



*... for a brighter future*

# Inelastic Neutron Scattering

Ray Osborn  
Materials Science Division  
Argonne National Laboratory

## Acknowledgements

Brian Rainford  
Department of Physics and Astronomy  
University of Southampton, UK

Toby Perring  
ISIS Pulsed Neutron Facility  
Rutherford Appleton Laboratory, UK

Taner Yildirim  
NIST Center for Neutron Research  
Gaithersburg, MD



U.S. Department  
of Energy

UChicago ►  
Argonne<sub>LLC</sub>

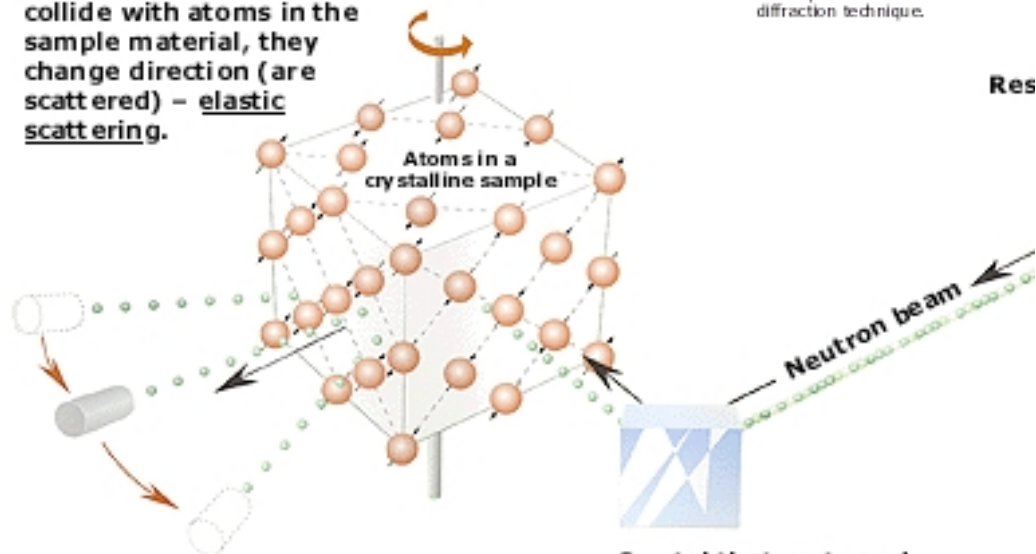


A U.S. Department of Energy laboratory  
managed by UChicago Argonne, LLC

# 1994 Nobel Prize in Physics

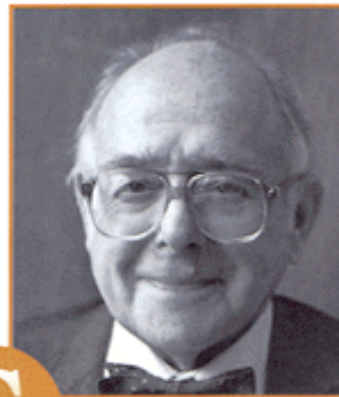
## Neutrons show where atoms are

When the neutrons collide with atoms in the sample material, they change direction (are scattered) – elastic scattering.



Detectors record the directions of the neutrons and a diffraction pattern is obtained.

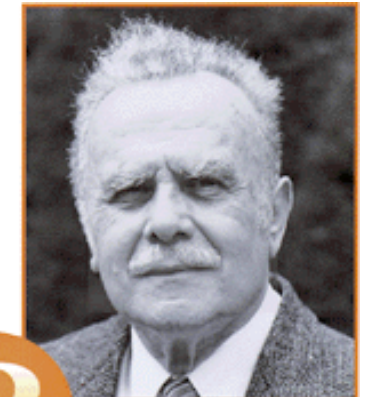
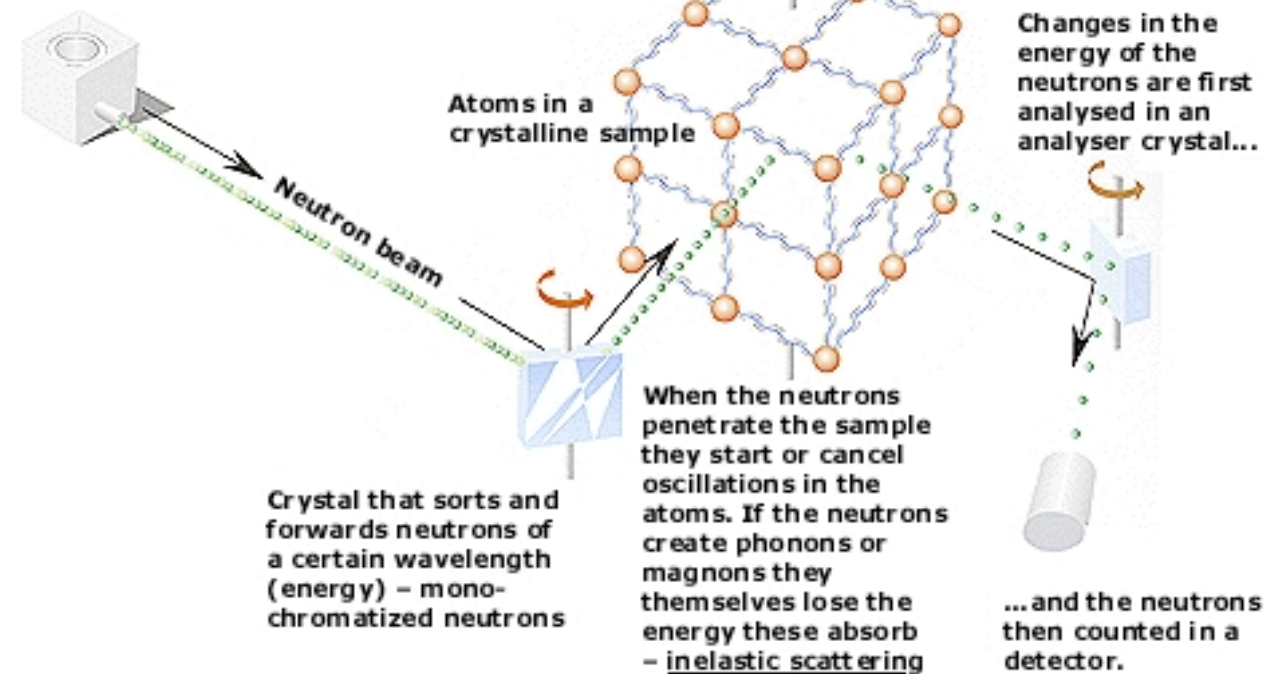
The pattern shows the positions of the atoms relative to one another.



**Clifford G. Shull**, MIT, Cambridge, Massachusetts, USA, receives one half of the 1994 Nobel Prize in Physics for development of the neutron diffraction technique.

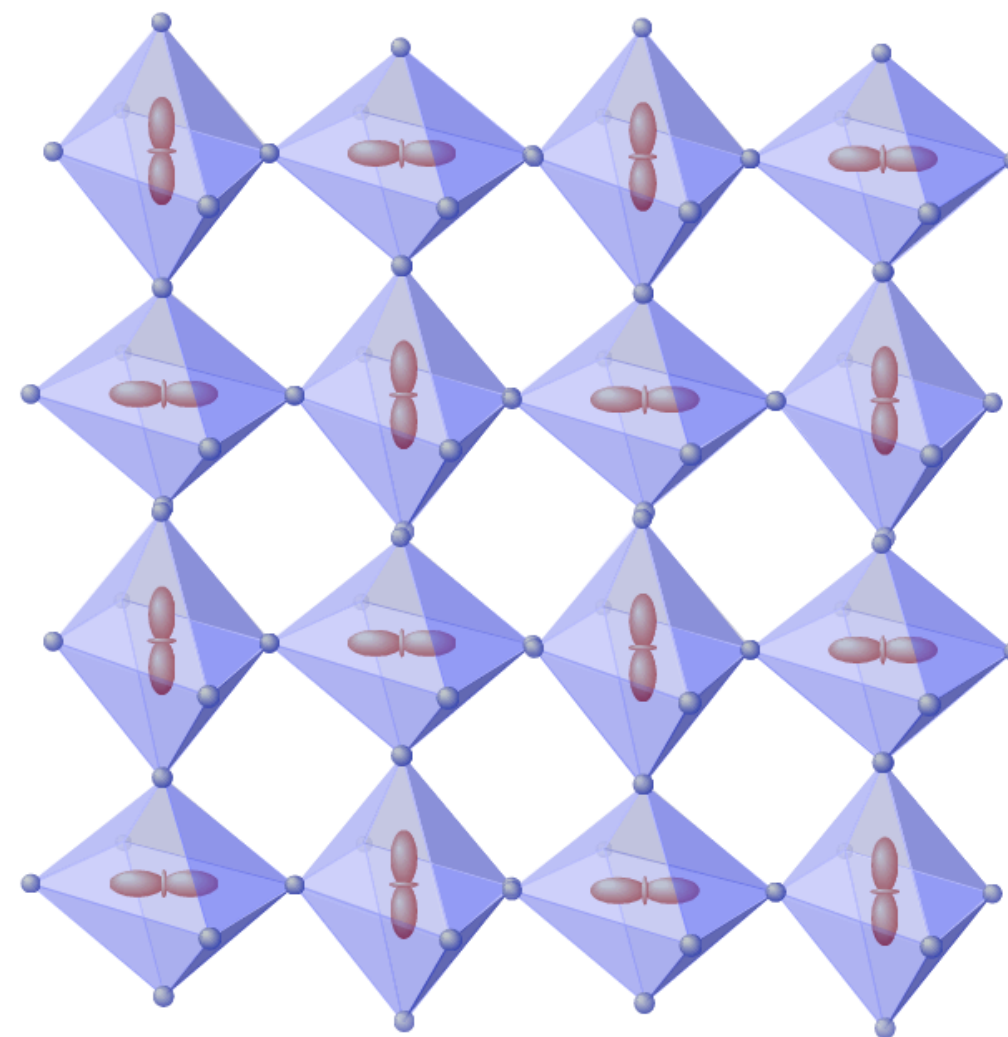
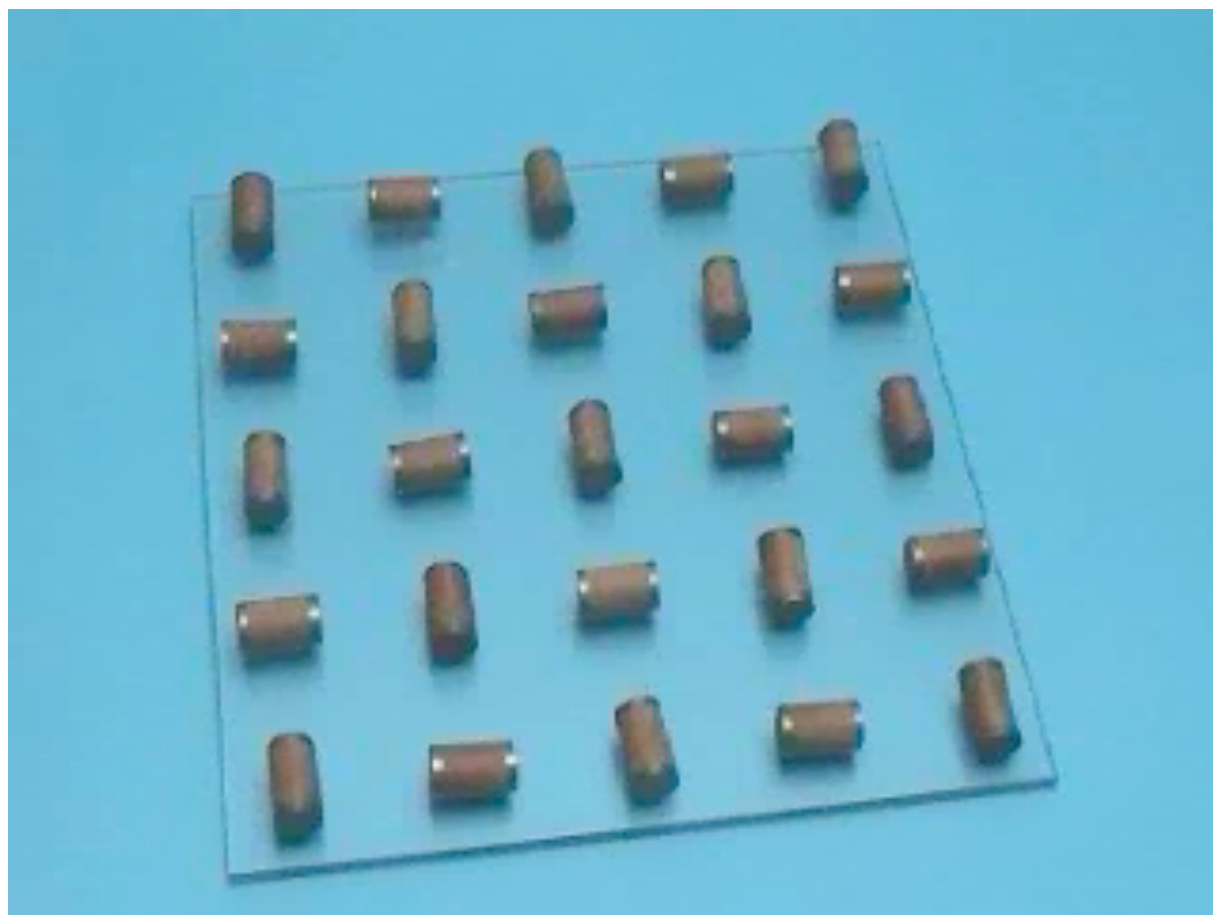
## Neutrons show what atoms do

3-axis spectrometer with rotatable crystals and rotatable sample



**Bertram N. Brockhouse**, McMaster University, Hamilton, Ontario, Canada, receives one half of the 1994 Nobel Prize in Physics for the development of neutron spectroscopy.

# The moving finger ...

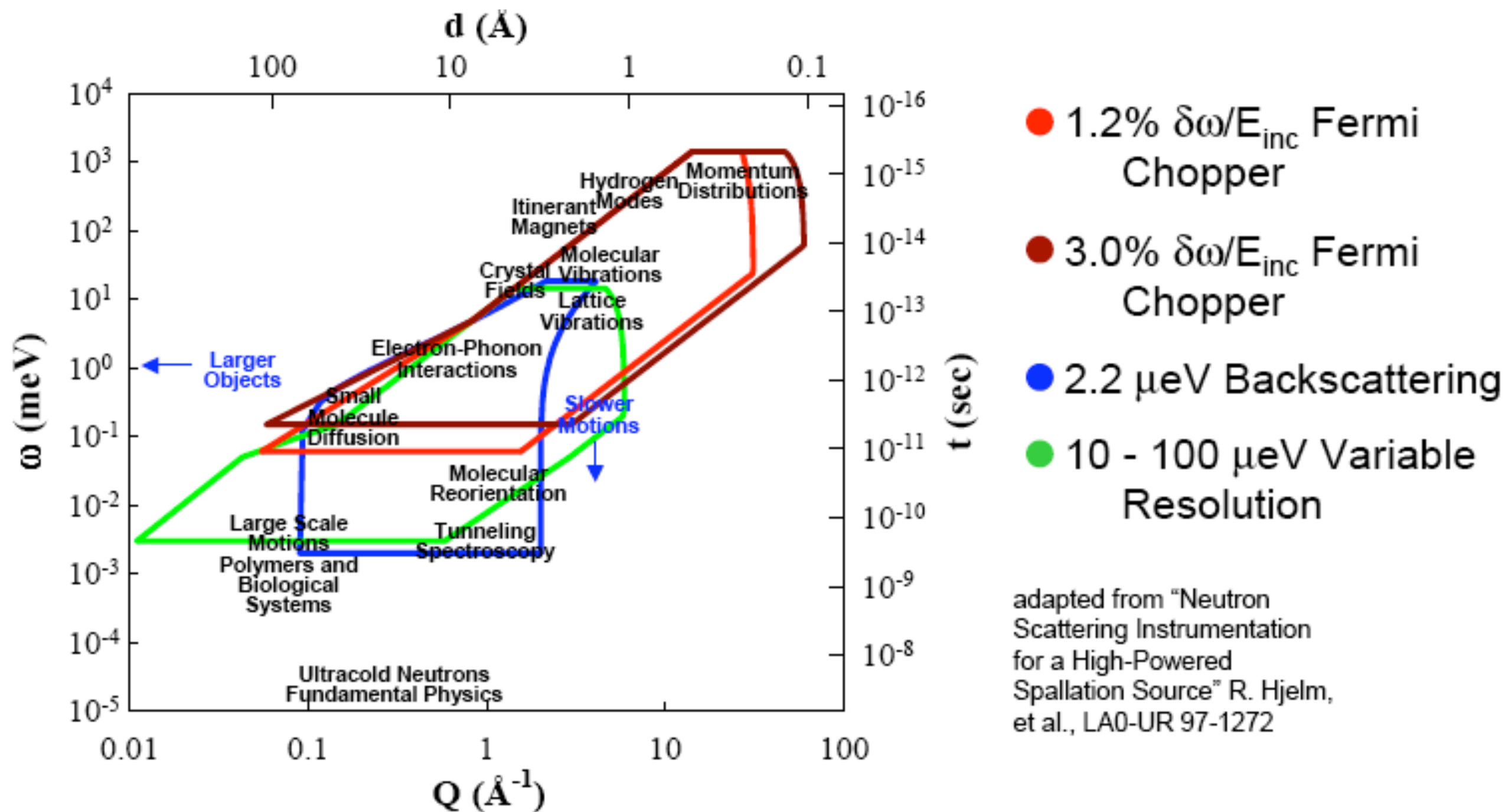


LaMnO<sub>3</sub>

# Useful properties of thermal neutrons

- Thermal neutrons have de Broglie wave-lengths comparable to typical interatomic distances and hence wavevectors,  $k = 2\pi/\lambda$ , that are on the scale of the Brillouin zone.
  - $\lambda \sim 0.1 - 10 \text{ \AA}$
  - $k \sim 0.6 - 60 \text{ \AA}^{-1}$
- Thermal neutrons have energies that are in the same range as those of typical excitations in condensed matter.
  - $\epsilon \sim 0.8 - 800 \text{ meV}$
- Thermal neutrons interact weakly with condensed matter.
  - The Born approximation is valid.
  - As a consequence, we need large samples.
- Thermal neutrons couple with both nuclei and magnetic spins
  - Nuclear force with nuclei  $\Rightarrow$  **lattice excitations**
  - Magnetic coupling to unpaired electrons  $\Rightarrow$  **magnetic excitations**

# Range of Inelastic Neutron Scattering Science



adapted from "Neutron Scattering Instrumentation for a High-Powered Spallation Source" R. Hjelm, et al., LA0-UR 97-1272

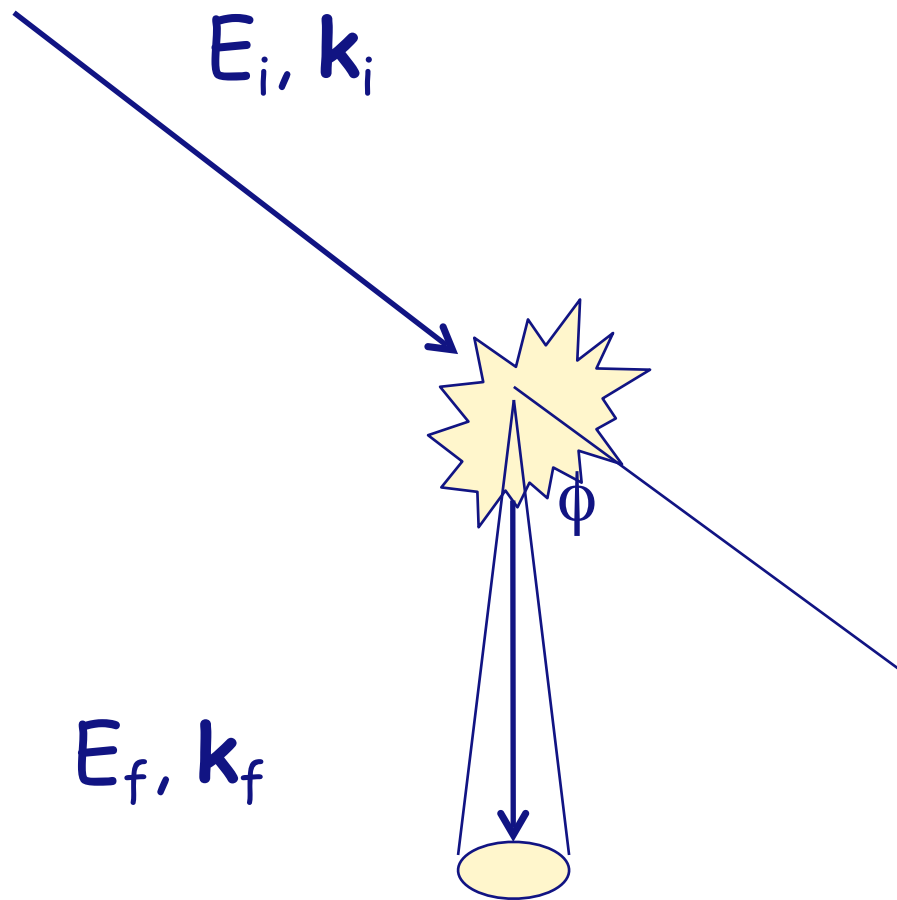
# Neutron Conversion Factors

$$E = \frac{\hbar^2 k^2}{2m} = \frac{h^2}{2m\lambda^2} = \frac{m}{2\tau^2}$$

where  $\tau$  is the time of flight, or inverse velocity ( $\tau = 1/v$ ).

- $E$  (meV) = 81.80  $\lambda^{-2}$  ( $\text{\AA}^{-2}$ )
- $E$  (meV) = 2.072  $k^2$  ( $\text{\AA}^{-2}$ )
- $E$  (meV) =  $5.227 \times 10^6 \tau^{-2}$  ( $\text{m}^2/\mu\text{sec}^2$ )
  
- $T$  (K) = 11.604  $E$  (meV)

# Inelastic Scattering Processes



$$\frac{d^2\sigma}{d\Omega dE_f} = \frac{k_f}{k_i} S(Q, \varepsilon)$$

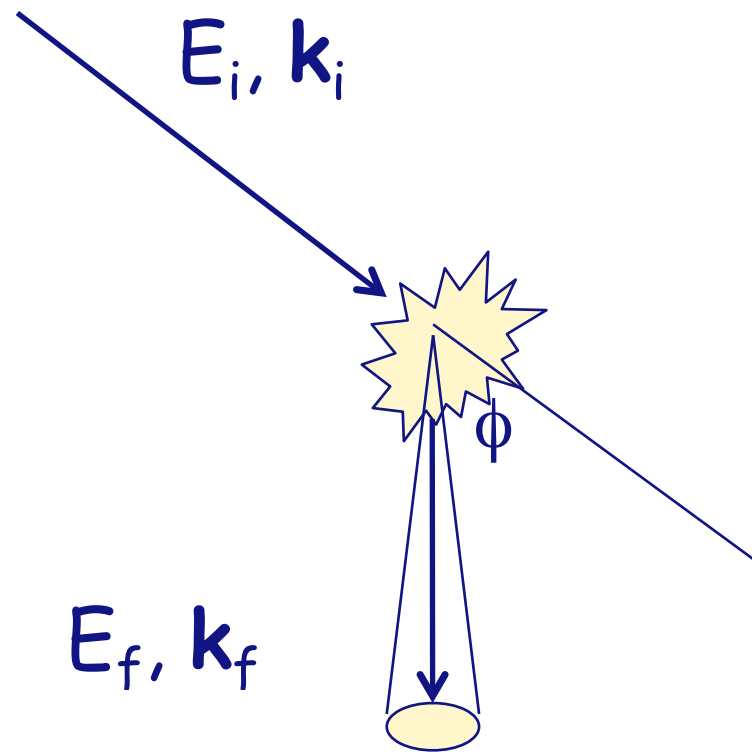
Conservation of energy

$$\varepsilon = E_i - E_f$$

Conservation of "momentum"

$$\vec{Q} = \vec{k}_i - \vec{k}_f$$

# Neutron Scattering Cross Sections



$$\mathbf{Q} = \mathbf{k}_i - \mathbf{k}_f$$

$$\hbar\omega = E_i - E_f$$

$$\left( \frac{d^2 \sigma}{d\Omega dE_f} \right)_{coh} = \frac{\sigma_{coh}}{4\pi} \frac{k_f}{k_i} NS(\mathbf{Q}, \omega)$$

$$S(\mathbf{Q}, \omega) = \frac{1}{2\pi\hbar} \int G(\mathbf{r}, t) \exp[i(\mathbf{Q} \cdot \mathbf{r} - \omega t)] d\mathbf{r} dt$$

$$G(\mathbf{r}, t) = \frac{1}{(2\pi)^3} \int I(\mathbf{Q}, t) \exp[-i\mathbf{Q} \cdot \mathbf{r}] d\mathbf{Q}$$

$$I(\mathbf{Q}, t) = \frac{1}{N} \sum_{i,j} \langle \exp[-i\mathbf{Q} \cdot \mathbf{R}_j(0)] \exp[-i\mathbf{Q} \cdot \mathbf{R}_i(t)] \rangle$$

$G(\mathbf{r}, t) d\mathbf{r}$  gives the probability that, given a nucleus at the origin at  $\mathbf{r} = 0$ , any nucleus (the same one or a different one) will be found within volume  $d\mathbf{r}$  at  $\mathbf{r}$  and at time  $t$

$$S(\mathbf{Q}) = \int S(\mathbf{Q}, \omega) d\omega = I(\mathbf{Q}, 0) = \int G(\mathbf{r}, 0) \exp(i\mathbf{Q} \cdot \mathbf{r}) d\mathbf{r}$$

where  $G(\mathbf{r}, 0) = \delta(\mathbf{r}) + g(\mathbf{r})$  so that

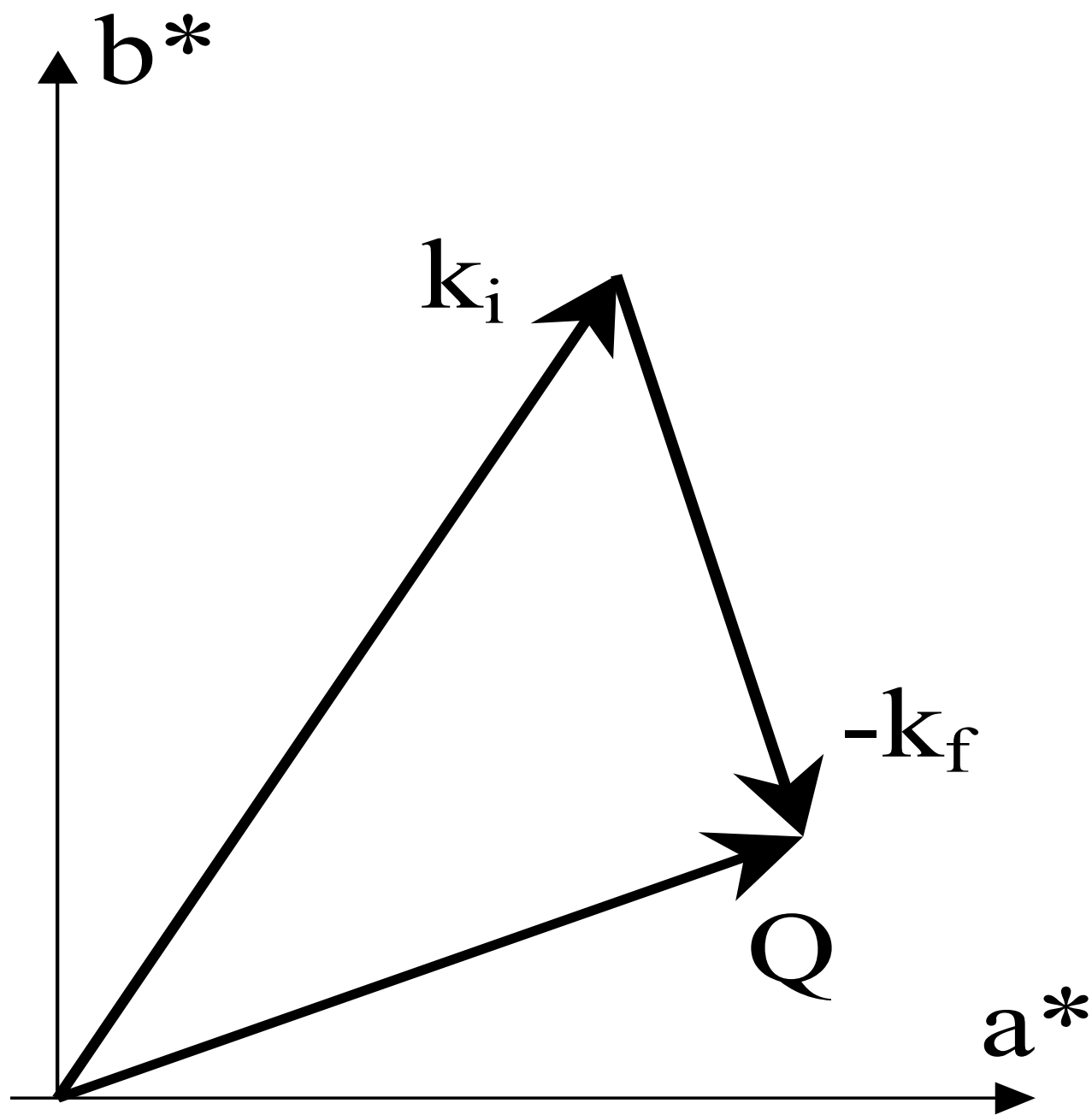
$$S(\mathbf{Q}) = 1 + \int g(\mathbf{r}) \exp(i\mathbf{Q} \cdot \mathbf{r}) d\mathbf{r}$$

$S(\mathbf{Q}) \Rightarrow$  Instantaneous Correlations

$S(\mathbf{Q}, \omega=0) \Rightarrow$  Static Correlations

# Reciprocal Space Construction

The scattering triangle

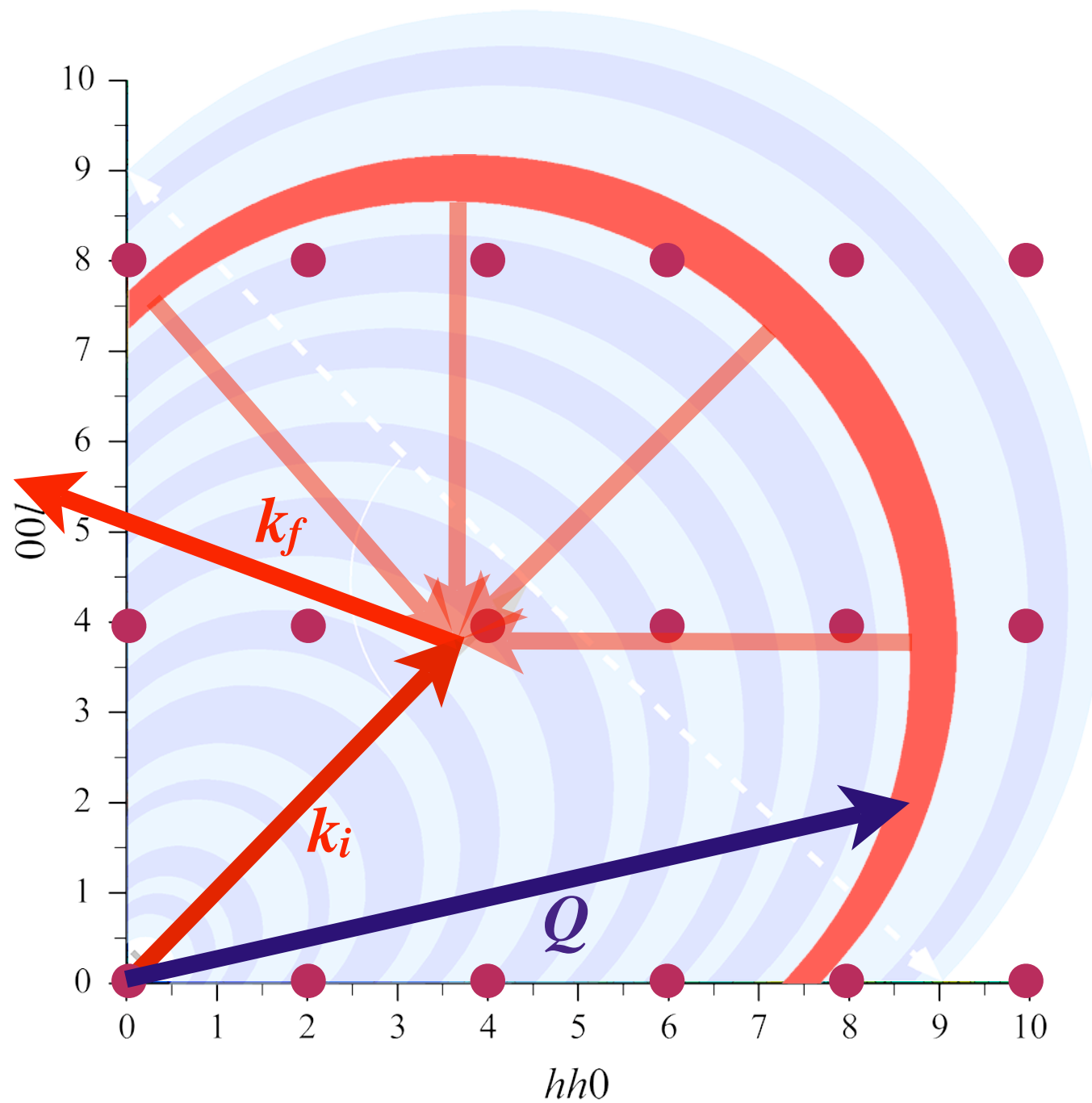


$$\vec{Q} = \vec{k}_i - \vec{k}_f$$

$$\varepsilon = E_i - E_f$$

$$= \frac{\hbar^2}{2m} (k_i^2 - k_f^2)$$

# Neutron Laue Diffraction

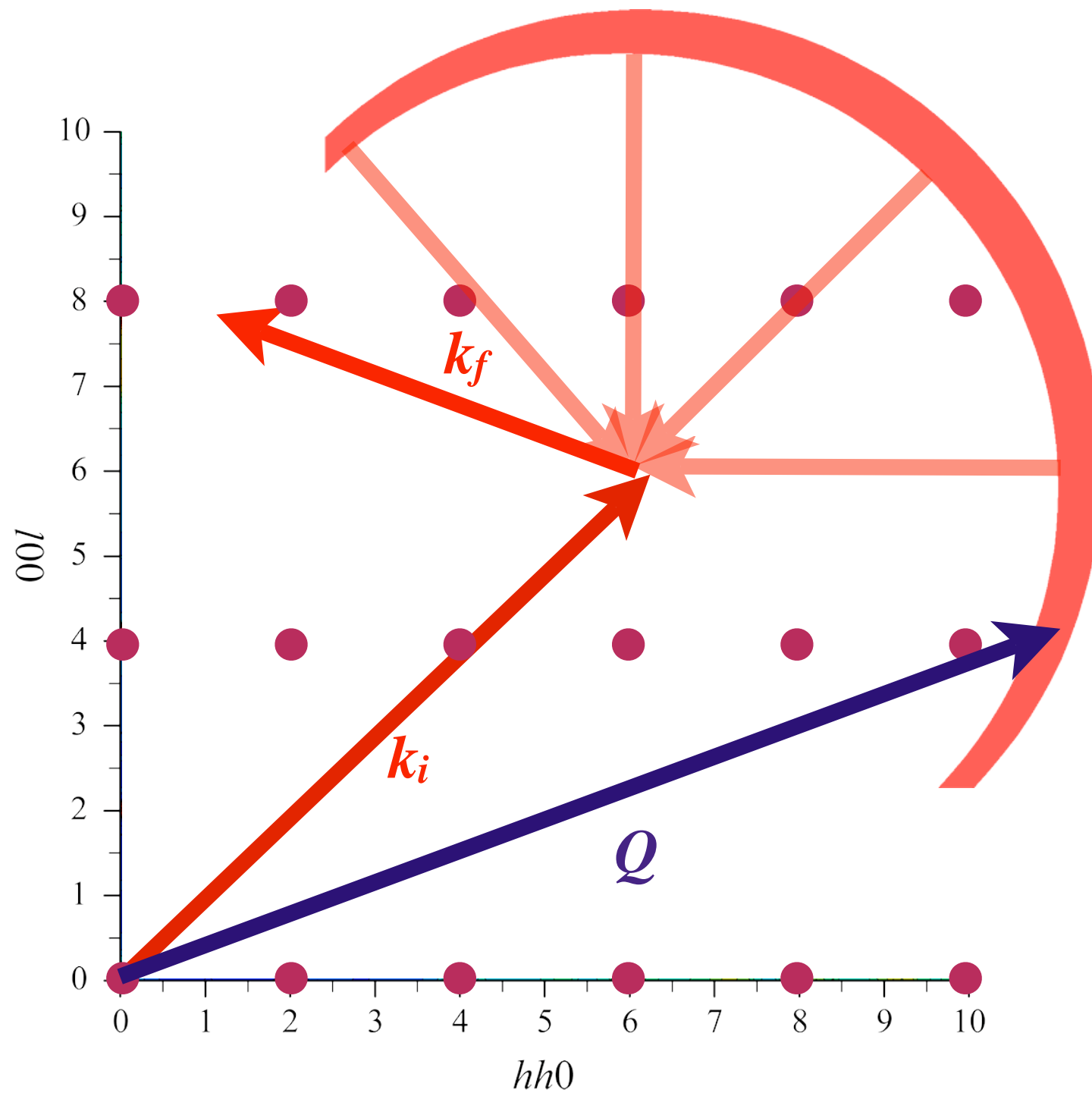


$$k_i = 2\pi / \lambda_i$$

$$k_f = 2\pi / \lambda_f$$

$$Q = k_i - k_f$$

# Ewald Spheres



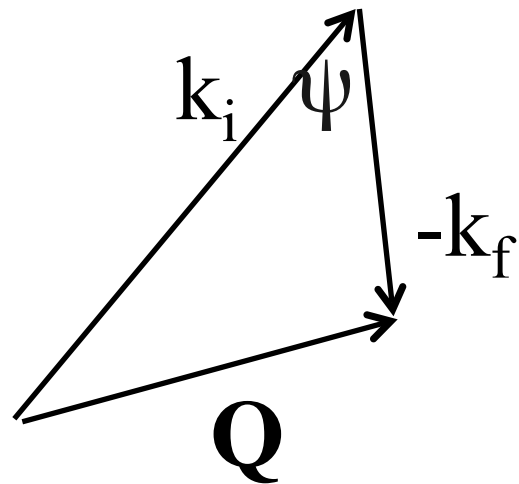
$$k_i = 2\pi / \lambda_i$$

$$k_f = 2\pi / \lambda_f$$

$$Q = k_i - k_f$$

# Kinematic Range

From the scattering triangle, we can see that



$$Q^2 = k_i^2 + k_f^2 - 2k_i k_f \cos(\psi)$$

from which it follows that

$$\frac{\hbar^2}{2m} Q^2 = E_i + E_f - 2\sqrt{E_i E_f} \cos(\psi)$$

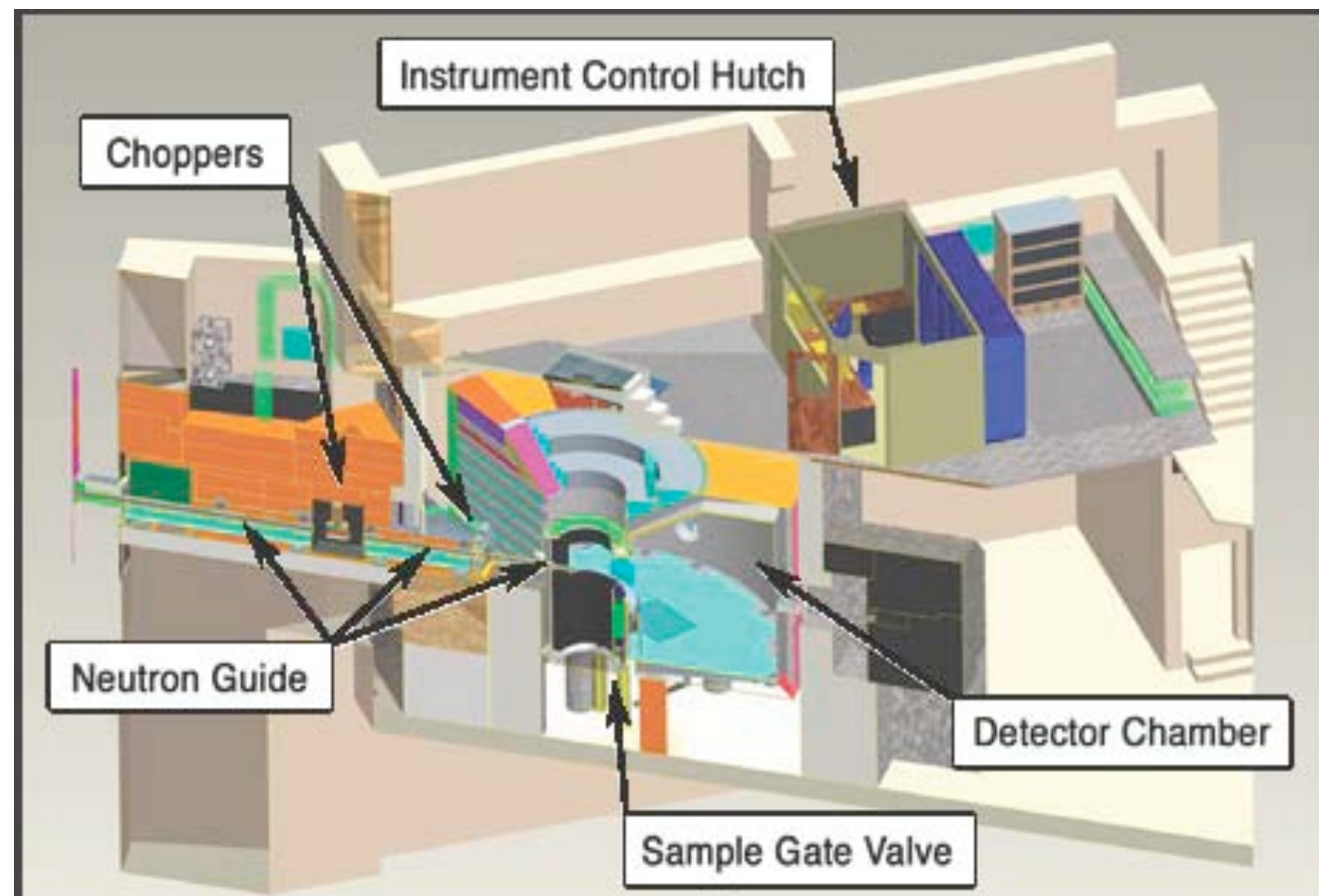
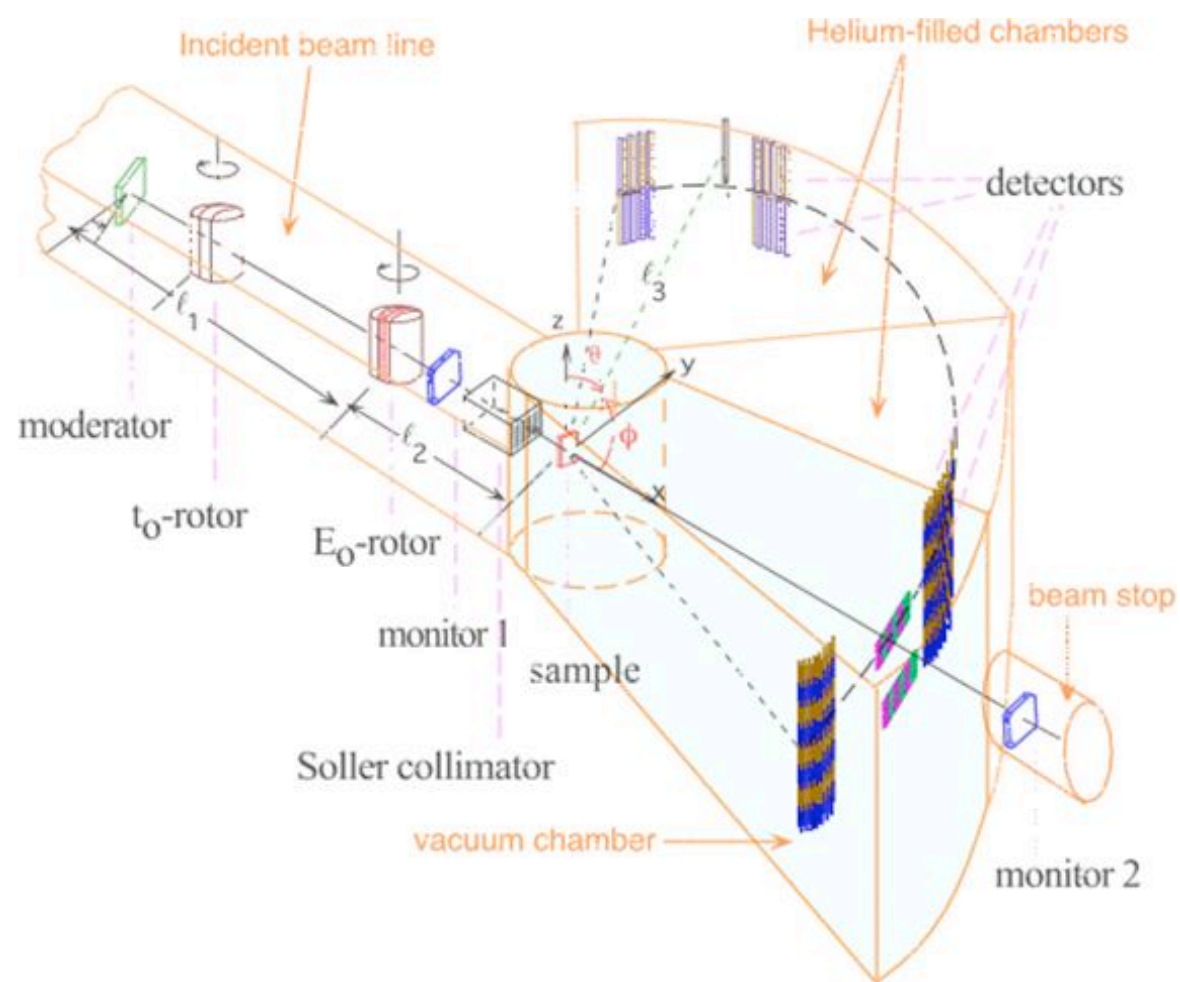
and so putting  $E_f = E_i - \varepsilon$

we get 
$$\frac{\hbar^2}{2m} Q^2 = 2E_i - \varepsilon - 2\sqrt{E_i(E_i - \varepsilon)} \cos(\psi)$$

This equation gives us the locus of  $(Q, \varepsilon)$  for a given scattering angle  $\psi$ .

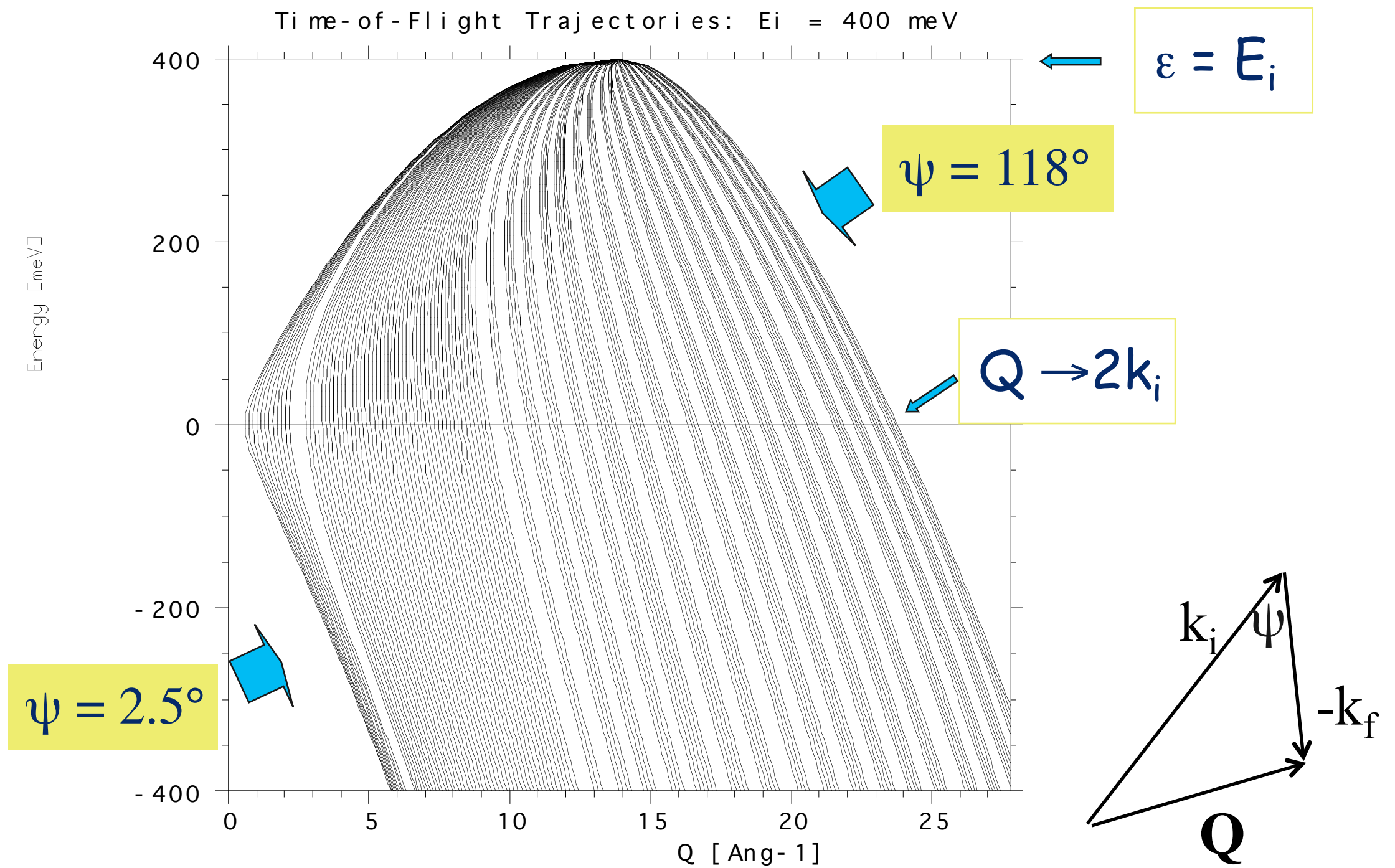
(N.B. we can write  $\hbar^2/2m=2.072$  for  $E(\text{meV})$  and  $Q$  in  $\text{\AA}^{-1}$ ).

# Time-of-Flight Spectrometer

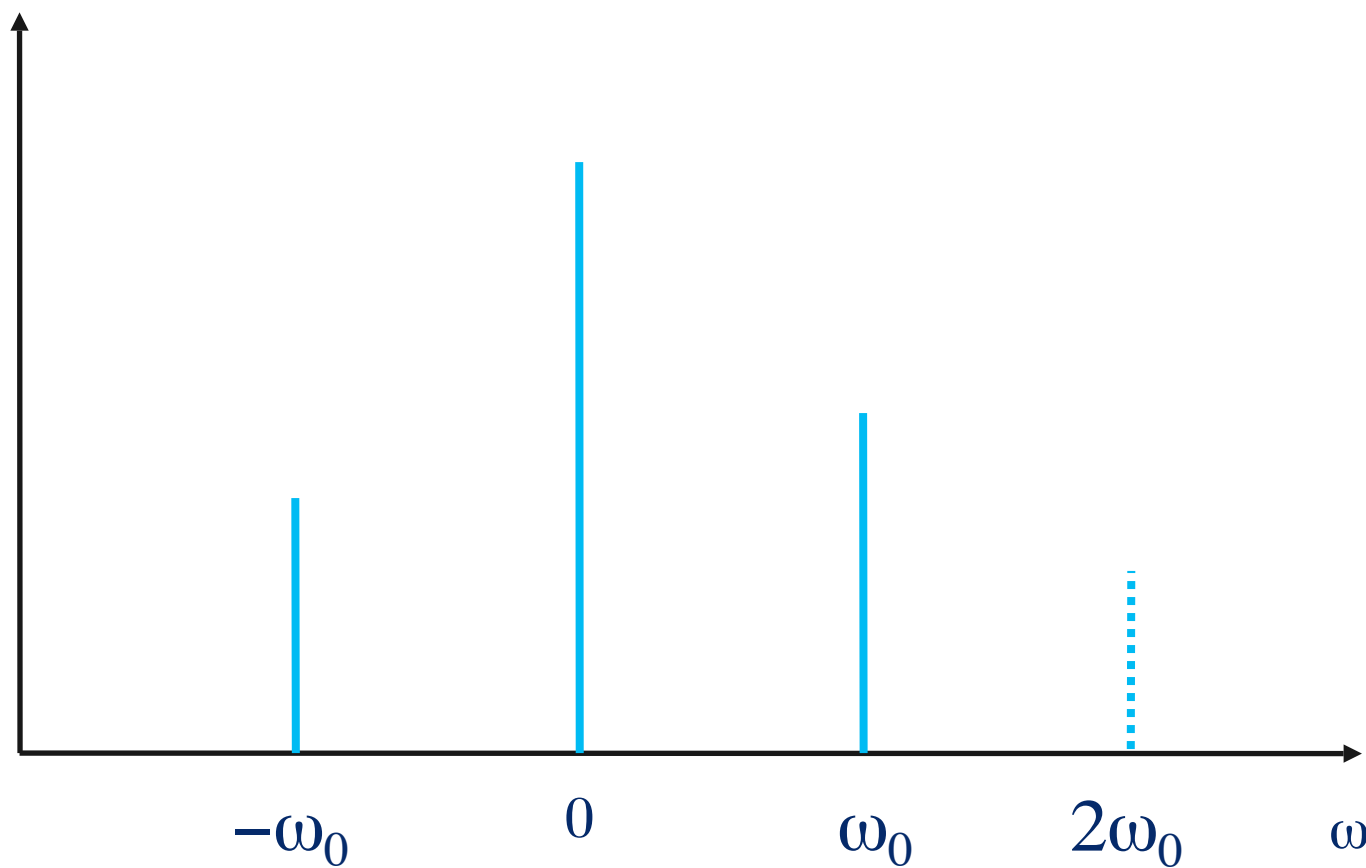
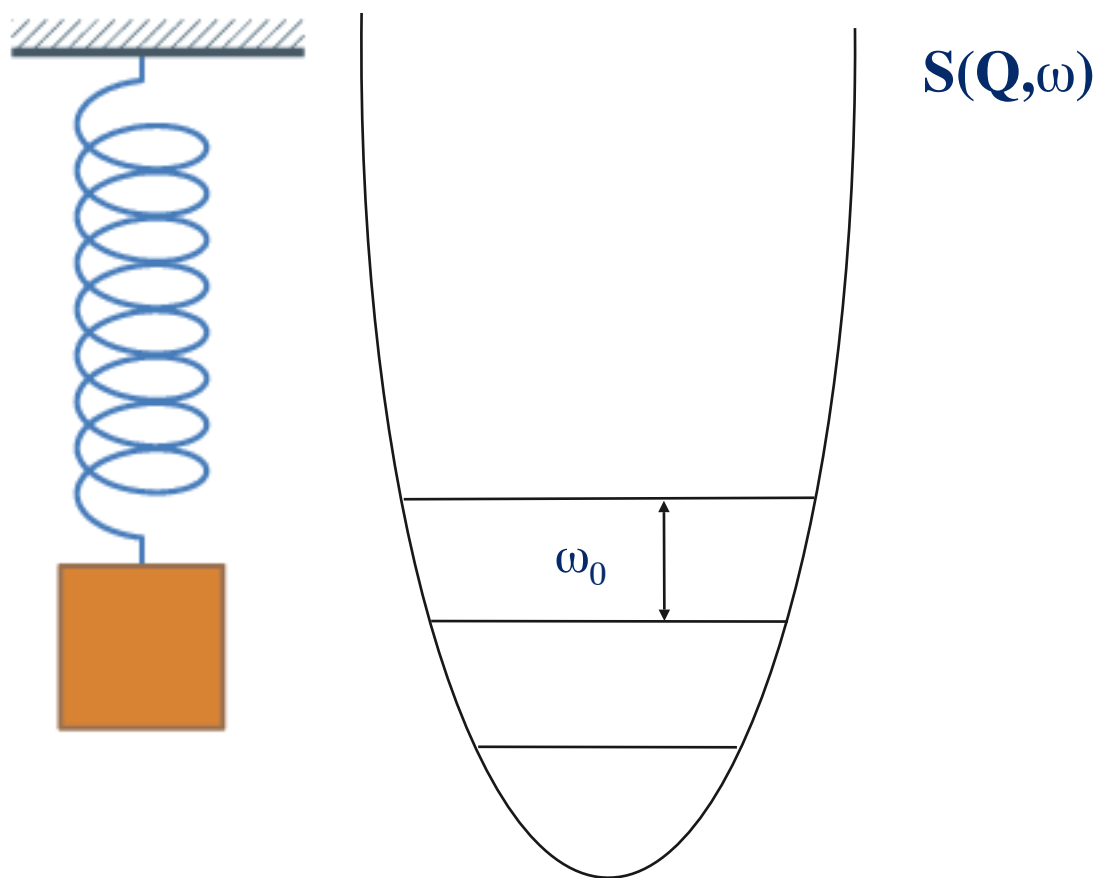


ARCS

# Locus of Neutrons in $(Q, \epsilon)$ Space



# Harmonic Oscillator



$$V = \frac{1}{2}kx^2$$

$$S(Q, \omega) = \exp\{-2W(Q)\} \left\{ \delta(\hbar\omega) + \left( \frac{Q^2}{2m\omega_0} \right) \{n(\omega) + 1\} [\delta(\omega - \omega_0) - \delta(\omega + \omega_0)] \right\}$$

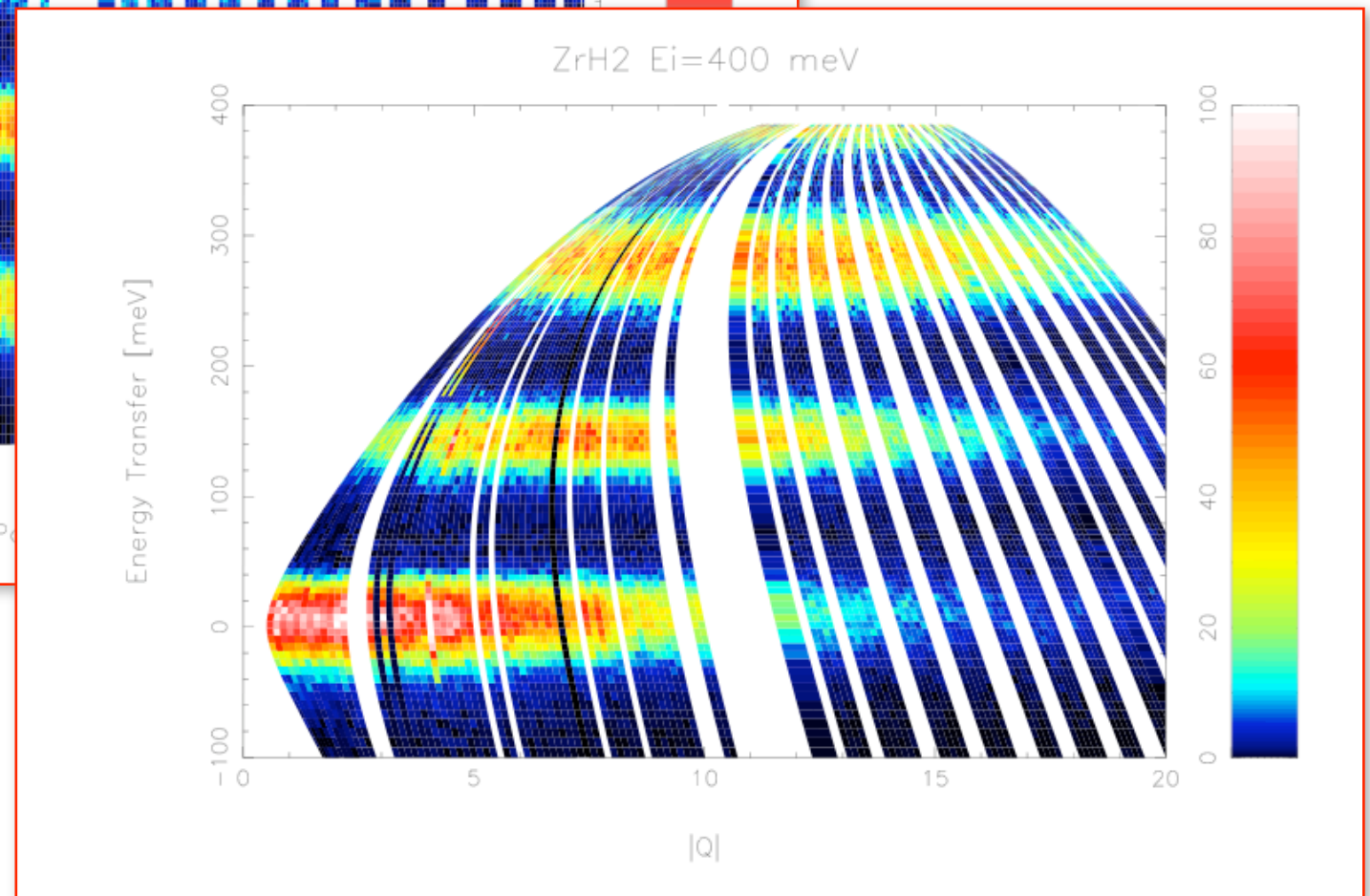
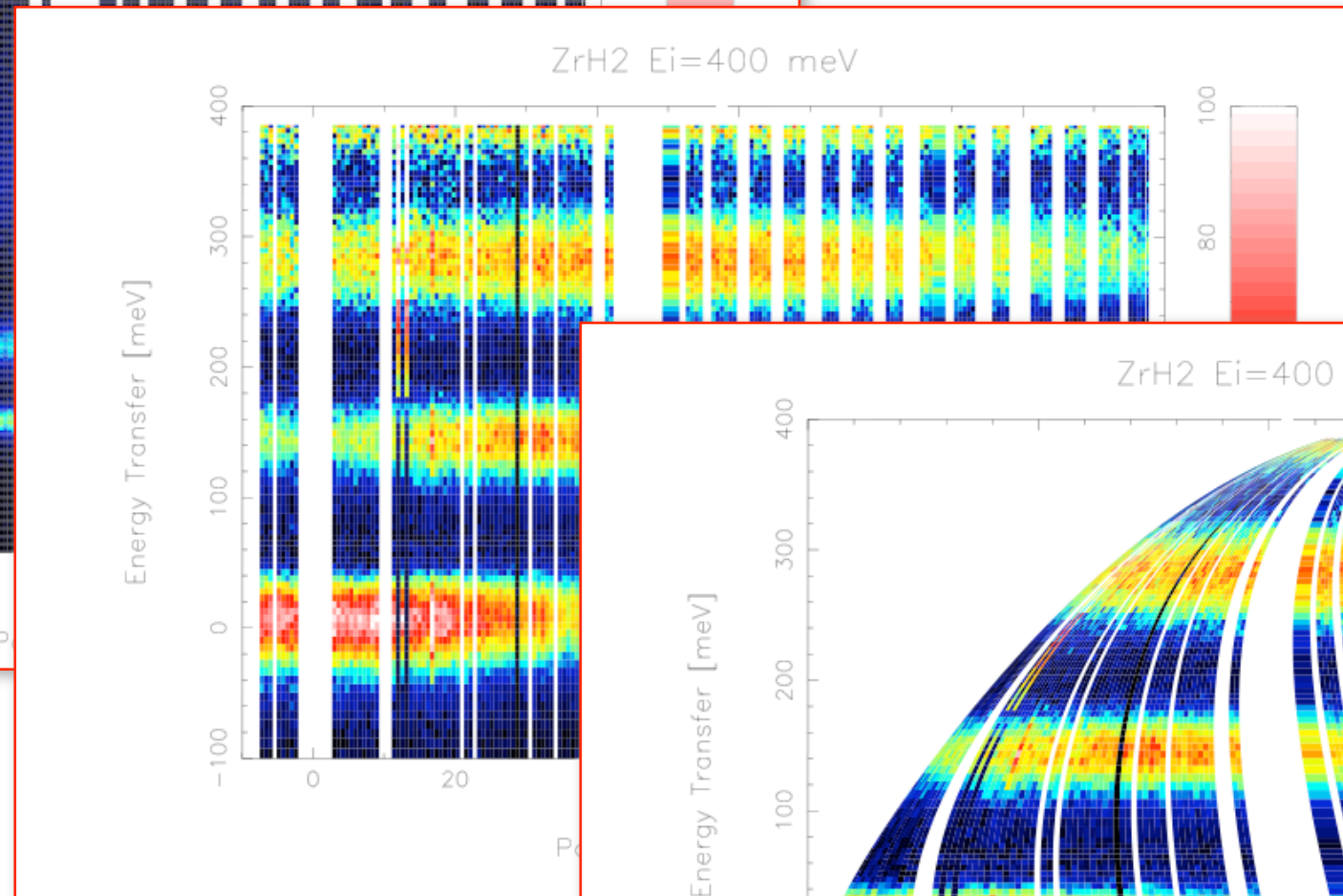
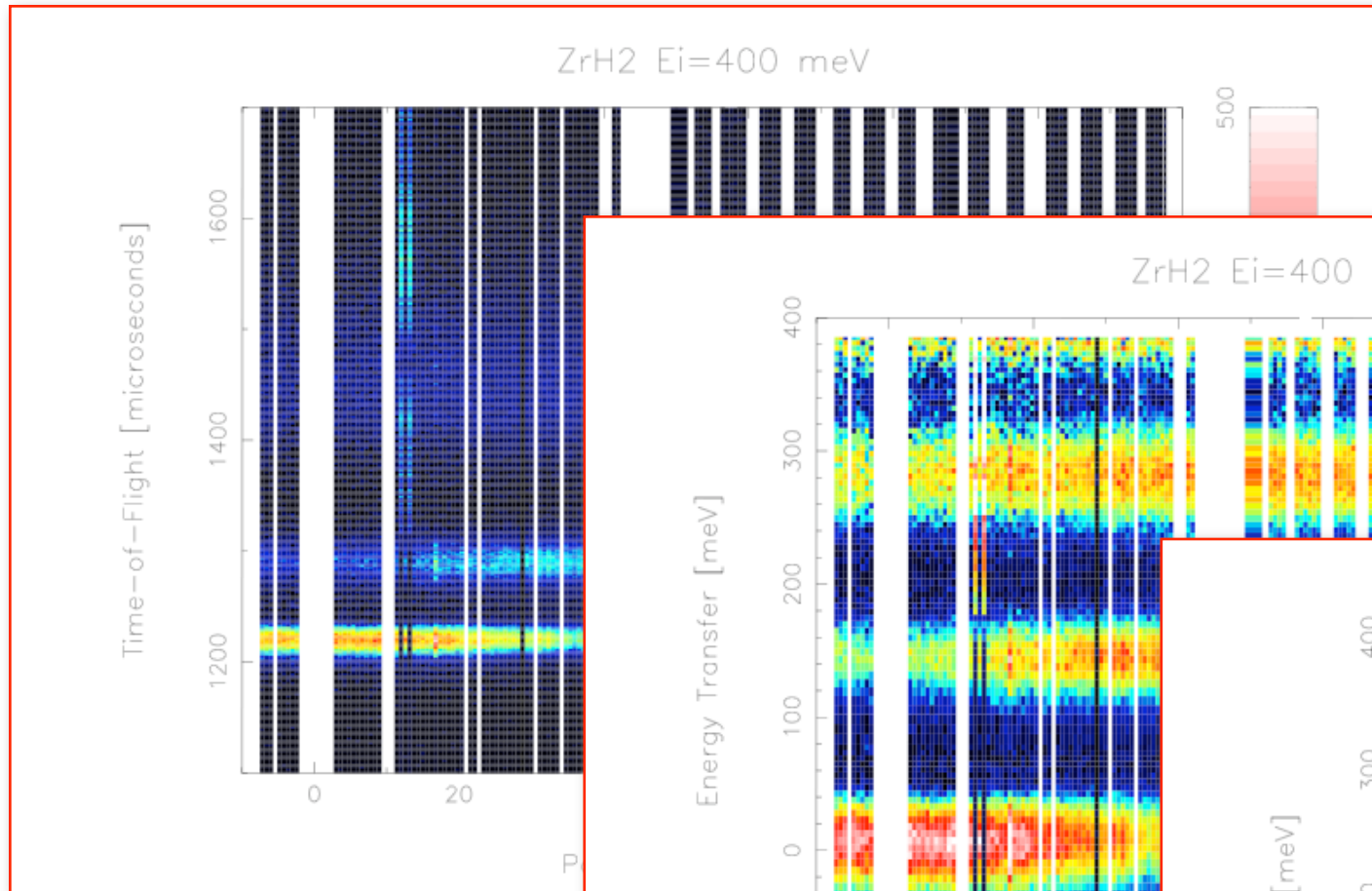
$$\{n(\omega) + 1\} = -n(-\omega) = [1 - \exp(-\hbar\omega/k_B T)]^{-1}$$

In general, the neutron can excite  $n$  phonons at once

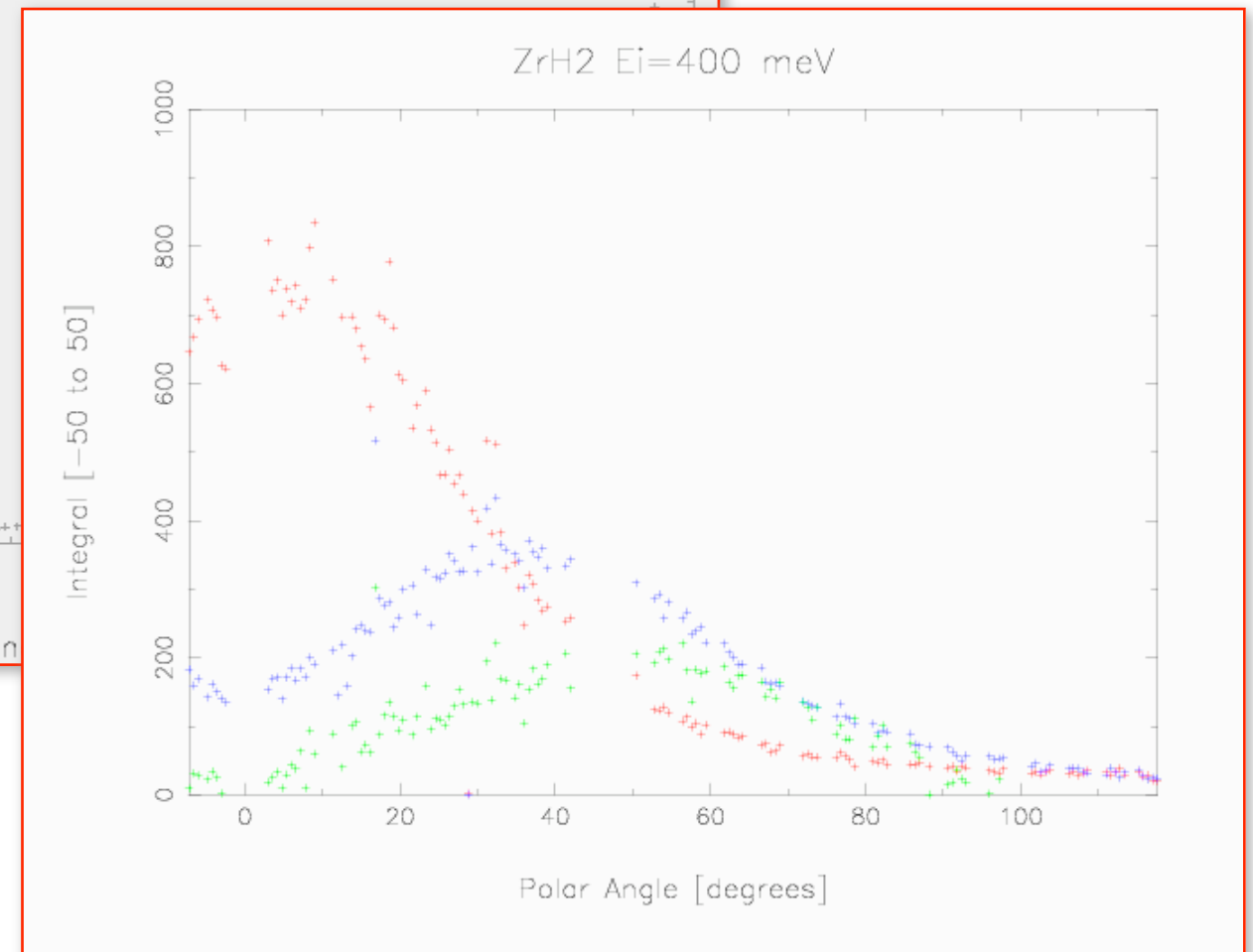
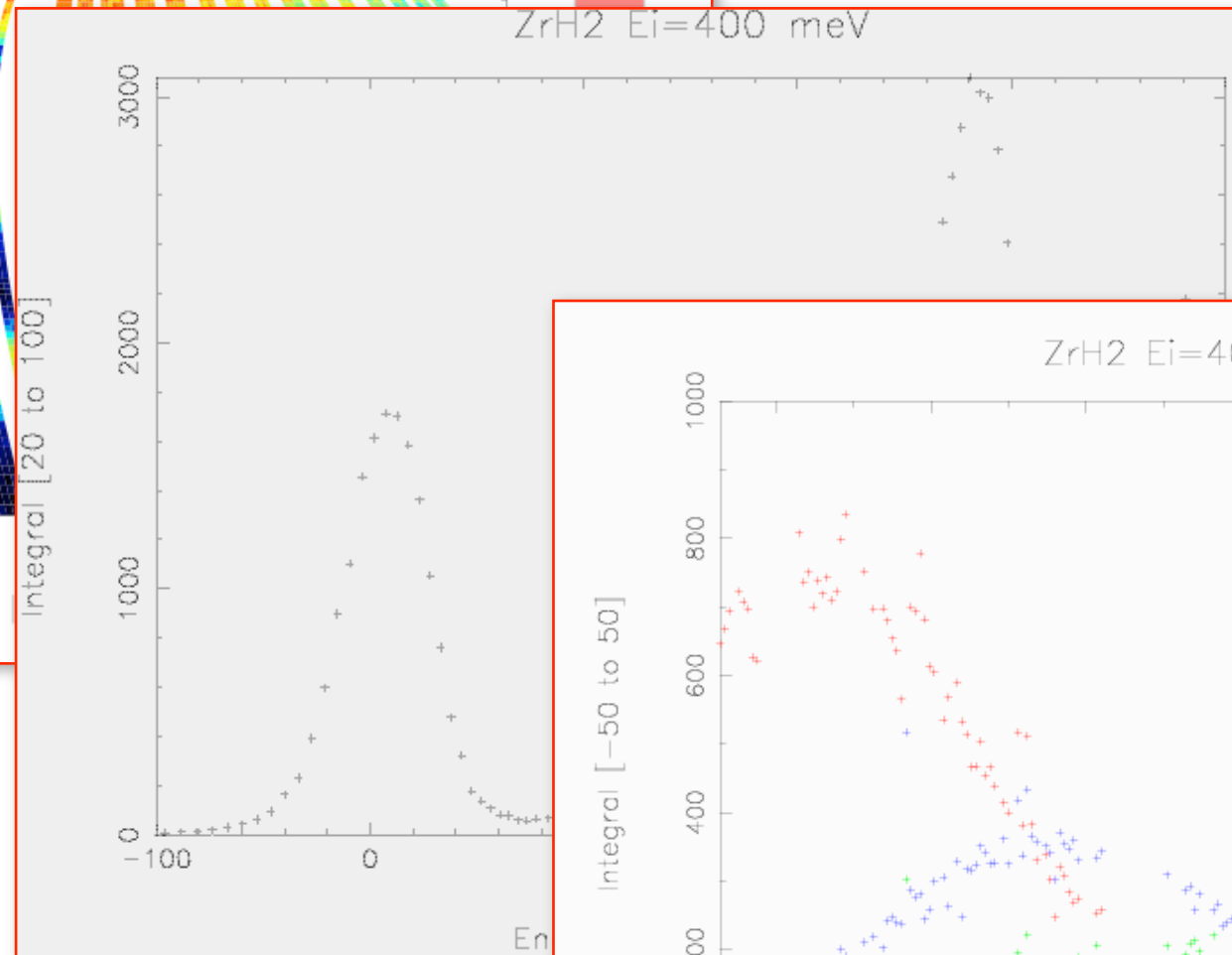
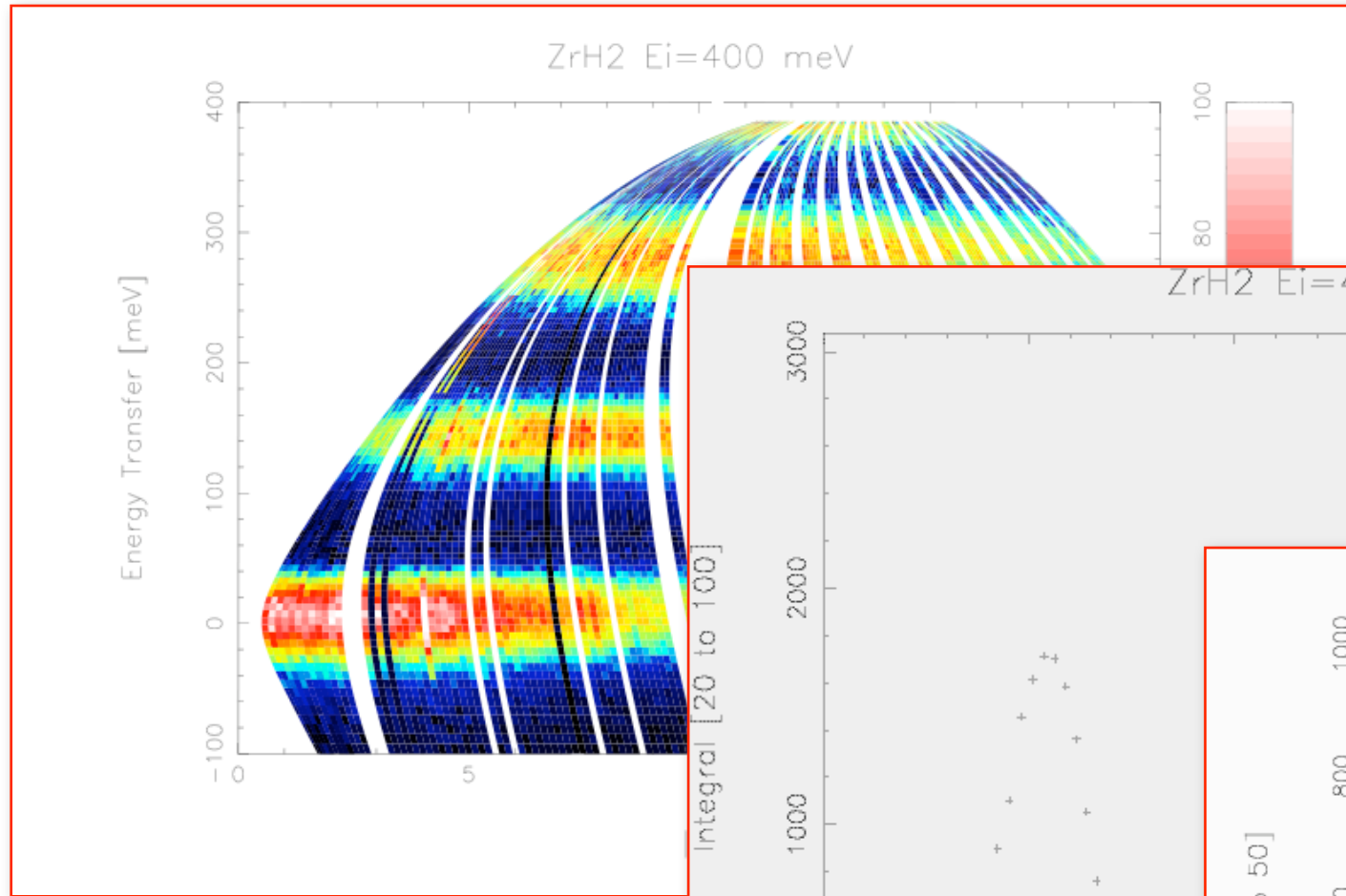
$$S(Q, \omega) = \exp\{-2W(Q)\} \sum_n \left( \frac{\hbar Q^2}{4mn\omega_0 \sinh \phi} \right)^n \exp(n\phi) \delta(\omega - n\omega_0)$$

where  $\phi = (\hbar\omega_0 / 2k_B T)$  and  $W(Q) = \hbar Q^2 \coth \phi / 4m\omega_0$

# Scattering in $\text{ZrH}_2$



# $(Q, \varepsilon)$ -Dependence of $ZrH_2$

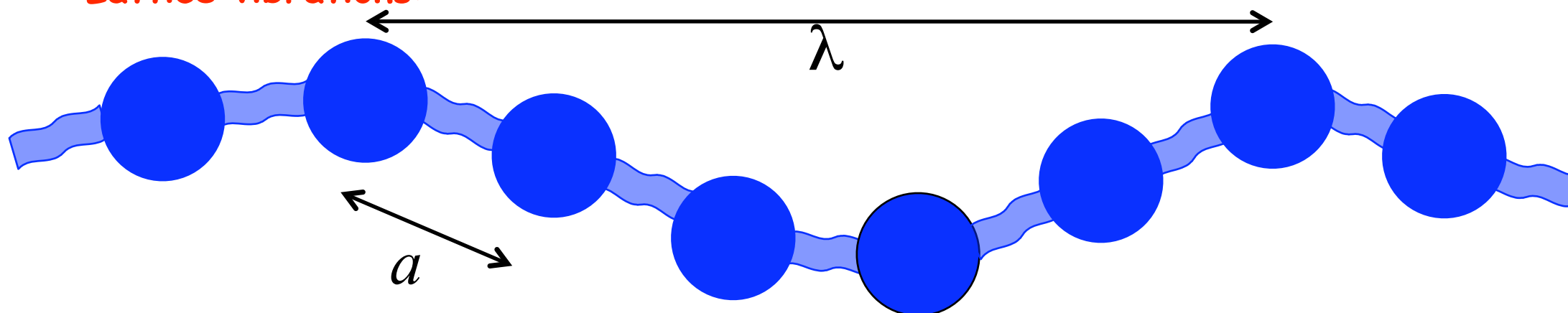


# Coherent Excitations

Processes in which a single excitation (quantum) is created or destroyed in the sample by the neutron.

Examples:

(i) **Lattice vibrations:**



e.g. simple linear chain of atoms, mass  $m$ , coupled together by bonds ("springs") with stiffness  $S$ .

Elementary excitations are wave-like with  $\lambda = 2\pi/q$  ;

Displacement of  $n$  th atom is:

$$\text{where } x_n = A \exp[i(qna - \omega_q t)]$$

A quantum, energy  $\hbar\omega_q$  is called a phonon.

$$\omega_q = \sqrt{\frac{4S}{m}} \sin\left(\frac{qa}{2}\right)$$

# Cross Section for Coherent Excitations

The neutron cross section for creating a single quantum (phonon or magnon) is:

$$\frac{d^2\sigma^{(+1)}}{d\Omega d\varepsilon} = A(Q) \sum_{\vec{G}} \langle n_q + 1 \rangle \delta(\vec{Q} - \vec{q} - \vec{G}) \delta(\varepsilon - \hbar\omega_q)$$

The cross section for annihilation is:

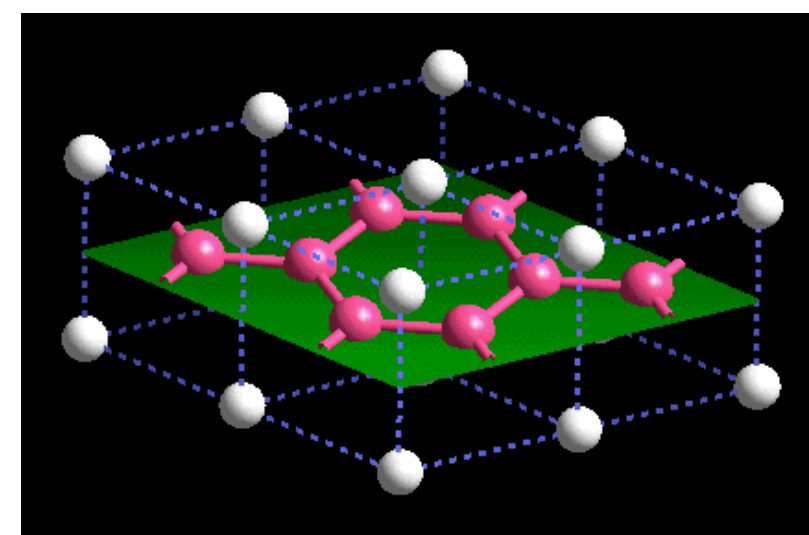
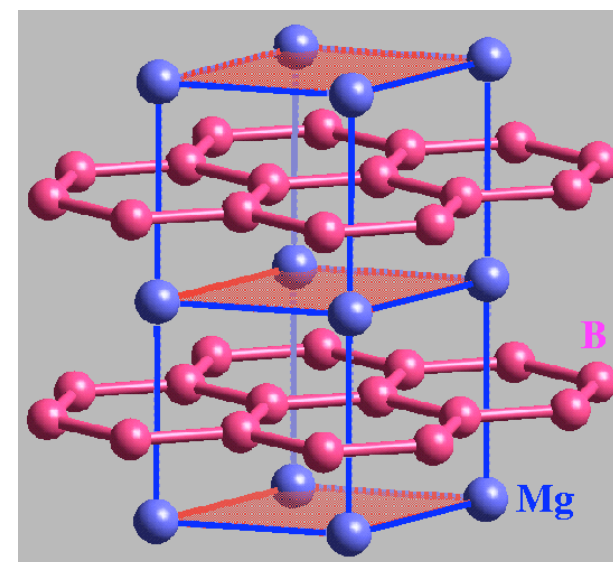
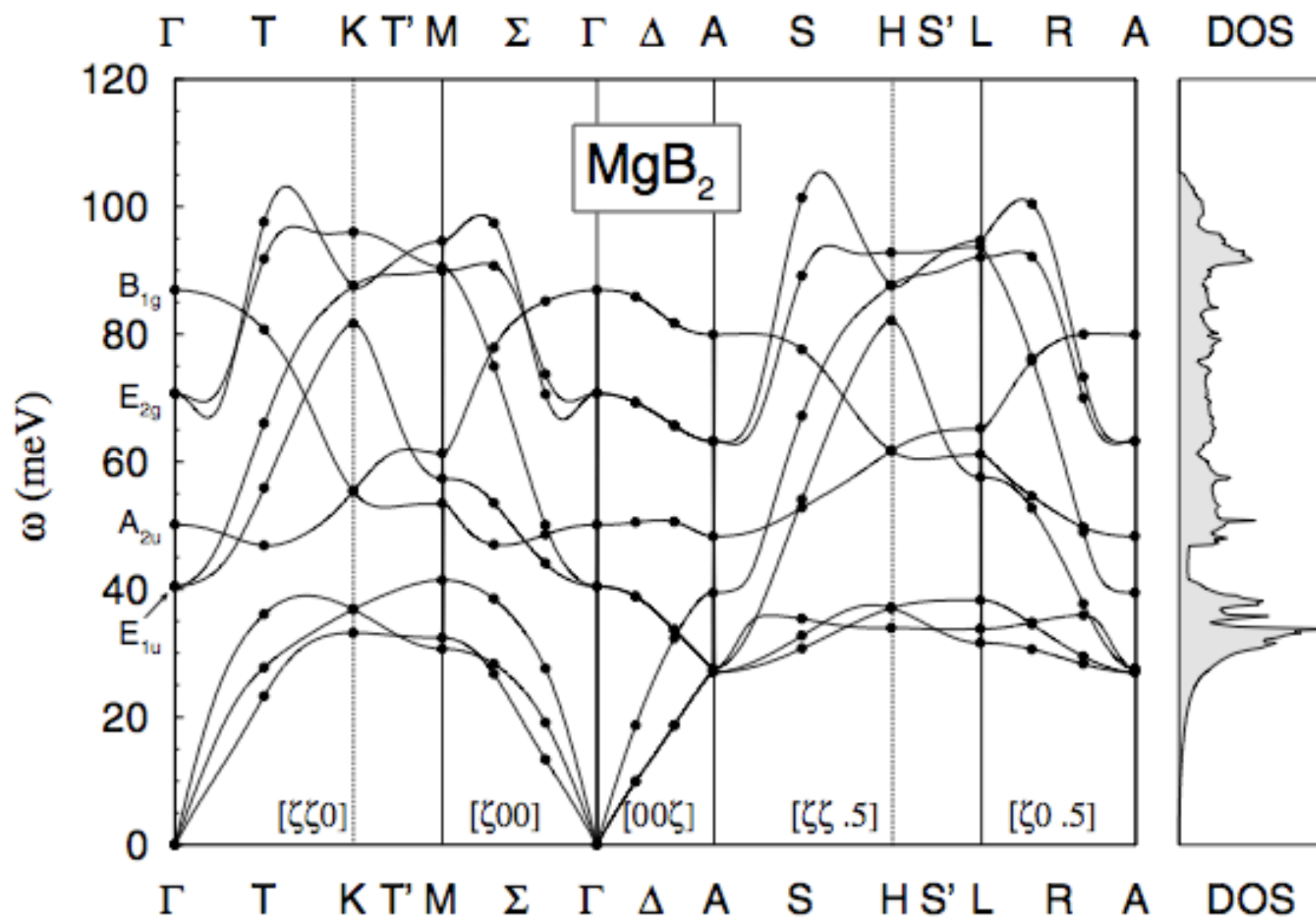
$$\frac{d^2\sigma^{(-1)}}{d\Omega d\varepsilon} = A(Q) \sum_{\vec{G}} \langle n_q \rangle \delta(\vec{Q} + \vec{q} - \vec{G}) \delta(\varepsilon + \hbar\omega_q)$$

The delta functions show that we get scattering only when:

$$\vec{Q} = \vec{G} \pm \vec{q} \quad \text{and} \quad \varepsilon = \pm \hbar\omega_q$$

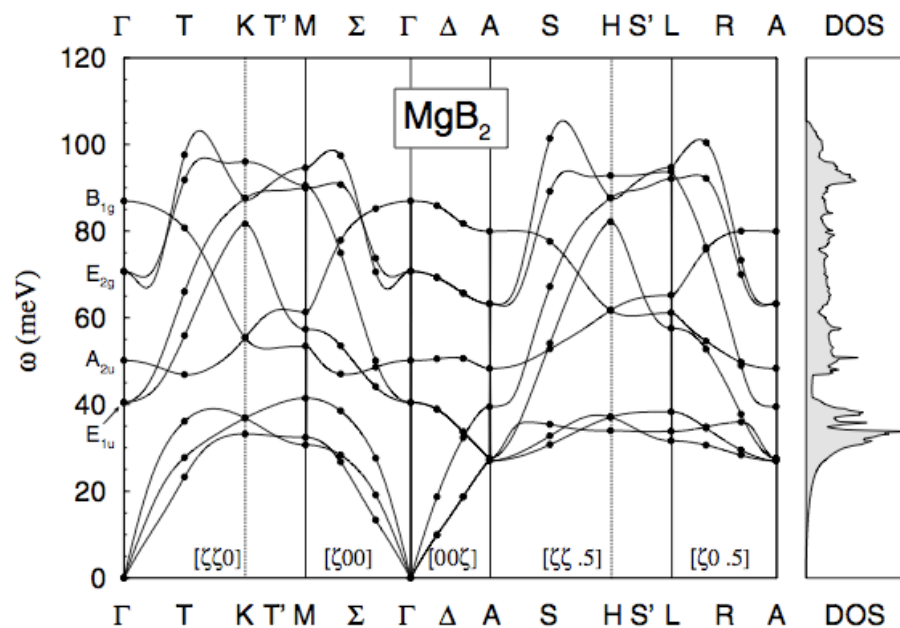
These conditions enable us to measure the dispersion relations.

# Phonon Dispersion in MgB<sub>2</sub>



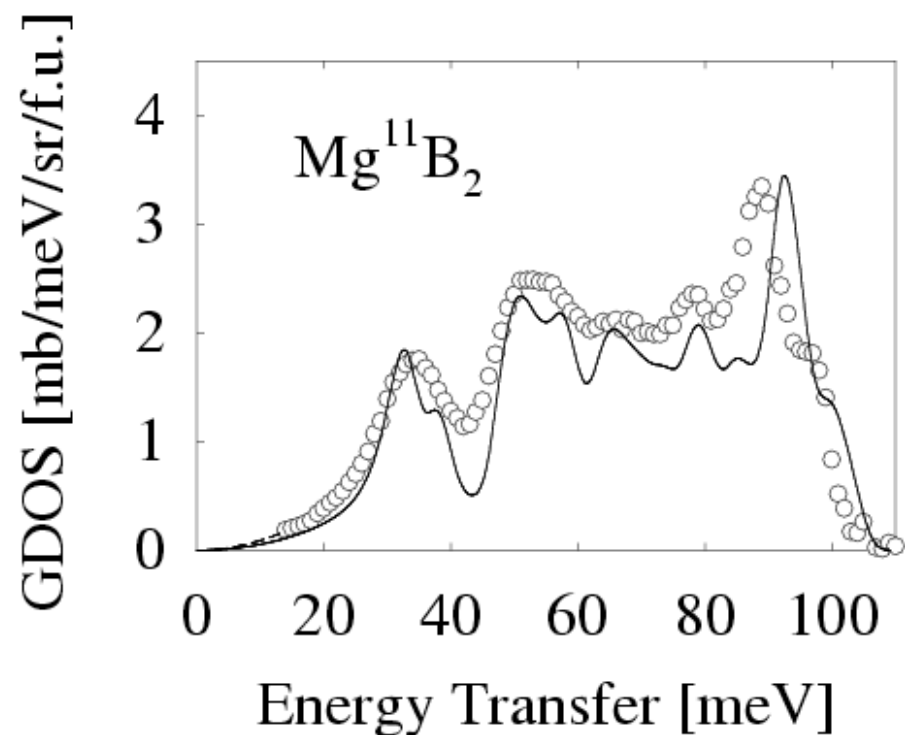
$\Gamma_{2g}$

# Phonon Density-of-States



When single crystals are available, phonon dispersion relations ( $\omega$  vs  $q$ ) can be measured.

However, it is often useful to measure the phonon density-of-states i.e. the sum over all phonon modes at each energy



In the incoherent approximation,

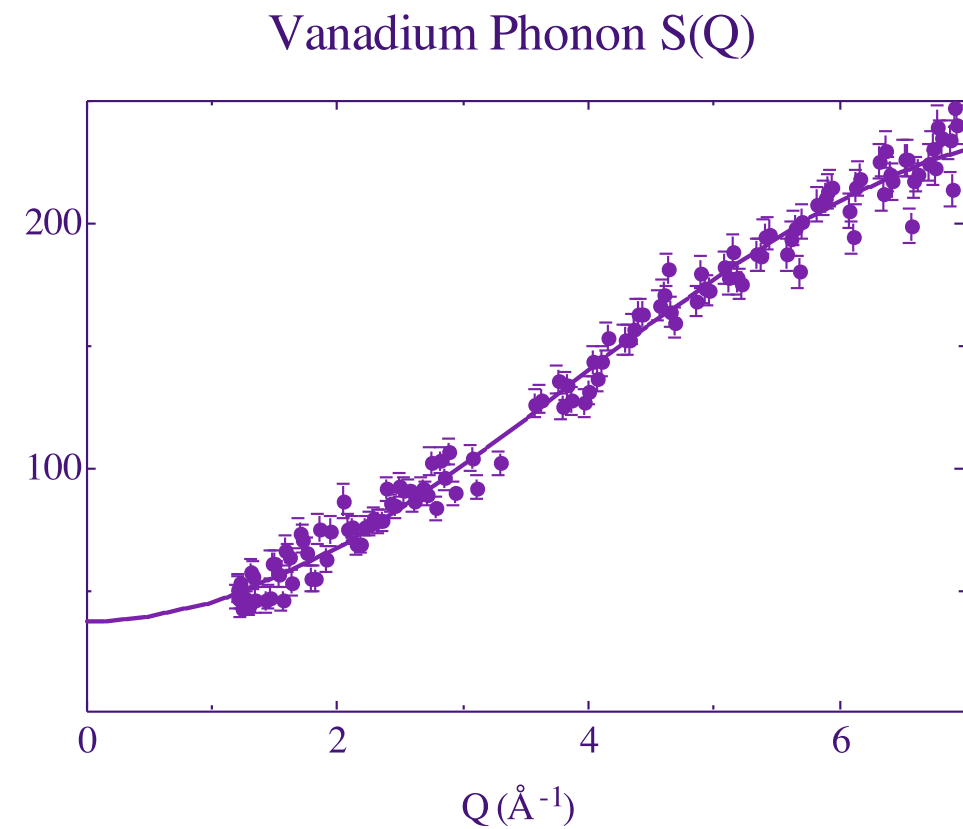
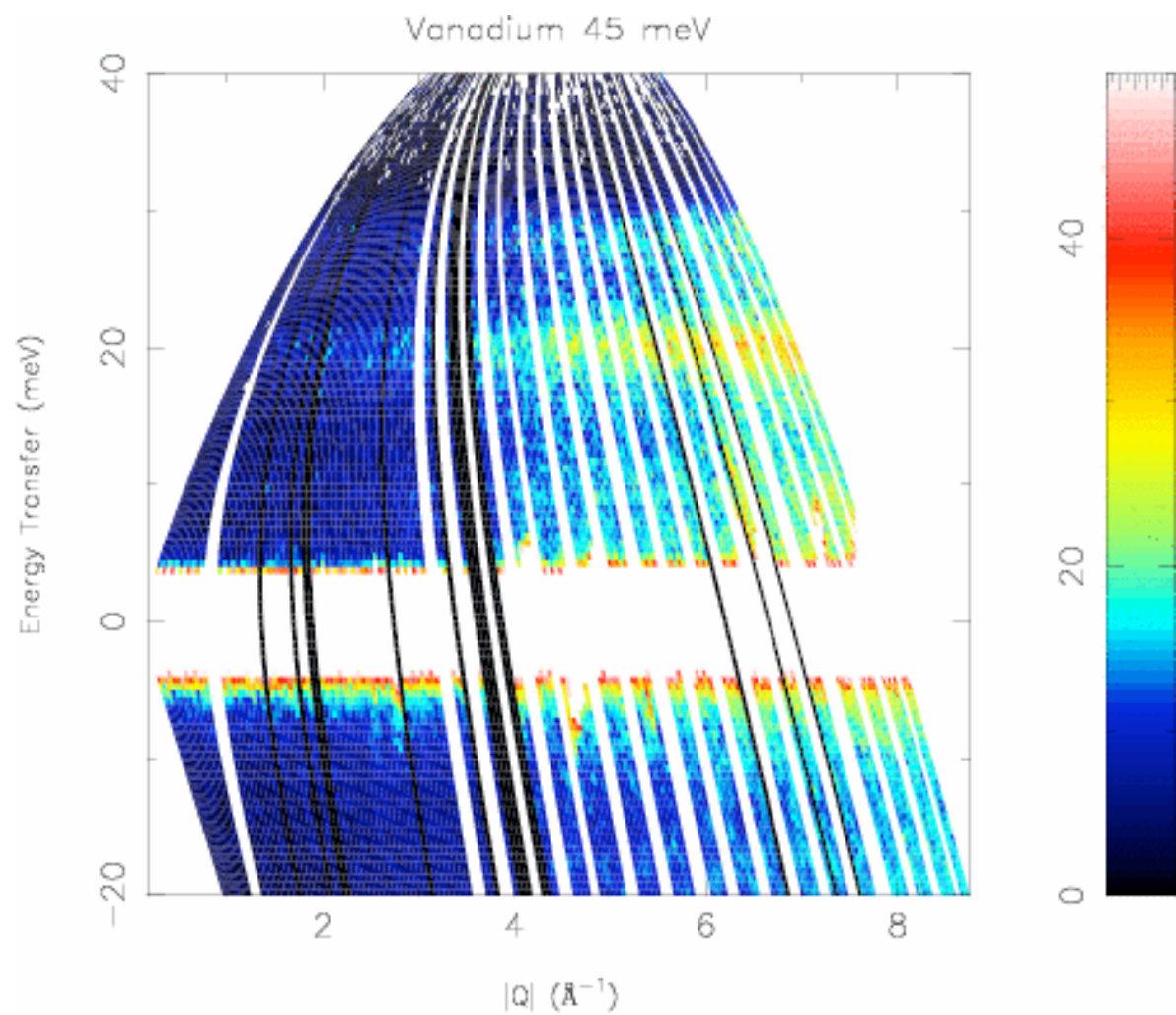
$$S(Q, \omega) = \exp[-2W(Q)] \left[ \delta(\hbar\omega) + \frac{\hbar Q^2}{2M} \frac{Z(\omega)}{\omega} \{n(\omega) + 1\} + \dots \right]$$

Strictly speaking, we measure a sum of the partial densities-of-state of each element weighted by  $\sigma_i/M_i$

# Vanadium: A Perfect Incoherent Scatterer

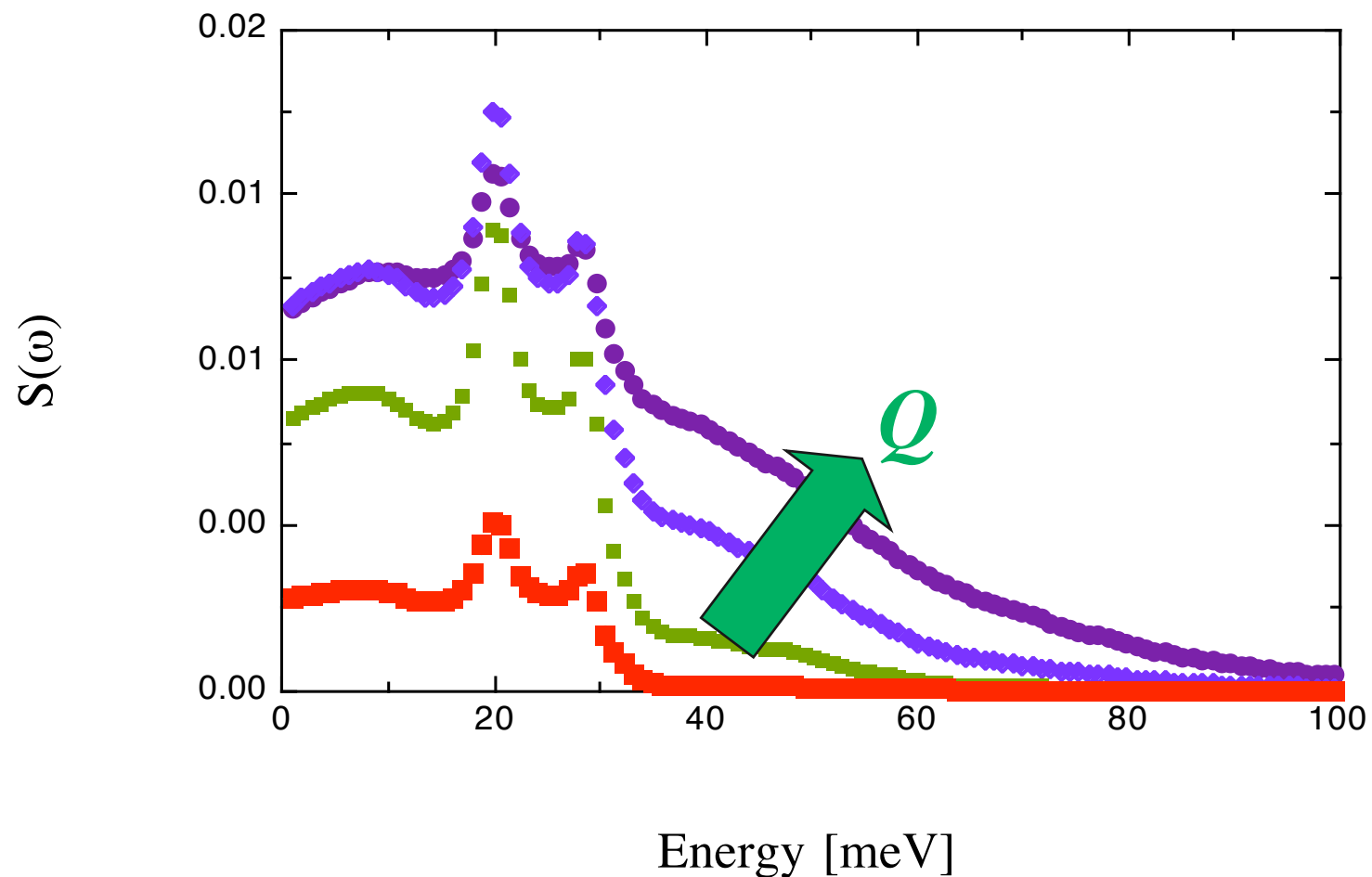
$$S(Q, \omega) = \sum_i \sigma_i \frac{\hbar Q^2}{2M_i} \exp(-2W_i) \frac{Z_i(\omega)}{\omega} [n(\omega) + 1]$$

$$W_i = \frac{1}{2} \langle (\mathbf{Q} \cdot \mathbf{u})^2 \rangle = \frac{\hbar Q^2}{2M_i} \int \frac{Z_i(\omega)}{\omega} [2n_B(\omega) + 1] d\omega$$



# Multi-phonon Scattering

## Vanadium Cross Section



Multi-phonon ( $n > 1$ ) scattering becomes larger with increasing  $Q$ .  
Eventually, the different terms merge into a single recoil peak.

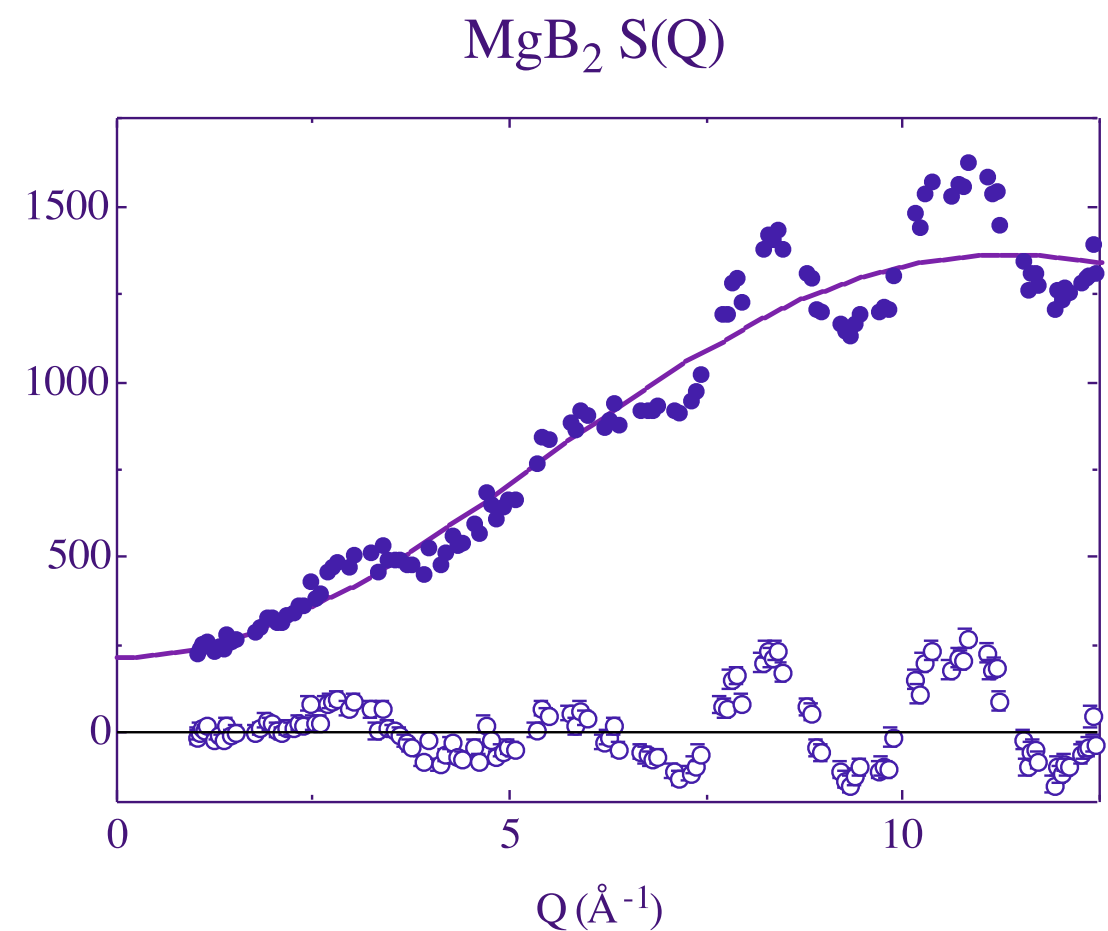
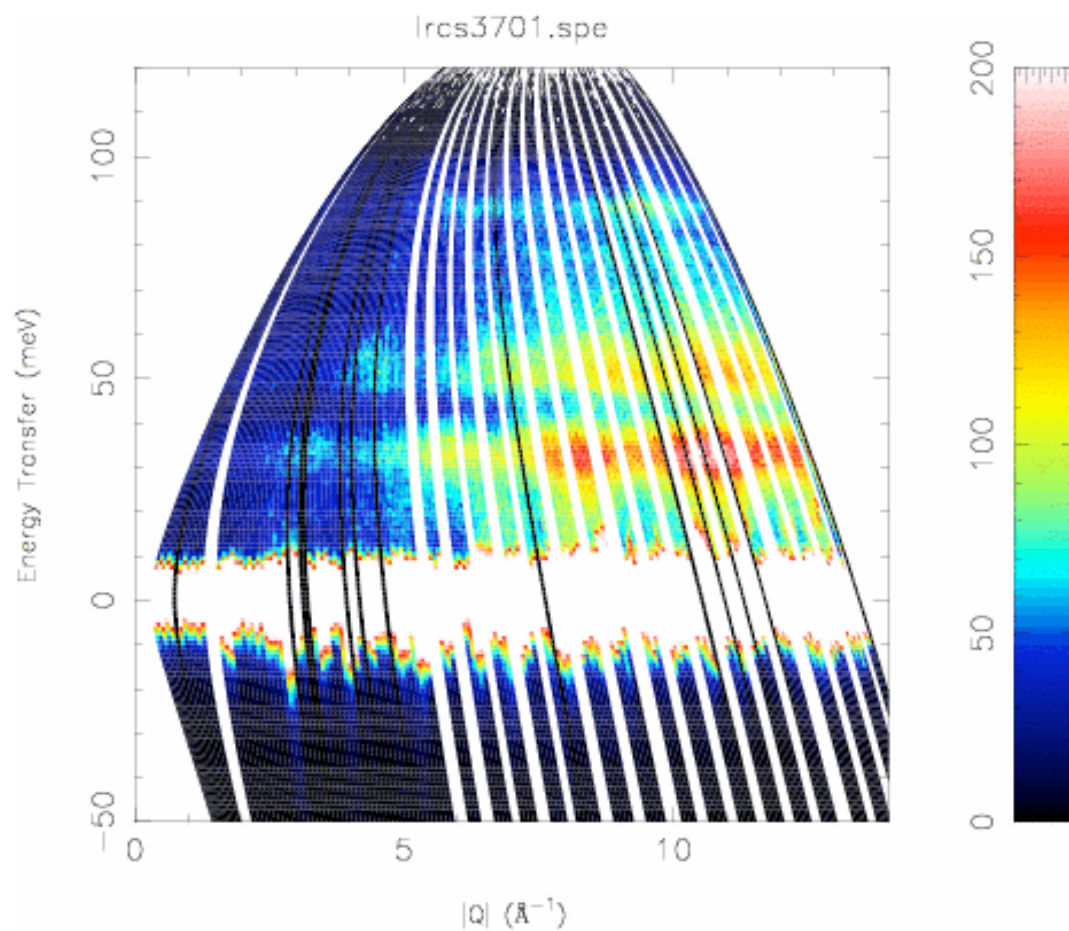
$$\langle \hbar\omega \rangle = \hbar Q^2 / 2M$$

*N.B.*  $S(Q) = \int S(Q, \omega) d\omega = 1$  for all values of  $Q$  (theoretically)

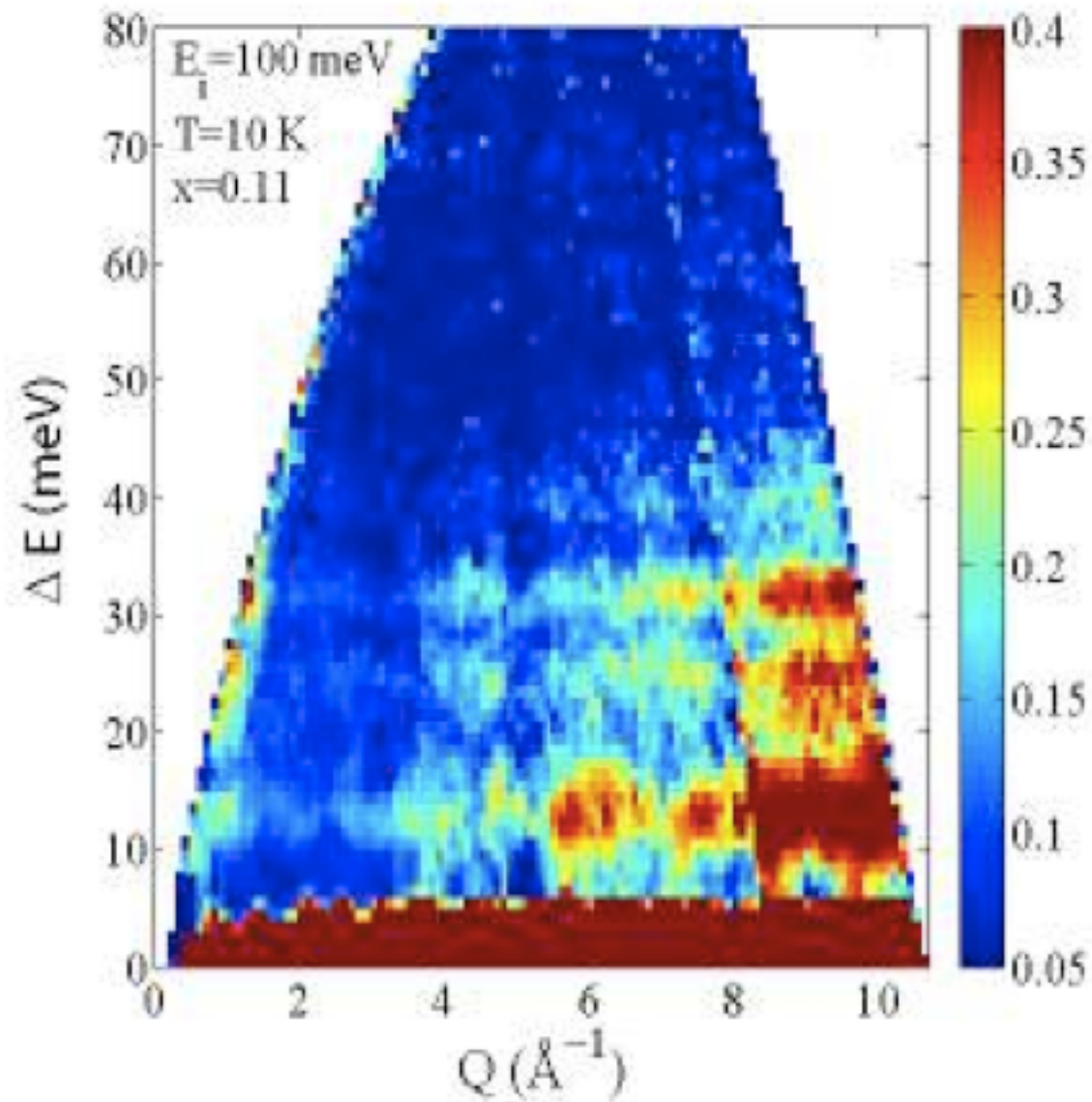
# MgB<sub>2</sub>: A Strongly Coherent Scatterer

- With a coherent scatterer, it is necessary to sum over a wide range of  $Q$  to generate an accurate phonon density-of-states

$$S(Q, \omega) = \exp[-2W(Q)] \left[ \delta(\hbar\omega) + \frac{\hbar Q^2}{2M} \frac{Z(\omega)}{\omega} \{n(\omega) + 1\} + \dots \right]$$

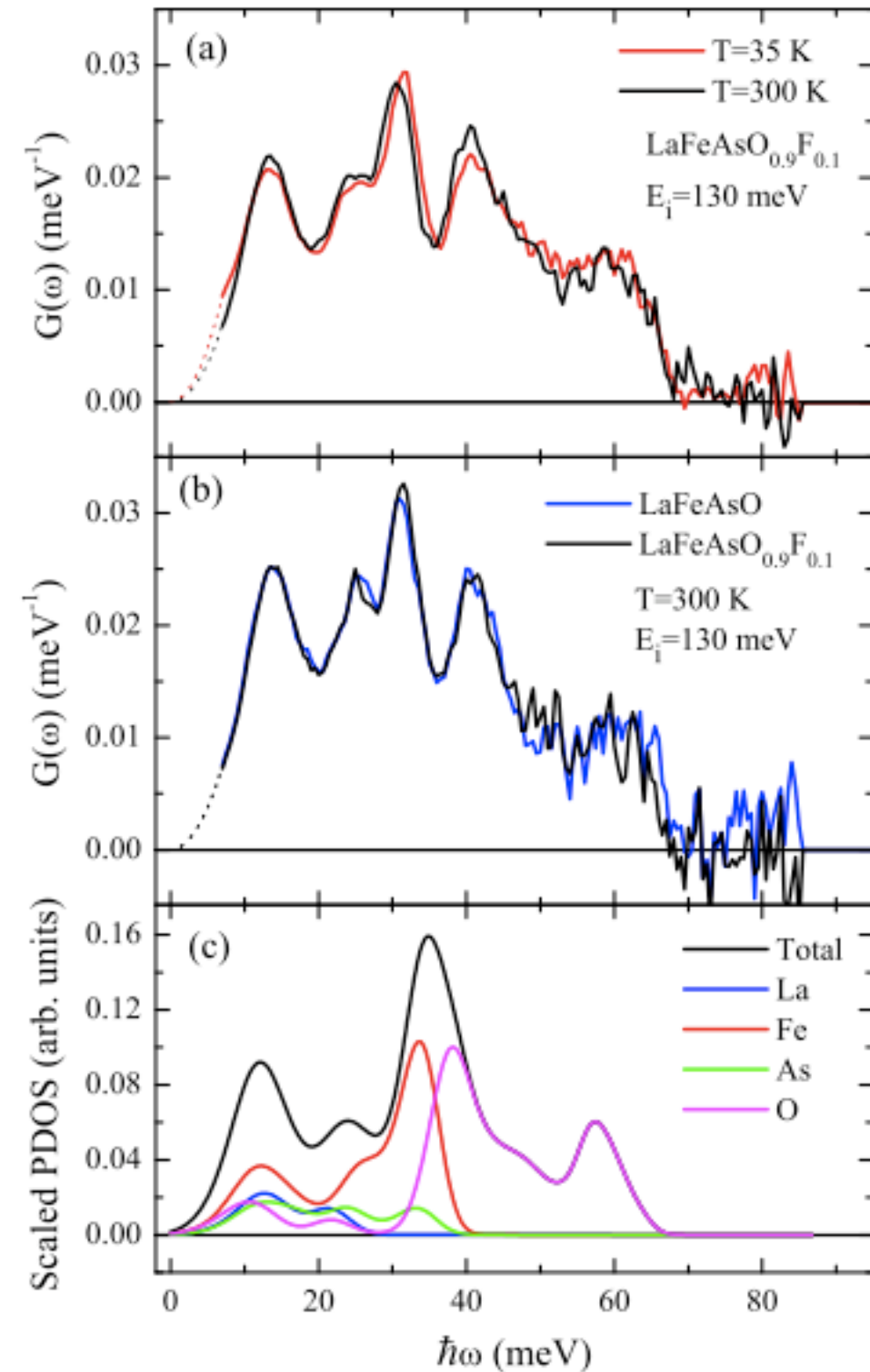


# Phonons in Superconducting $\text{LaFeAsO}_{1-x}\text{F}_x$



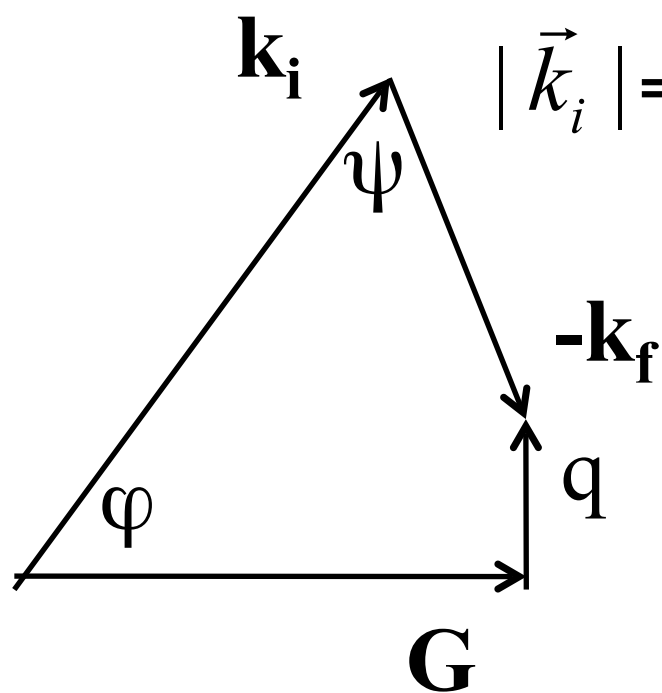
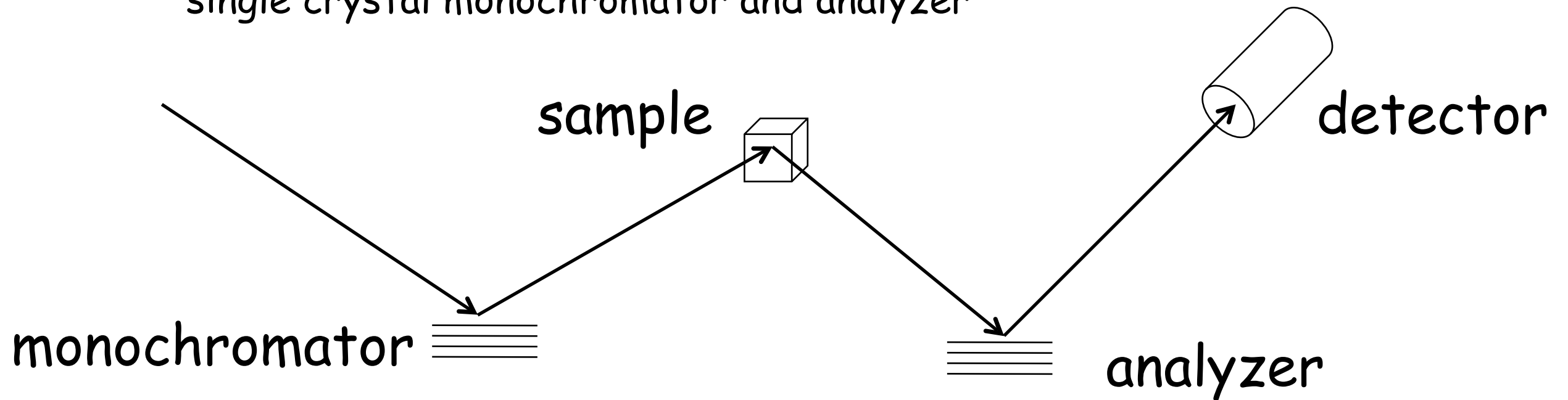
ARCS Data

Christianson et al, PRL to be published



# Triple Axis Spectrometer

Flexible inelastic instrument used at steady state neutron sources, in which  $E_i$ ,  $k_i$  and  $E_f$ ,  $k_f$  are selected by Bragg diffraction from a single crystal monochromator and analyzer

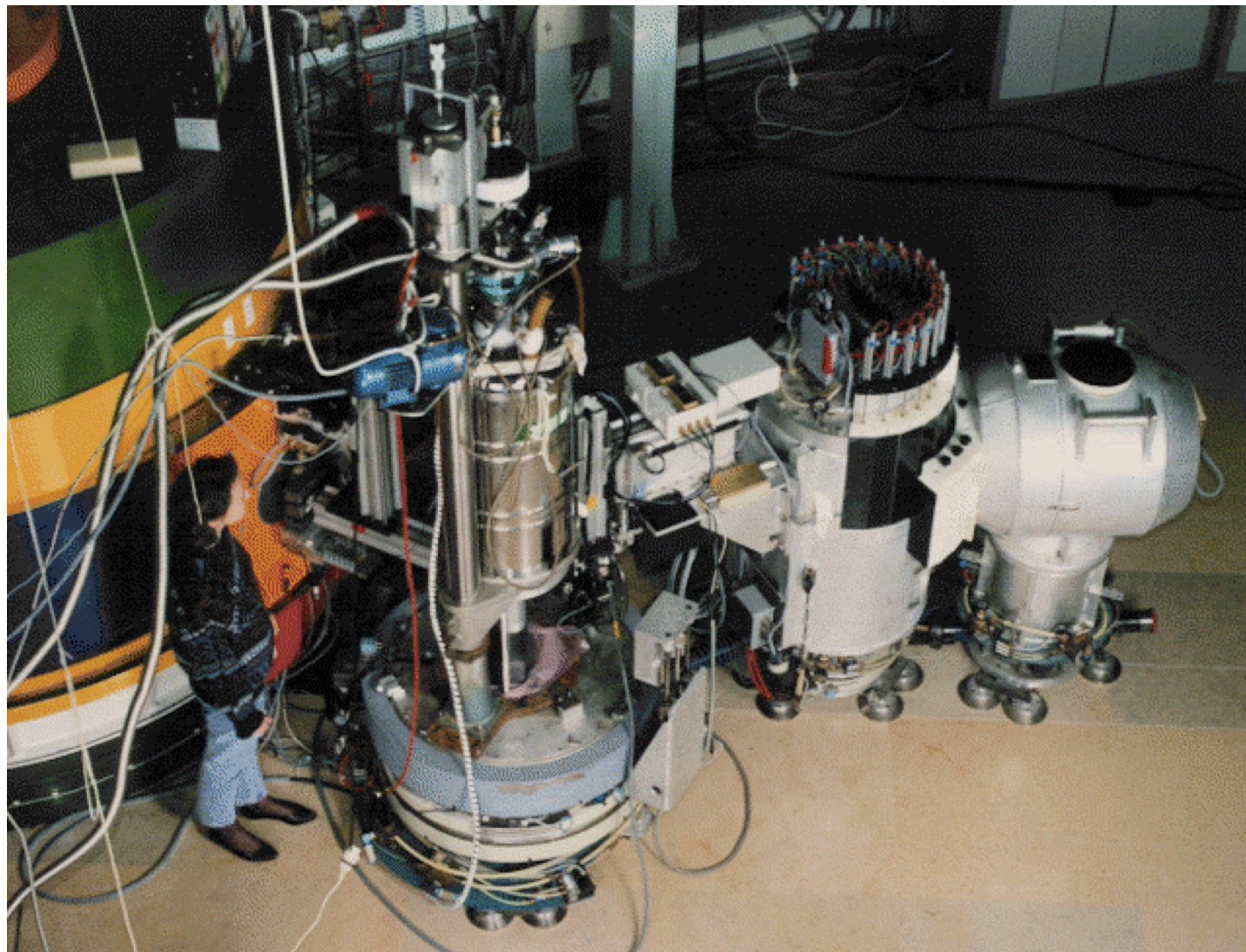


$$|\vec{k}_i| = \frac{\pi}{d_M \sin(\theta_M)}$$

$$|\vec{k}_f| = \frac{\pi}{d_A \sin(\theta_A)}$$

Varying two lengths  $k_i$ ,  $k_f$  and two angles  $\psi$ ,  $\varphi$  allow flexible scans to be chosen, e.g. Constant Q or Constant  $\varepsilon$

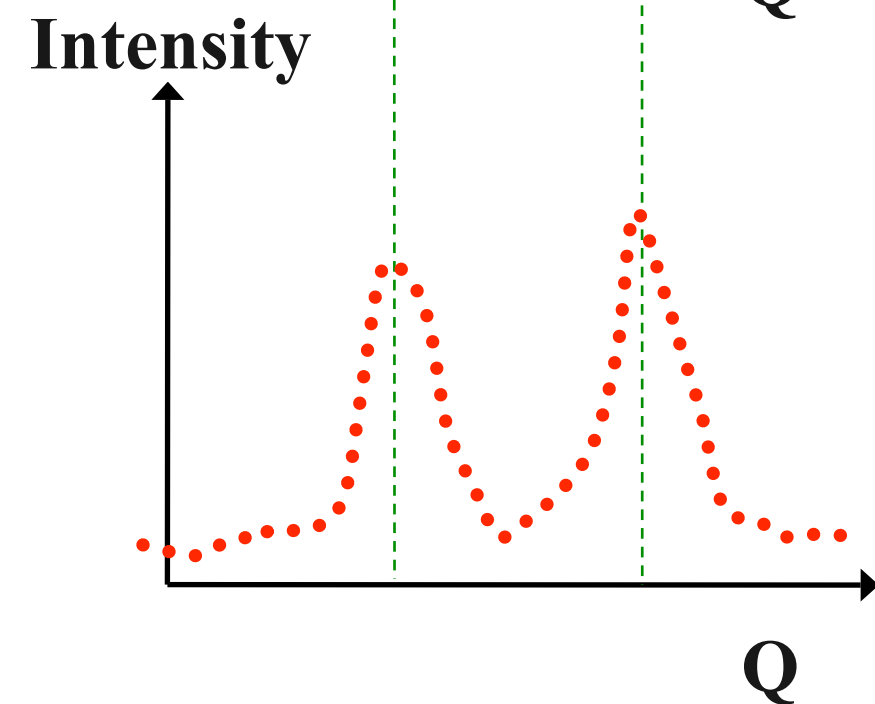
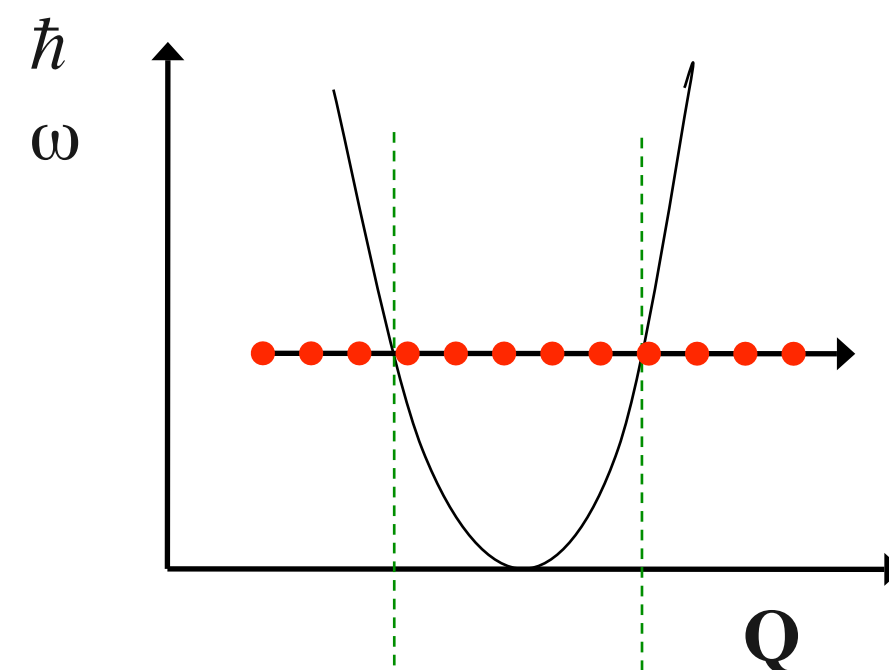
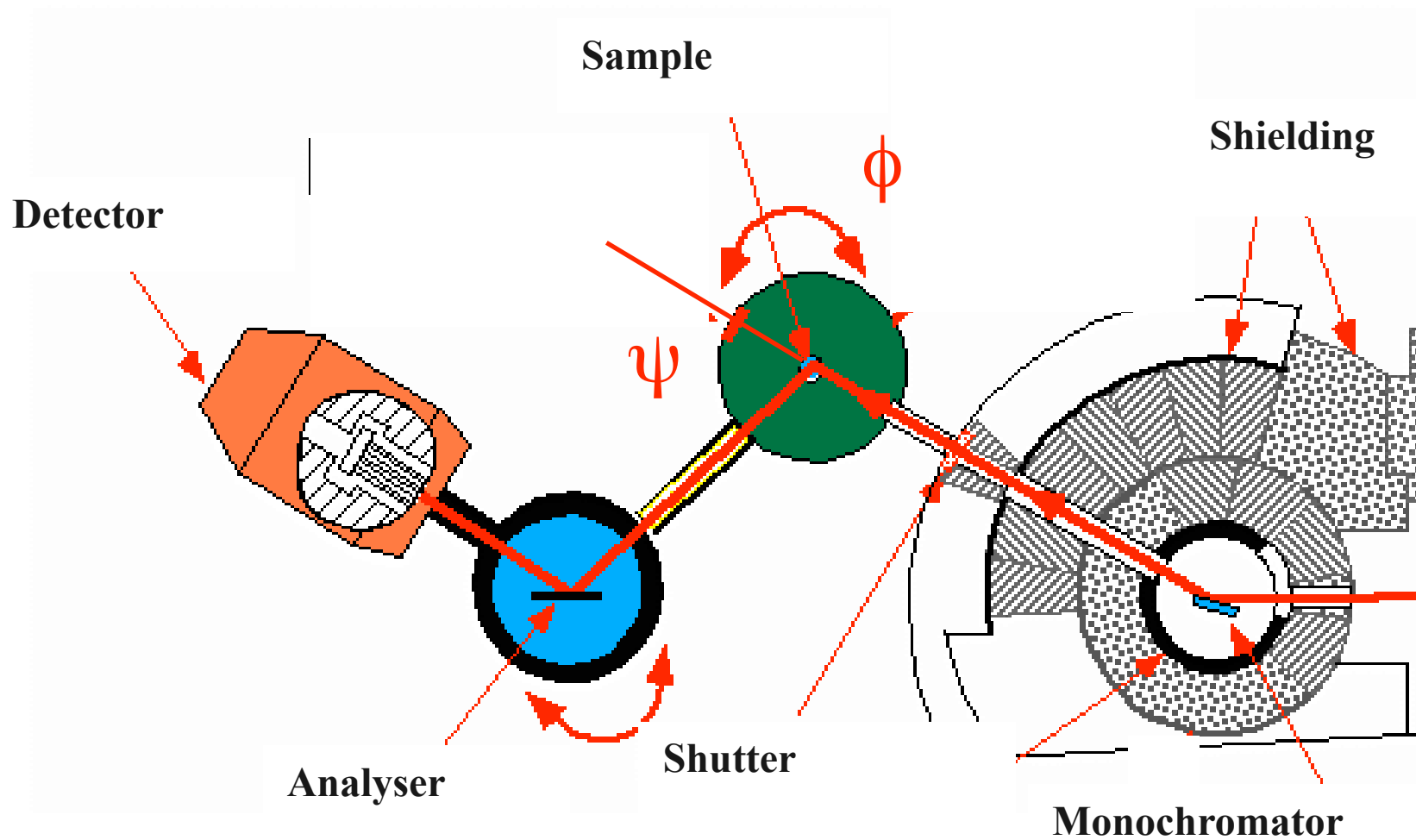
# Triple Axis Spectrometer



- Supreme instrument at a reactor to measure excitations for 40 years
- Every research reactor has one or a suite of TAS optimised for different energy ranges
- Design principles essentially unchanged
- Constantly evolves as technology improves

IN20 (ILL)

# Triple Axis Spectrometer



Monochromator

$$\Rightarrow E_I$$

Analyser

$$\Rightarrow E_F$$

Scattering angle,  $\psi$

$$\Rightarrow |Q|$$

Crystal orientation,  $\phi$

$$\Rightarrow Q$$

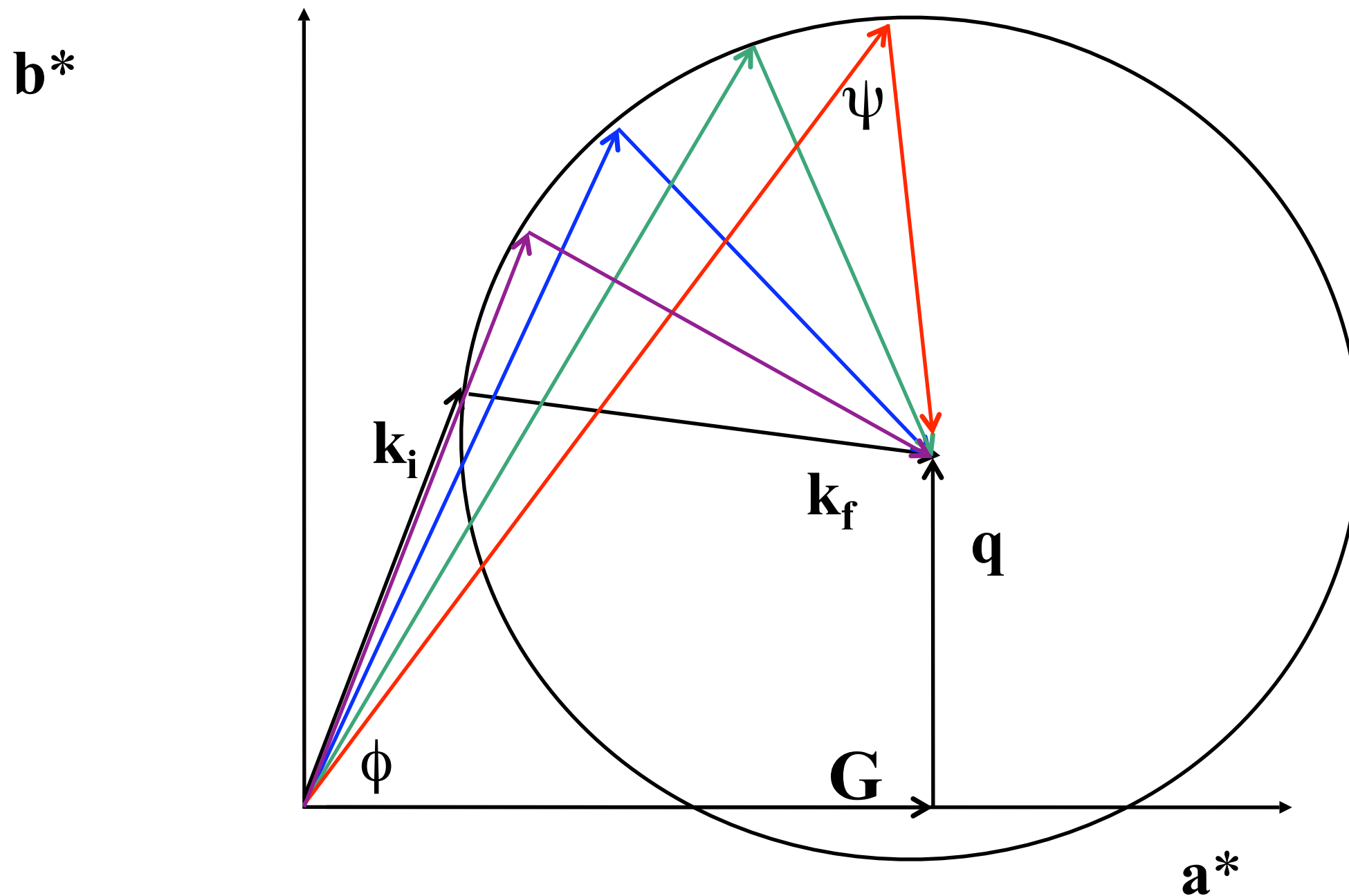
- One point per setting -

**Serial Operation**

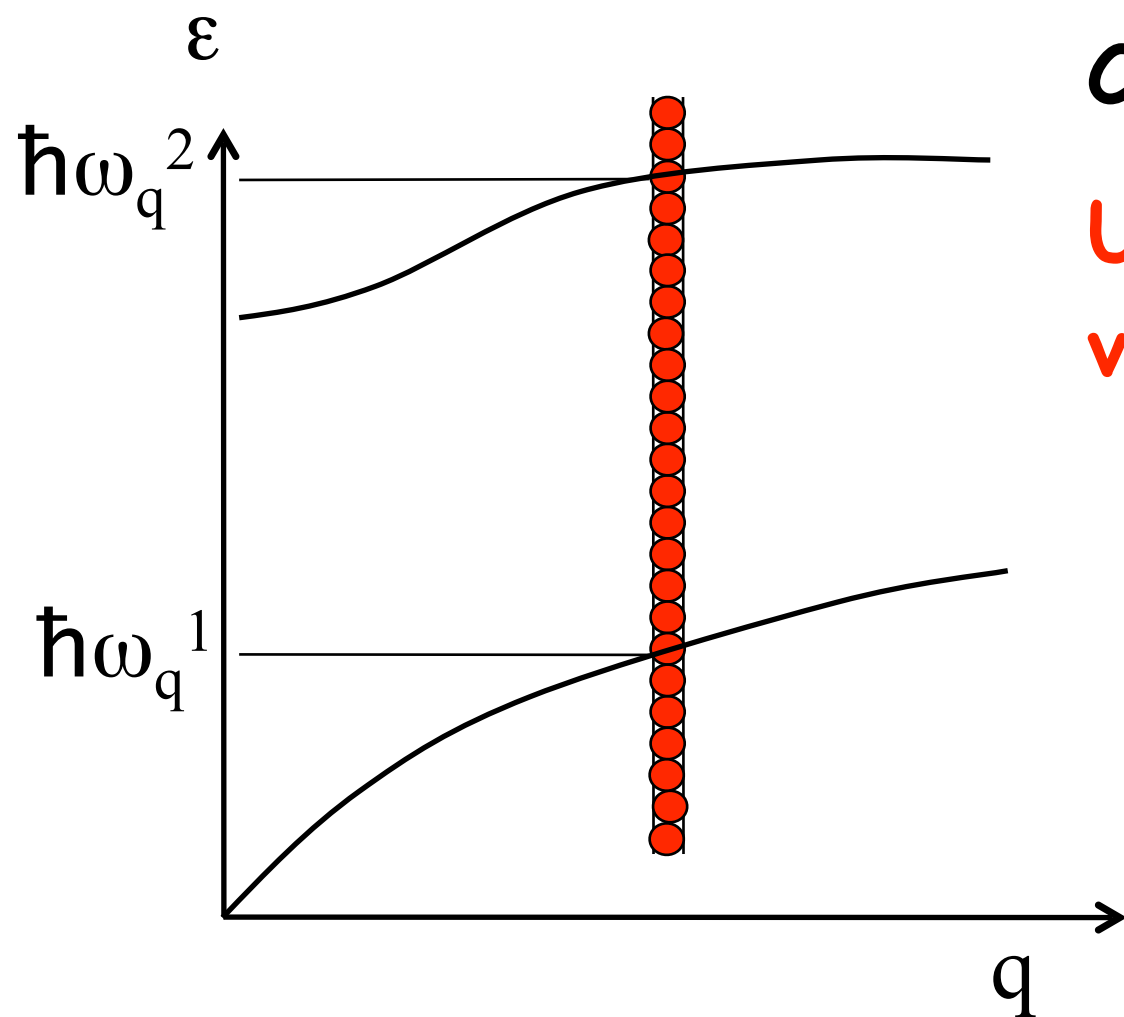
# Constant Q-scans

We have the flexibility to keep  $|k_i|$  or  $|k_f|$  constant.

Below is an example of a constant Q scan with fixed  $|k_f|$ .



# Constant Q and Constant $\epsilon$ Scans

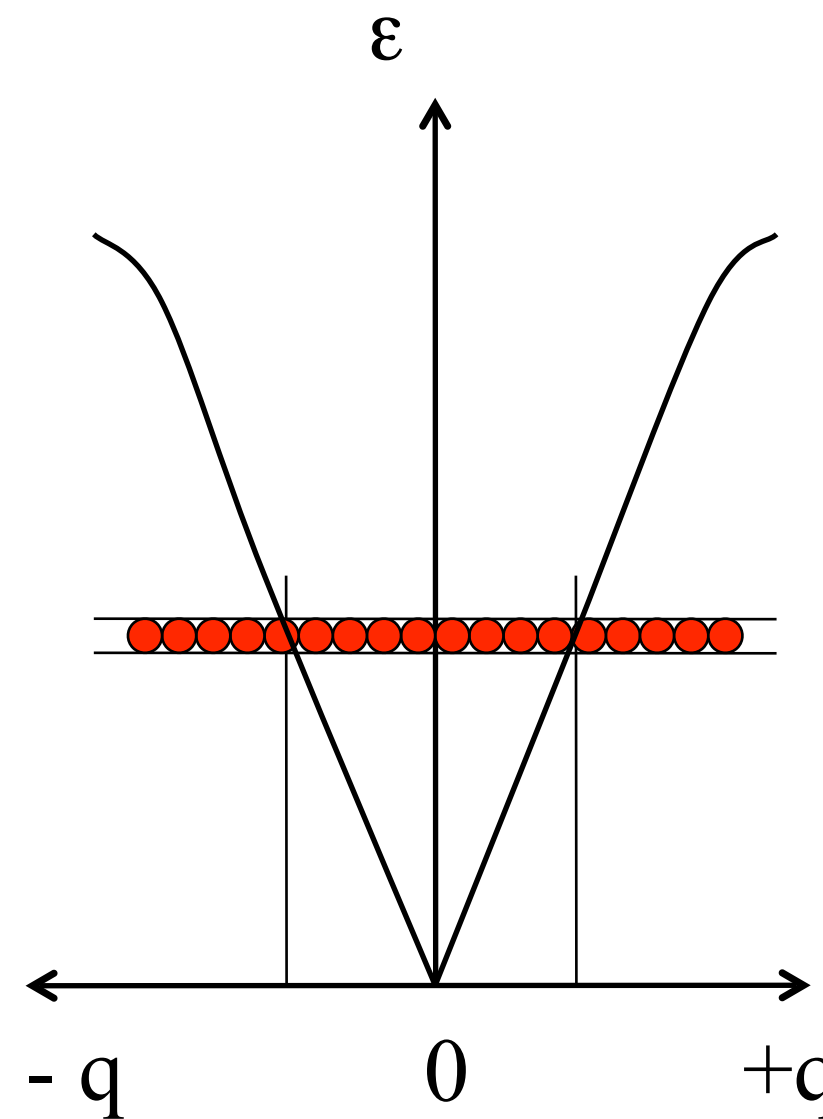


**Constant Q scan**

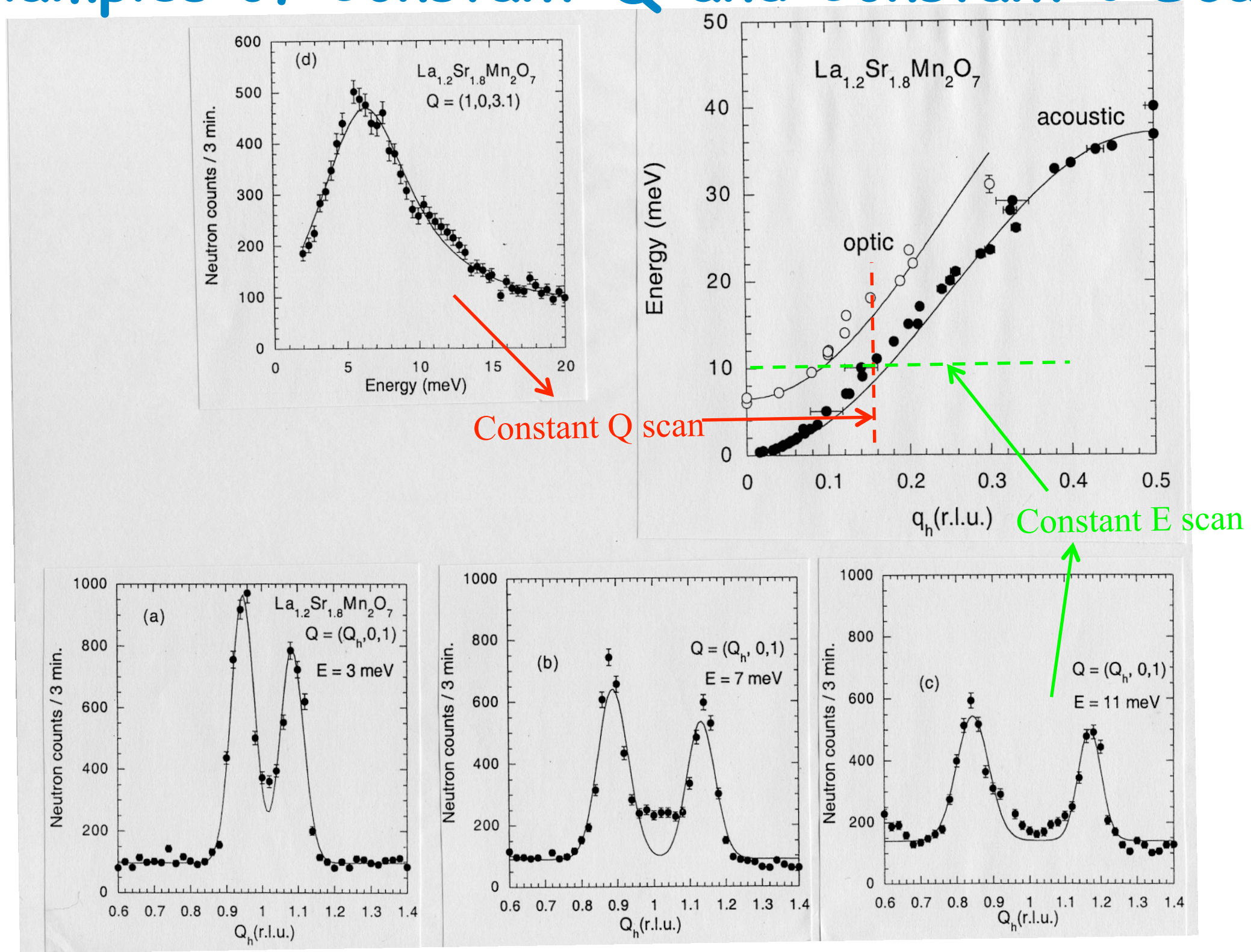
Used to measure slowly varying dispersion relations.

**Constant  $\epsilon$  scan**

Used to measure steep Dispersion relations.



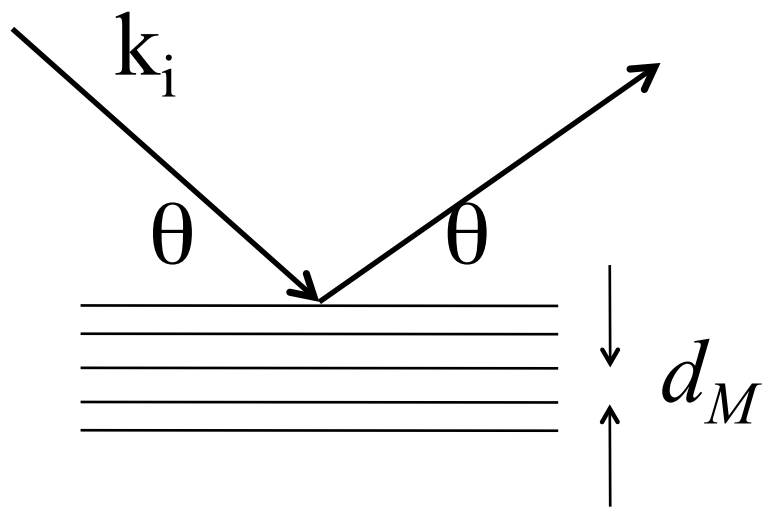
# Examples of Constant Q and Constant $\epsilon$ Scans



# Triple Axis Resolution

Contribution to energy resolution of spectrometer arising from monochromator:

$$\lambda_M = 2d_M \sin(\theta_M)$$



Uncertainty in  $\lambda_M$  due to angular collimation  $\delta\theta$  and fluctuation in plane spacing of crystal  $\delta d_M$  is :

$$\frac{\delta\lambda_M}{\lambda_M} = \sqrt{(\cot(\theta_M) \delta\theta_M)^2 + \left(\frac{\delta d_M}{d_M}\right)^2}$$

The corresponding uncertainties in the energy and the wavevector are

$$\frac{\delta E_i}{E_i} = 2 \frac{\delta\lambda_M}{\lambda_M} \quad \text{and} \quad \frac{\delta k_i}{k_i} = \frac{\delta\lambda_M}{\lambda_M}$$

The analyzer has similar contributions to the uncertainties in  $E_f$  and  $k_f$ .

# Resolution (contd)

The wavelength spreads from monochromator and analyser combine with the angular collimations before and after the sample to produce a four dimensional resolution function for the triple axis  $R(\vec{Q}, \varepsilon)$ . The width of a peak in a scan will be determined by the convolution of the cross section with this resolution function.

$$I(Q_0, \varepsilon_0) = \int R(\vec{Q} - \vec{Q}_0, \varepsilon - \varepsilon_0) \sigma(\vec{Q}, \varepsilon) d\vec{Q} d\varepsilon$$

The form of the resolution function is Gaussian:

$$R(\vec{x}) = R_0 \exp \{ -\vec{x} \vec{M} \vec{x} \}$$

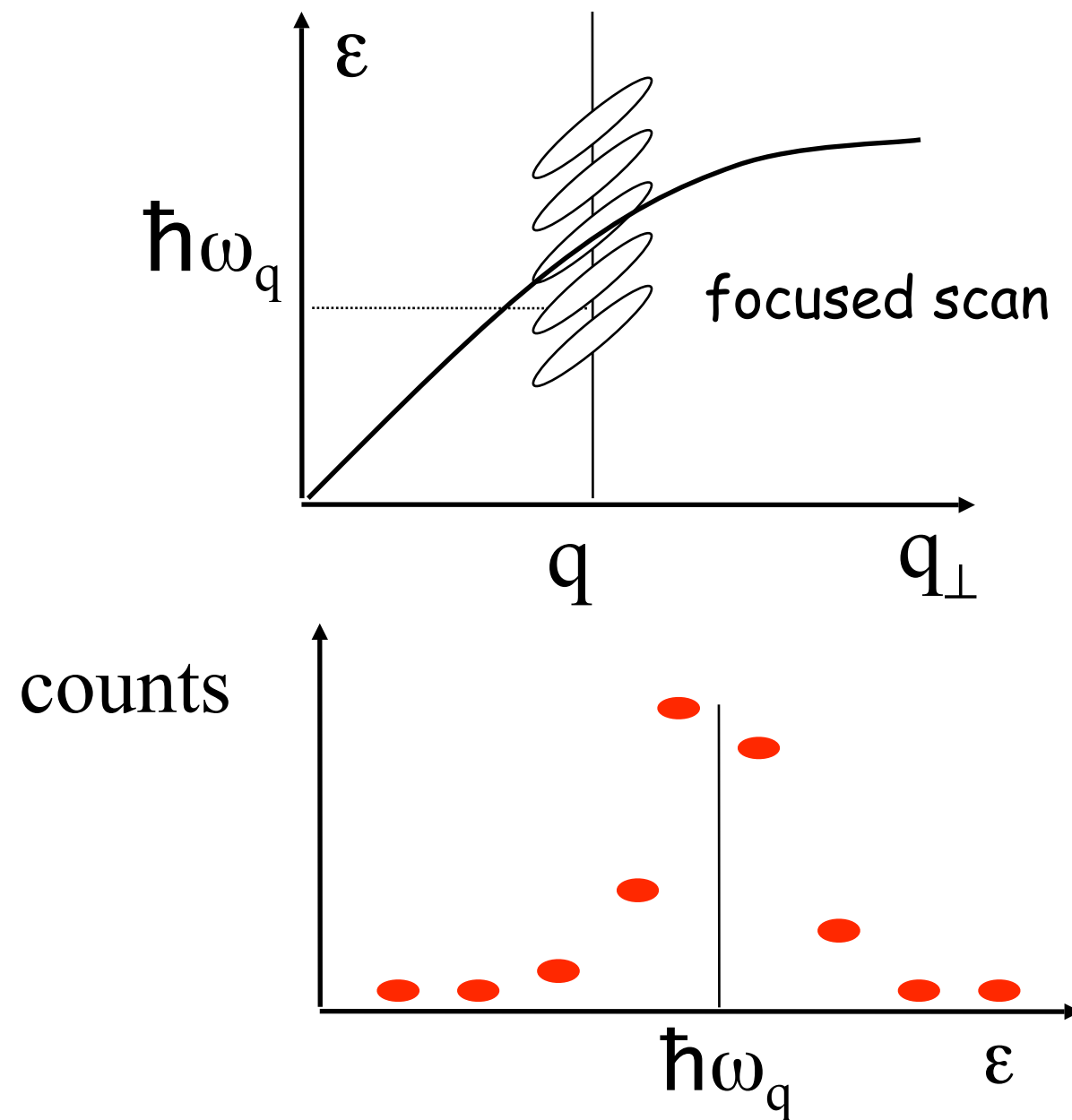
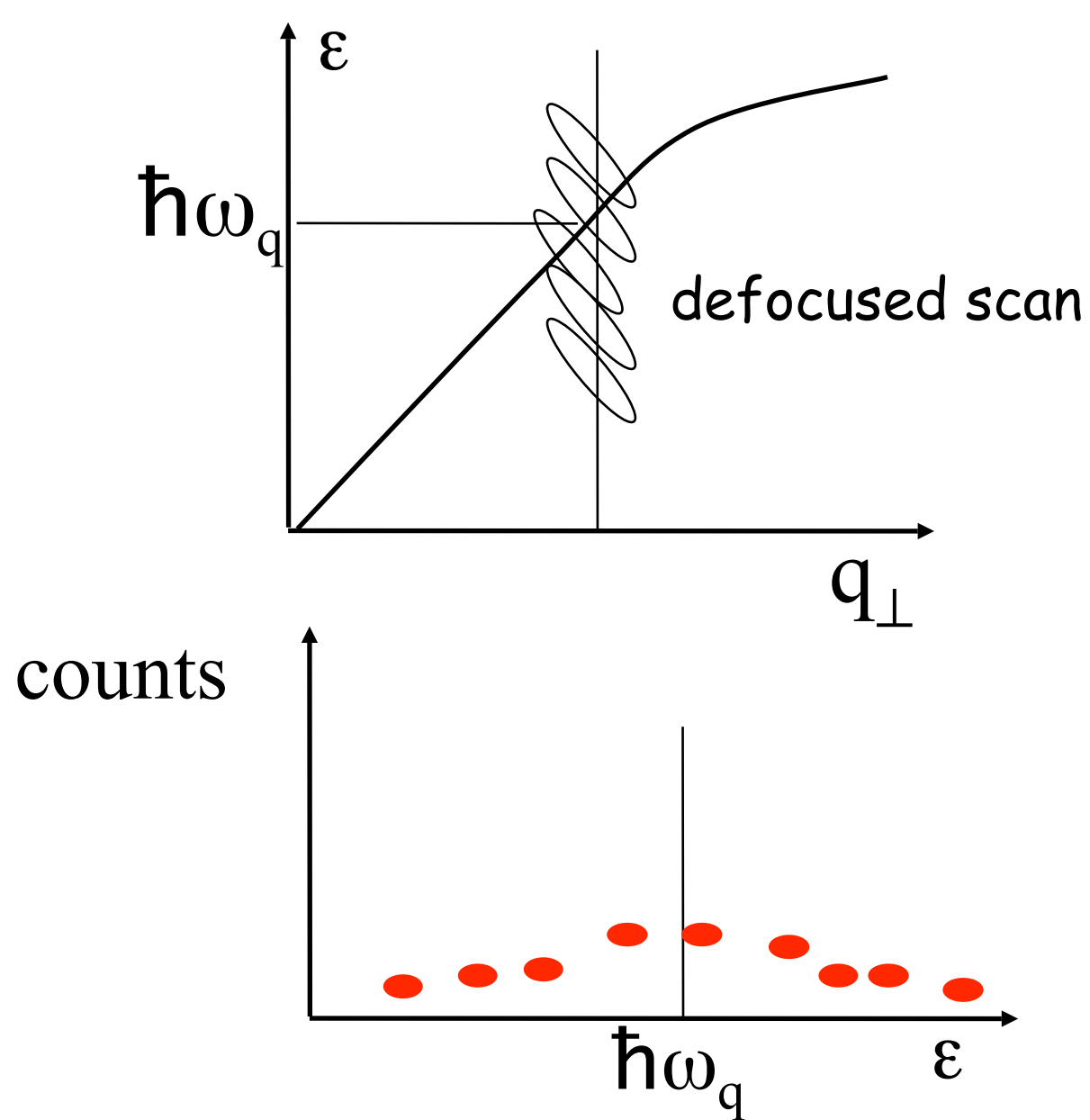
where  $\vec{x}$  denotes a four dimensional vector  $\vec{x} = (\vec{Q}, \varepsilon)$ .

A contour of  $R$  is an ellipsoid in this four dimensional space  $(Q_x, Q_y, Q_z, \varepsilon)$ .

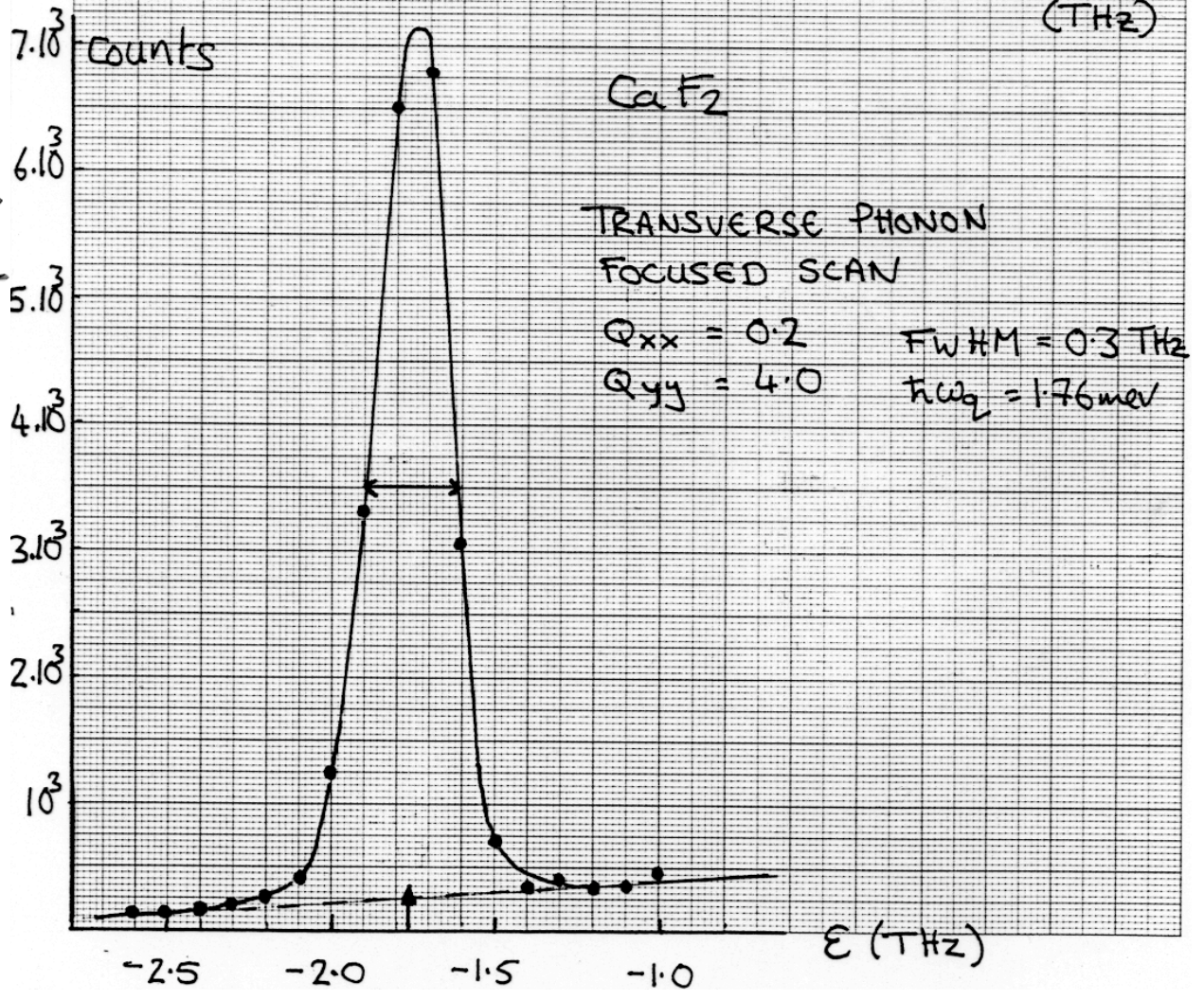
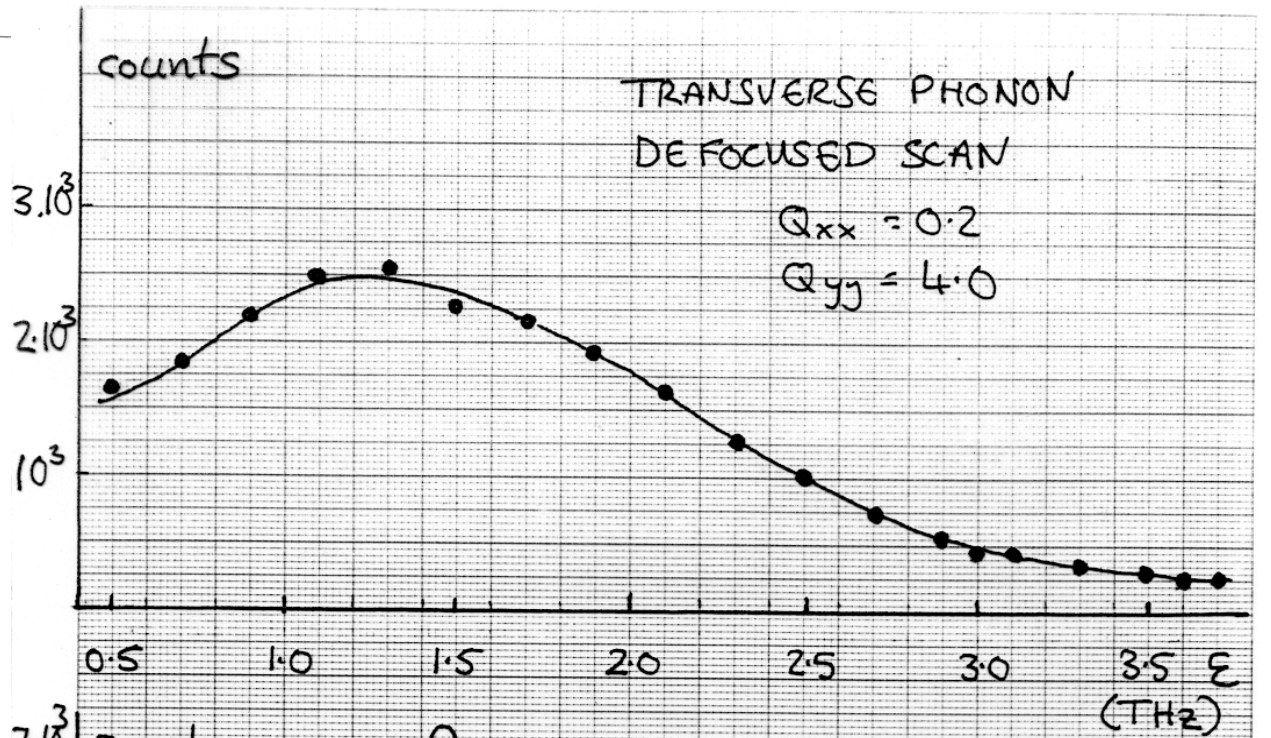
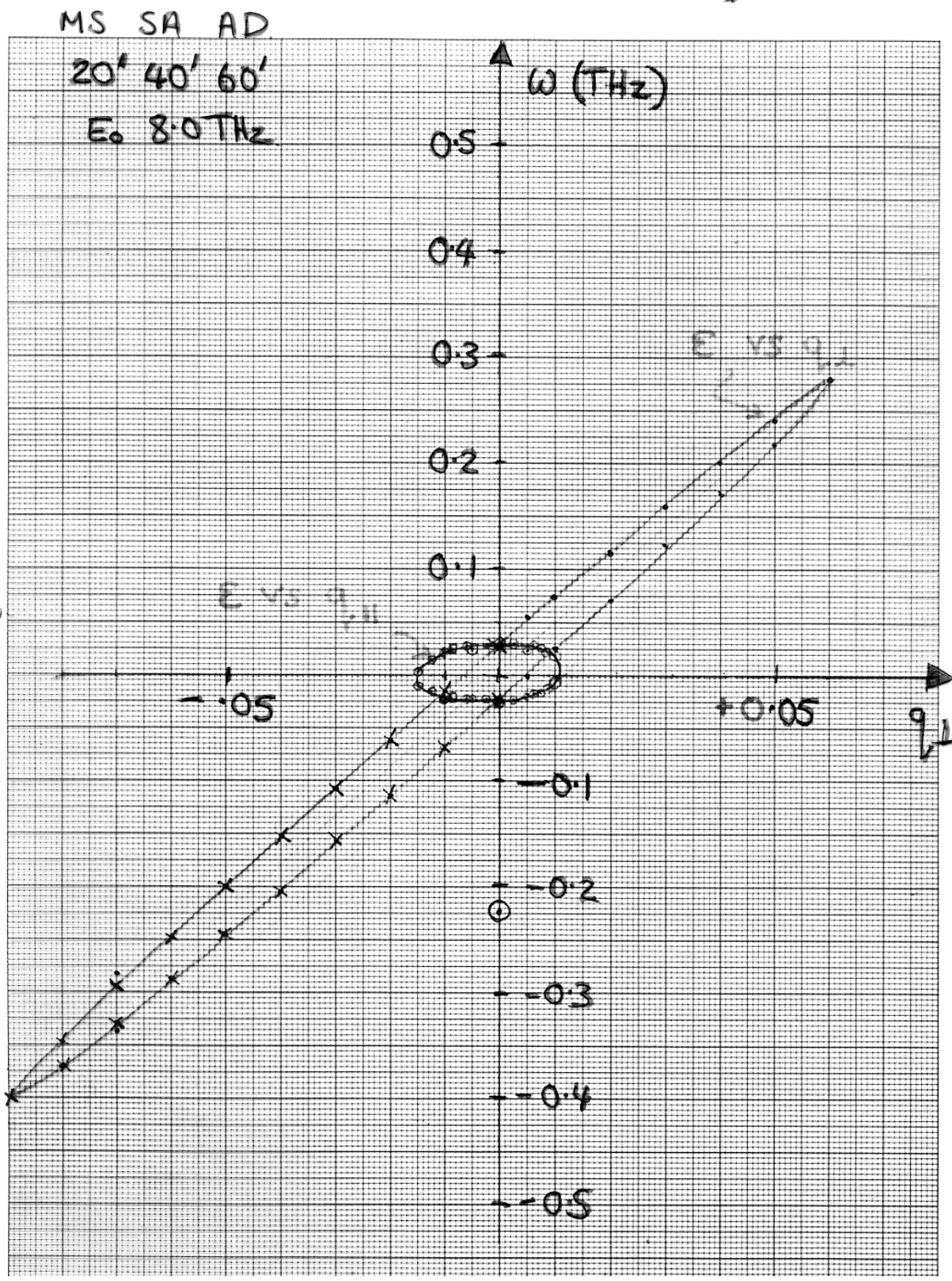
To visualize this we will represent the ellipsoid at its half height contour.

# Focussing in Triple Axis Scans

It turns out that the components of the resolution matrix  $M$  are highly correlated in the  $\varepsilon, q_{\perp}$  plane, where  $q_{\perp}$  is the component of  $q$  perpendicular to the scattering vector  $Q$ . The resolution function can be a very elongated cigar shape in this plane. This can lead to strong focussing effects

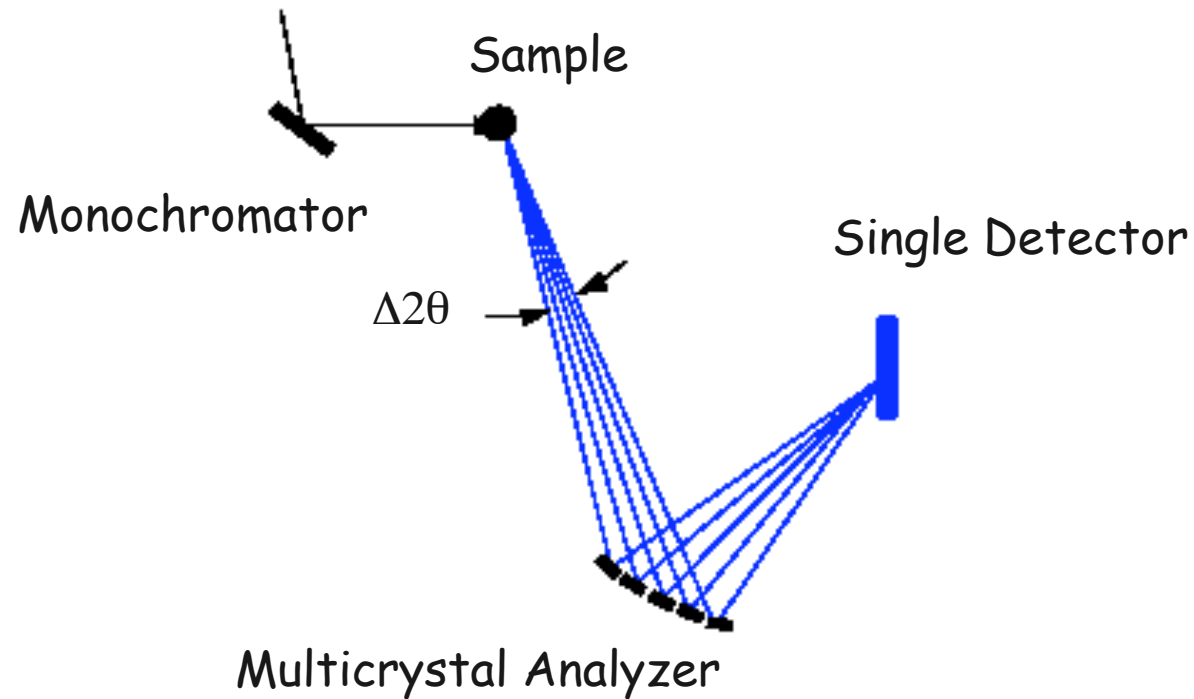


# Resolution function at (220) CaF<sub>2</sub>

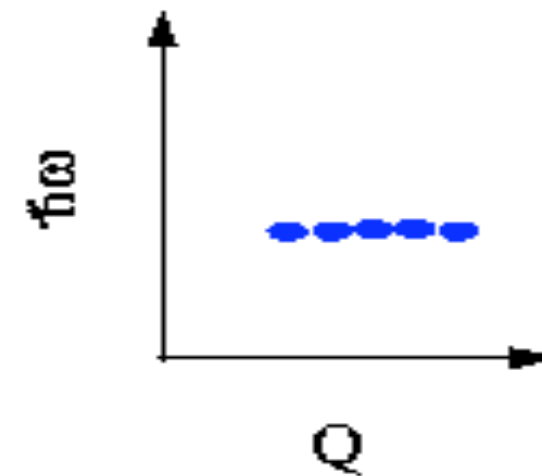


# Beyond the Triple-Axis (SPINS/NIST)

## Multiple Analyzers



## Relaxed Q-resolution



$L$  = distance from sample to HF analyzer

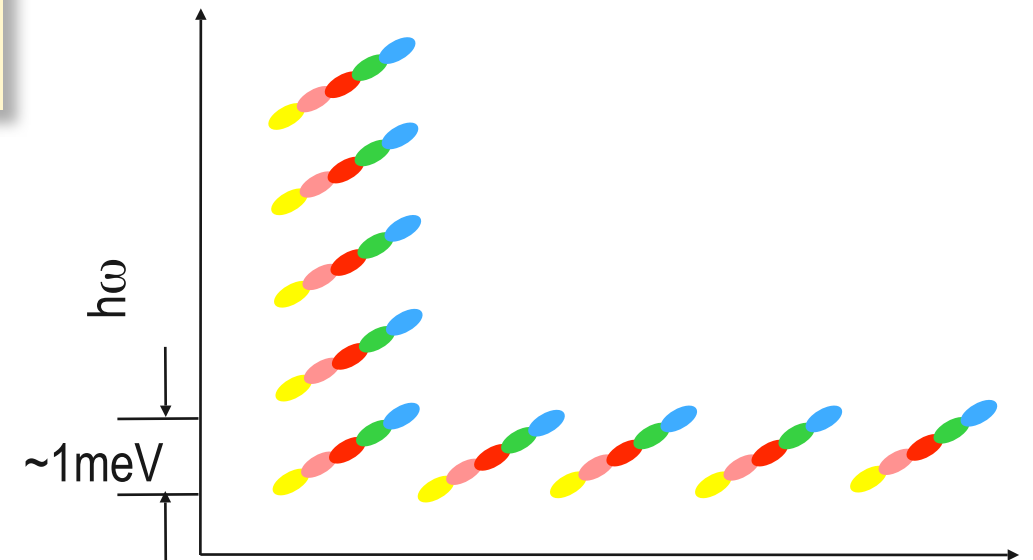
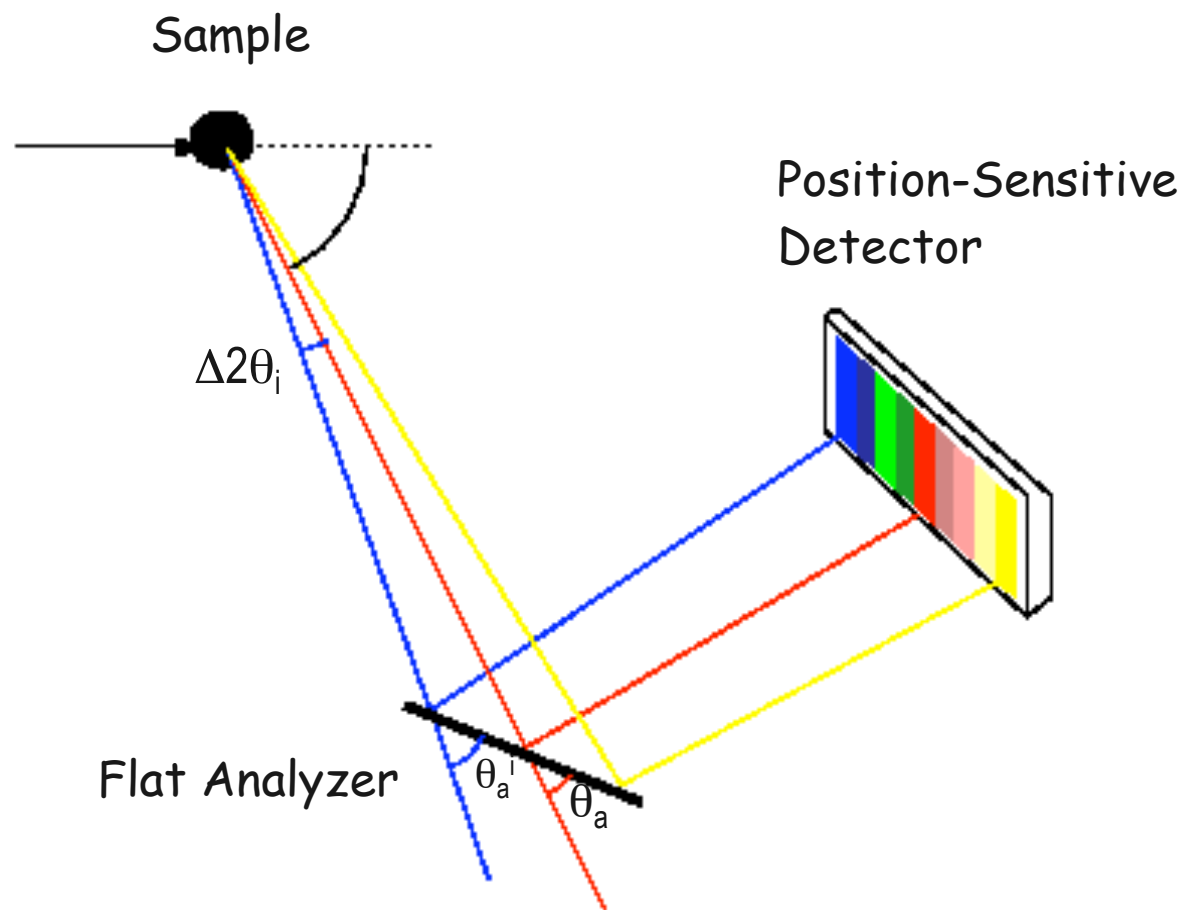
$w_a$  = total width of HF analyzer

$$\Delta 2\theta = w_a \sin\theta_a / L \sim 9 \text{ degree for } E_f = 5 \text{ meV at SPINS}$$

Useful for studying systems with short-range correlations

# Beyond the Triple-Axis (SPINS/NIST)

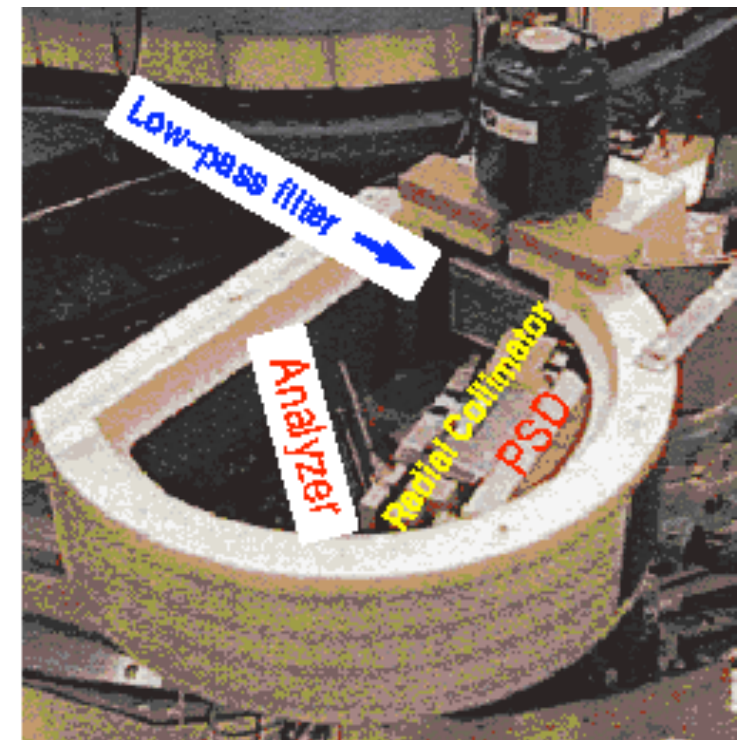
## Position-Sensitive Detectors



$$\theta_a^i = \theta_a + \Delta 2\theta_i = \theta_a - \text{atan}(x \sin\theta_a / (L + x \cos\theta_a))$$
$$k_f^i = \tau_a / 2 \sin\theta_a^i$$
$$Q_i = k - k^i$$

Probes scattering events at different energy and momentum transfers simultaneously

Survey  $(\omega, Q)$  space by changing the incident energy and scattering angle



# Types of TOF Spectrometer

## ■ Direct Geometry

- Fix incident energy with a chopper or crystal monochromator
- Determine final energy from total neutron time-of-flight

*e.g.* PHAROS, LRMECS, HRMECS, HET, MARI, MAPS, INC,  
(ARCS, SEQUOIA, HYSPEC, CNCS...), IN4, IN5, IN6, DCS,  
FOCUS

## ■ Indirect Geometry

- Fix final energy with crystal analyzers
- Determine incident energy from total neutron time-of-flight

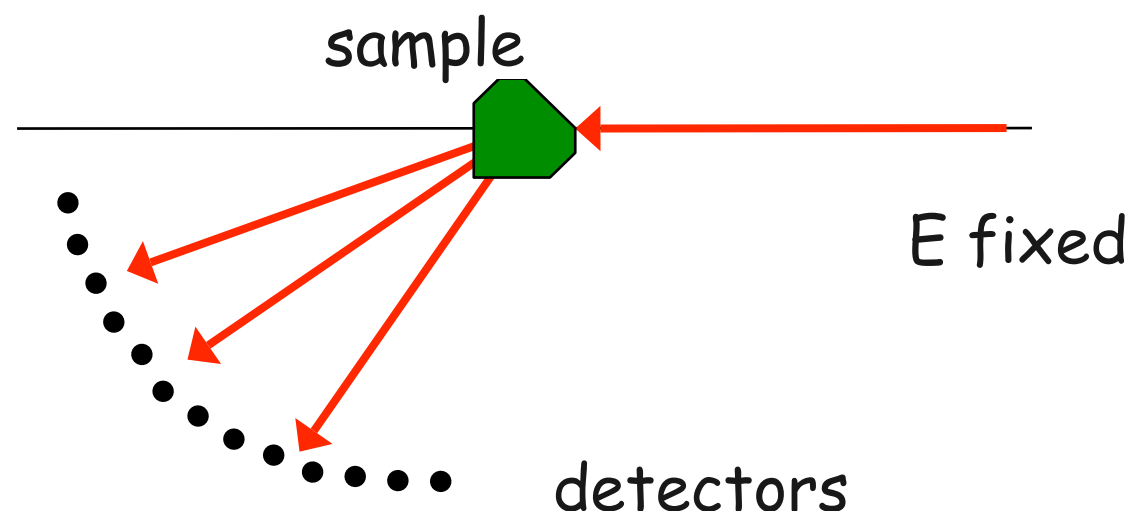
*e.g.* QENS, IRIS, OSIRIS, LAM80  
(SNS Backscattering Spectrometer...)  
IN10, IN13, NG2

# Direct Geometry vs Indirect Geometry

## Direct geometry

- Fixed incident energy
- All final energies

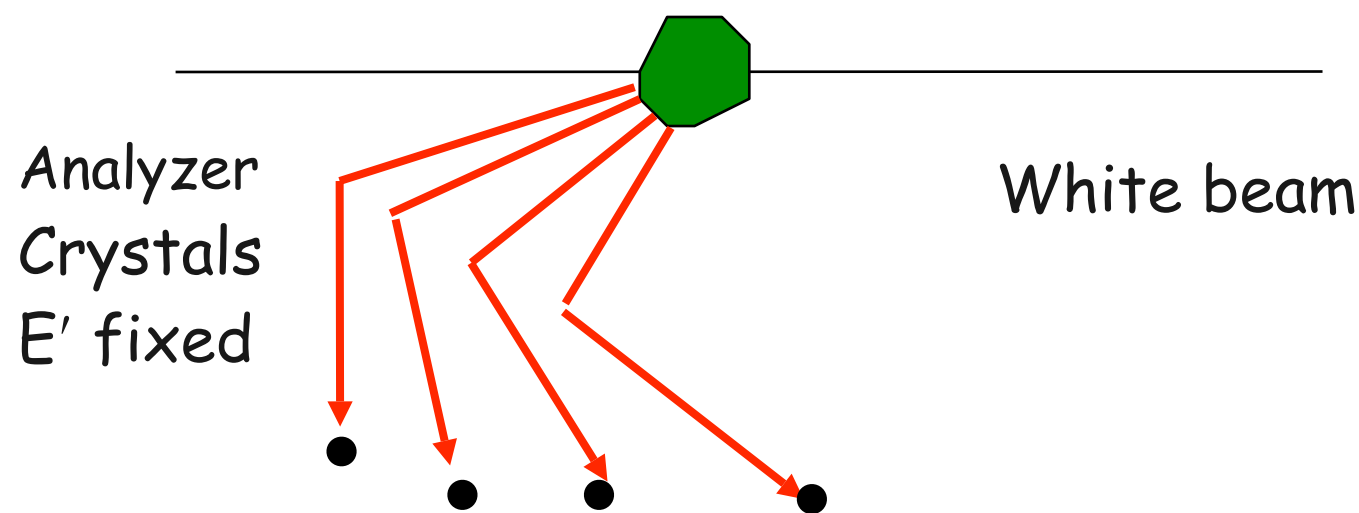
$$\rightarrow -\infty < \hbar\omega < E$$



## Indirect geometry

- All incident energies E
- Fixed final energy E'

$$\rightarrow -E' < \hbar\omega < \infty$$



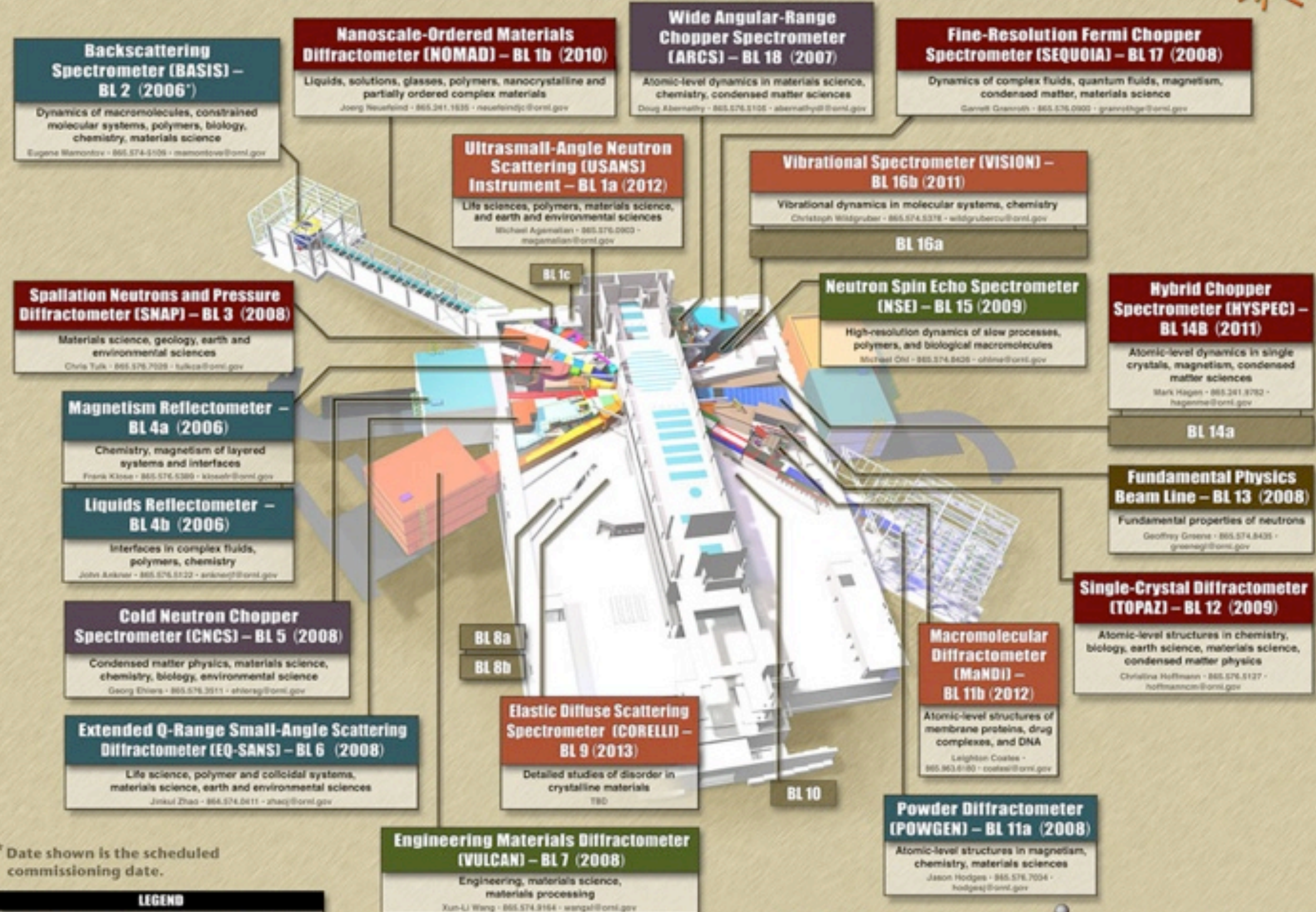
Intrinsically parallel operation

## Simultaneously measure:

- Wide range of energy transfer
- Large number of detectors

→ maps of scattering intensity

# Spallation Neutron Source



**Backscattering Spectrometer (BASIS) – BL 2 (2006\*)**  
 Dynamics of macromolecules, constrained molecular systems, polymers, biology, chemistry, materials science  
 Eugene Mamontov - 865.574.3106 - mamontov@ornl.gov

**Nanoscale-Ordered Materials Diffractometer (NOMAD) – BL 1b (2010)**  
 Liquids, solutions, glasses, polymers, nanocrystalline and partially ordered complex materials  
 Joerg Neufeld - 865.574.1635 - neufeldj@ornl.gov

**Wide Angular-Range Chopper Spectrometer (ARCS) – BL 18 (2007)**  
 Atomic-level dynamics in materials science, chemistry, condensed matter sciences  
 Doug Abernathy - 865.576.5106 - abernathyd@ornl.gov

**Fine-Resolution Fermi Chopper Spectrometer (SEQUOIA) – BL 17 (2008)**  
 Dynamics of complex fluids, quantum fluids, magnetism, condensed matter, materials science  
 Garrett Granroth - 865.576.0900 - granrothg@ornl.gov

**Ultra-small-Angle Neutron Scattering (USANS) Instrument – BL 1a (2012)**  
 Life sciences, polymers, materials science, and earth and environmental sciences  
 Michael Agamalian - 865.576.0900 - magamalian@ornl.gov

**Vibrational Spectrometer (VISION) – BL 16b (2011)**  
 Vibrational dynamics in molecular systems, chemistry  
 Christoph Wildgruber - 865.574.5376 - wildgruberu@ornl.gov

**Spallation Neutrons and Pressure Diffractometer (SNAP) – BL 3 (2008)**  
 Materials science, geology, earth and environmental sciences  
 Chris Tulk - 865.576.7028 - tulkca@ornl.gov

**Neutron Spin Echo Spectrometer (NSE) – BL 15 (2009)**  
 High-resolution dynamics of slow processes, polymers, and biological macromolecules  
 Michael Chi - 865.574.8426 - chi@ornl.gov

**Hybrid Chopper Spectrometer (HYSPEC) – BL 14b (2011)**  
 Atomic-level dynamics in single crystals, magnetism, condensed matter sciences  
 Mark Hagen - 865.574.5782 - hagenm@ornl.gov

**Magnetism Reflectometer – BL 4a (2006)**  
 Chemistry, magnetism of layered systems and interfaces  
 Frank Klöser - 865.576.5389 - kloeserf@ornl.gov

**Liquids Reflectometer – BL 4b (2006)**  
 Interfaces in complex fluids, polymers, chemistry  
 John Arltner - 865.576.5122 - arltnerj@ornl.gov

**Fundamental Physics Beam Line – BL 13 (2008)**  
 Fundamental properties of neutrons  
 Geoffrey Greene - 865.574.8426 - greenej@ornl.gov

**Cold Neutron Chopper Spectrometer (CNCS) – BL 5 (2008)**  
 Condensed matter physics, materials science, chemistry, biology, environmental science  
 Georg Ehlers - 865.576.2911 - ehlersg@ornl.gov

**Extended Q-Range Small-Angle Scattering Diffractometer (EQ-SANS) – BL 6 (2008)**  
 Life science, polymer and colloidal systems, materials science, earth and environmental sciences  
 Jinkui Zhao - 865.574.0611 - zhaoj@ornl.gov

BL 8a  
BL 8b

**Elastic Diffuse Scattering Spectrometer (CORELLI) – BL 9 (2013)**  
 Detailed studies of disorder in crystalline materials  
 TBD

**Macromolecular Diffractometer (MaNDI) – BL 11b (2012)**  
 Atomic-level structures of membrane proteins, drug complexes, and DNA  
 Leighton Coates - 865.963.6180 - coatesl@ornl.gov

**Single-Crystal Diffractometer (TOPAZ) – BL 12 (2009)**  
 Atomic-level structures in chemistry, biology, earth science, materials science, condensed matter physics  
 Christina Hoffmann - 865.576.5127 - hoffmanncc@ornl.gov

**Engineering Materials Diffractometer (VULCAN) – BL 7 (2008)**  
 Engineering, materials science, materials processing  
 Xun-Li Wang - 865.574.9164 - wangxl@ornl.gov

**Powder Diffractometer (POWGEN) – BL 11a (2008)**  
 Atomic-level structures in magnetism, chemistry, materials sciences  
 Jason Hodges - 865.576.7004 - hodgesj@ornl.gov

\* Date shown is the scheduled commissioning date.

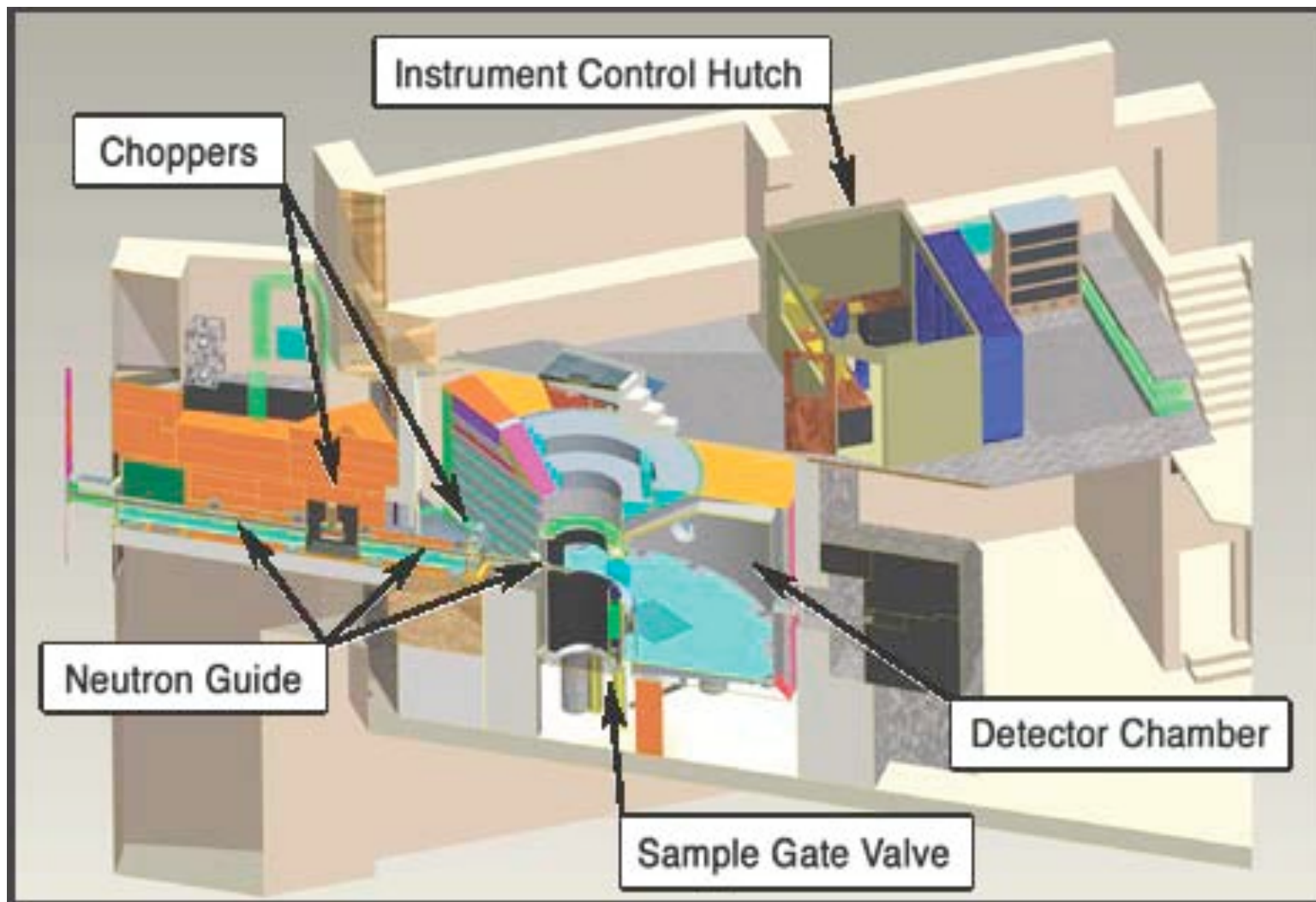
LEGEND		
	SNS TPC	
	DOE Grant	
	SNS I	
	DOE NP	
	SNS II	
	Non U.S.	



NEUTRON SCIENCES

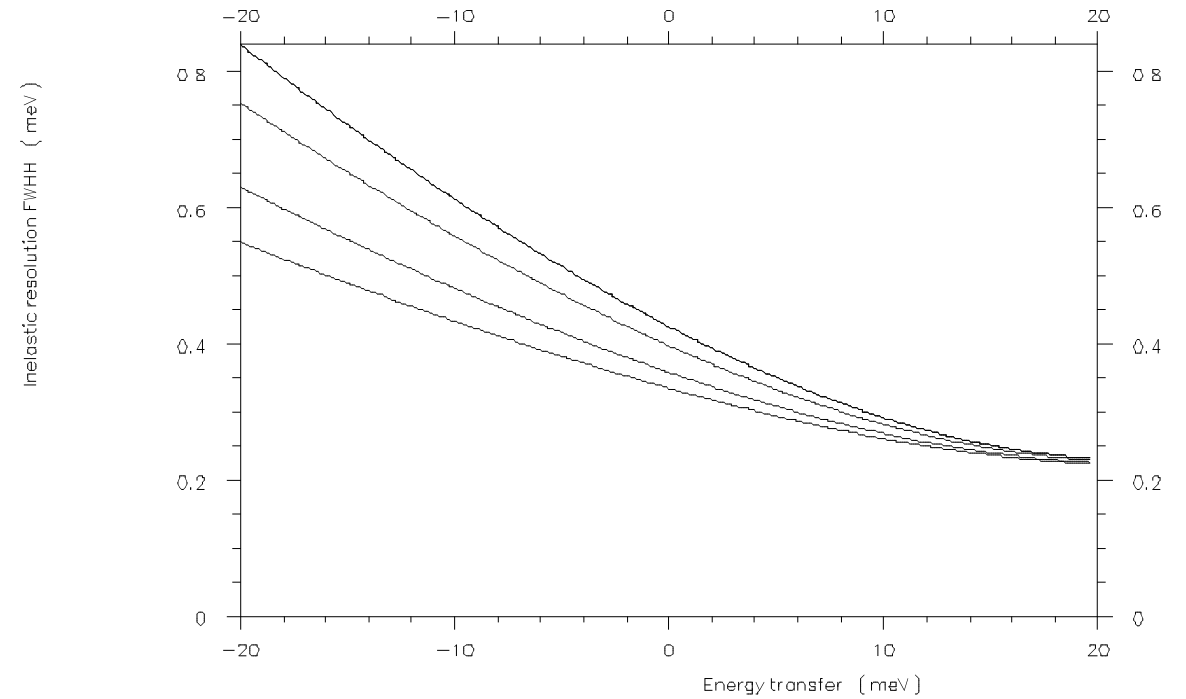
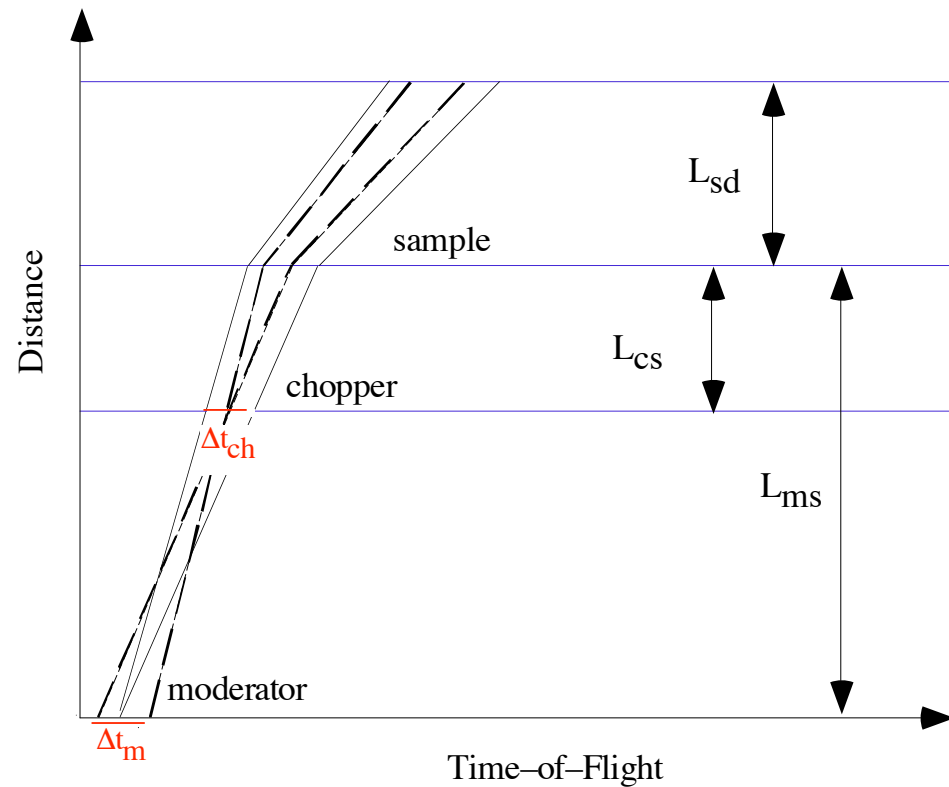
# Direct Geometry Chopper Spectrometer

## ARCS - A wide Angular Range Chopper Spectrometer



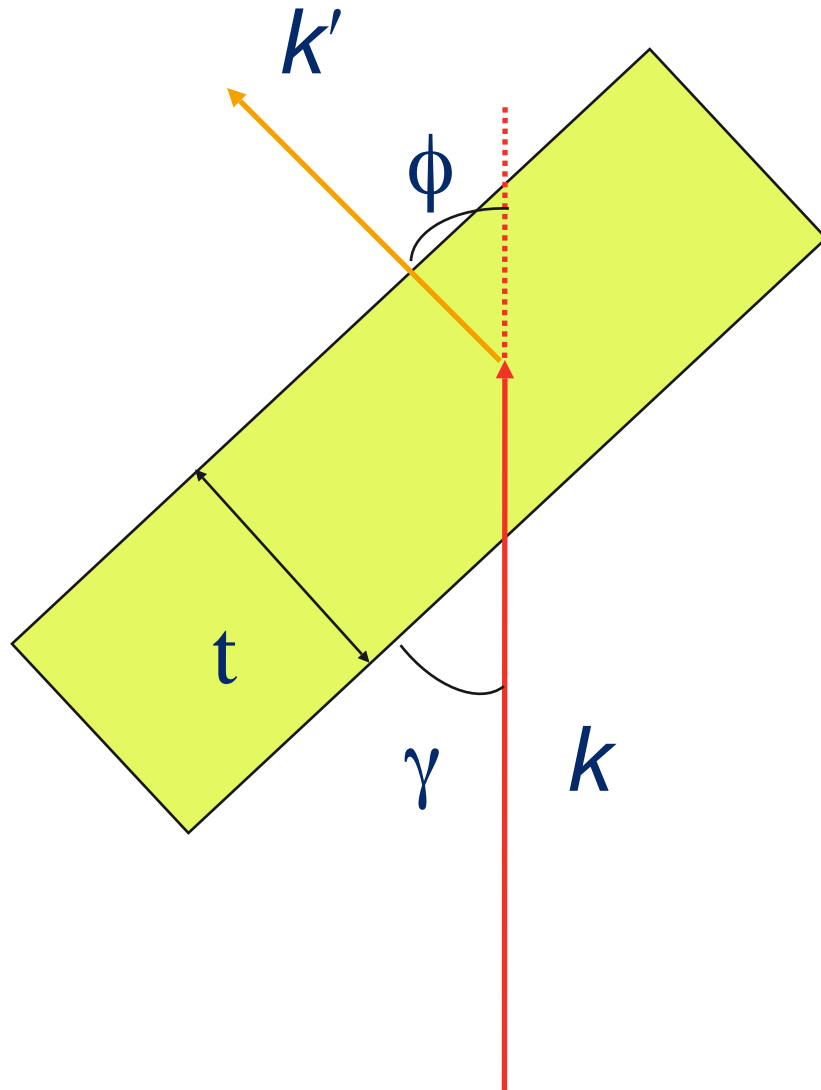
- Primary Flight Path: 11.6m
- Secondary Flight Path: 3m
- Angular range :
  - 30° -150° (Horizontal)
  - 30° -30° (Vertical)
- Incident energy : 10meV-1.5eV
- Energy resolution : 2-5% $E_i$
- Detectors : Position sensitive
- Supermirror guide
- Oscillating collimator
- Provision for polarization analysis

# Chopper Resolution



$$\frac{\Delta \epsilon}{E_i} = \left[ \left\{ 2 \frac{\Delta t_{ch}}{t_{ch}} \left( 1 + \frac{L_{ms}}{L_{sd}} \left[ 1 - \frac{\epsilon}{E_i} \right]^{\frac{3}{2}} \right) \right\}^2 \right]^{\frac{1}{2}} + \left[ \left\{ 2 \frac{\Delta t_m}{t_{ch}} \left( 1 + \frac{L_{cs}}{L_{sd}} \left[ 1 - \frac{\epsilon}{E_i} \right]^{\frac{3}{2}} \right) \right\}^2 \right]^{\frac{1}{2}}$$

# Self-Shielding



$$\text{Transmission} = \exp(-\mu t \sec \gamma)$$

Self-shielding:

$$\frac{\exp[-\mu_i t \sec(\gamma)] - \exp[-\mu_i t \sec(\phi - \gamma)]}{\mu_f t \sec(\phi - \gamma) - \mu_f t \sec(\gamma)}$$

(in transmission)

$$\frac{\exp[\mu_i t \sec(\phi - \gamma) - \mu_i t \sec(\gamma)] - 1}{\mu_f t \sec(\phi - \gamma) - \mu_f t \sec(\gamma)}$$

(in reflection)

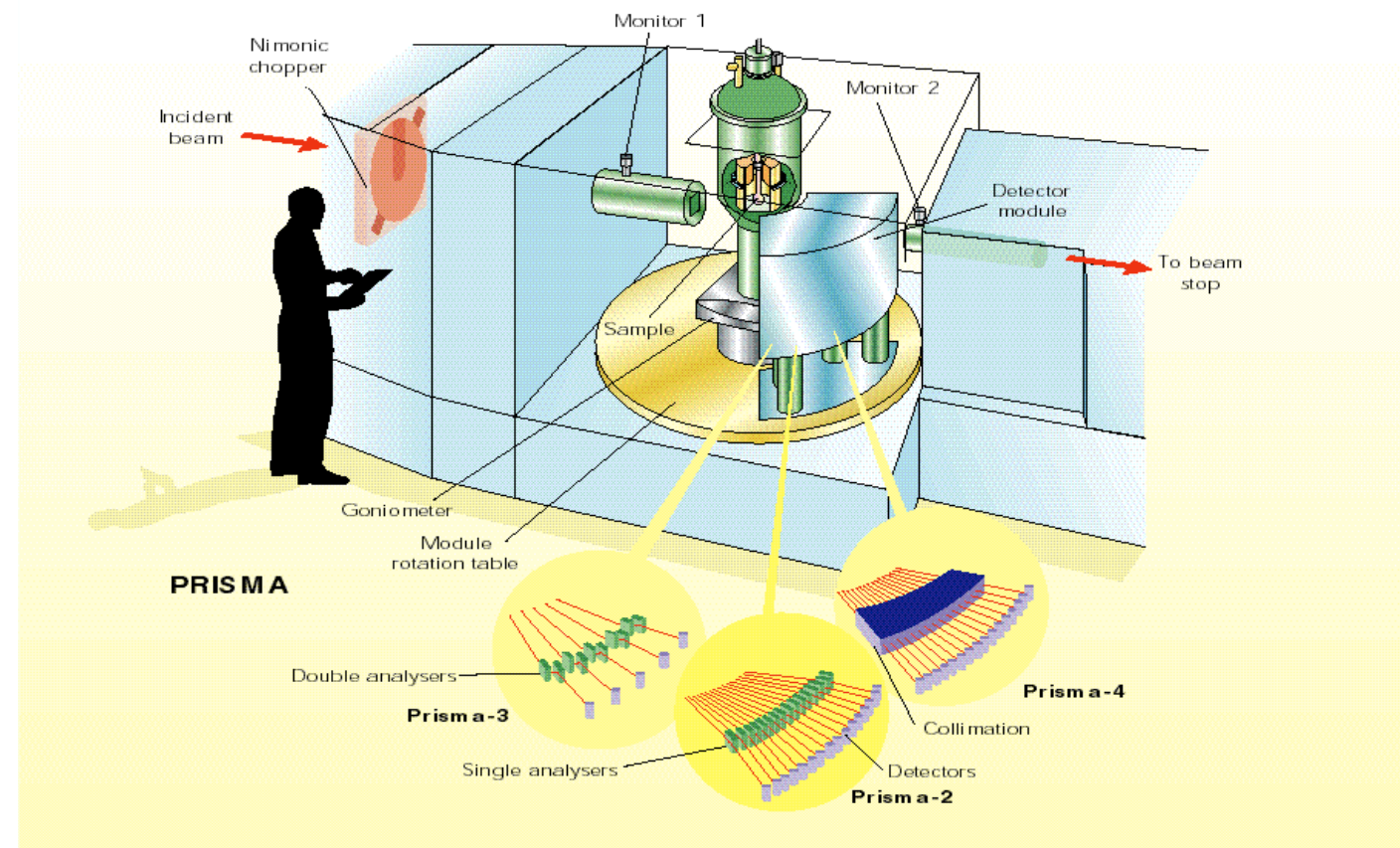
$$\mu = \mu_s + \mu_a \left(\frac{\lambda}{\lambda_0}\right) \quad \lambda_0 = 1.8 \text{ \AA}$$

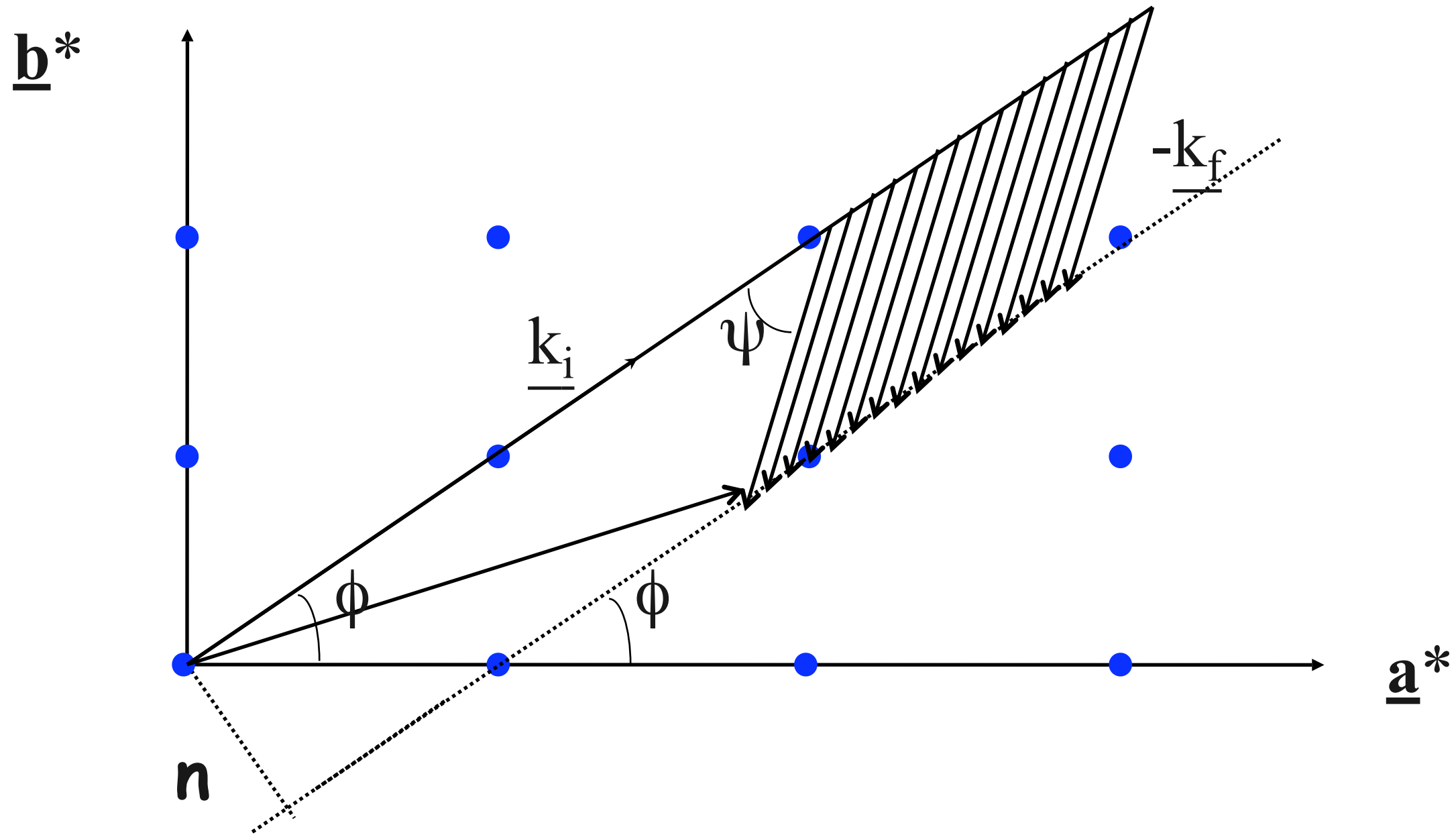
# Crystal Analyzer Spectrometer

This does the equivalent job on a pulsed source to the triple axis spectrometer at a reactor.

It is an example of an indirect geometry instrument in which the time of flight of the incident neutrons determines  $k_i$  and a Bragg reflection from an analyzer determines  $k_f$ .

PRISMA

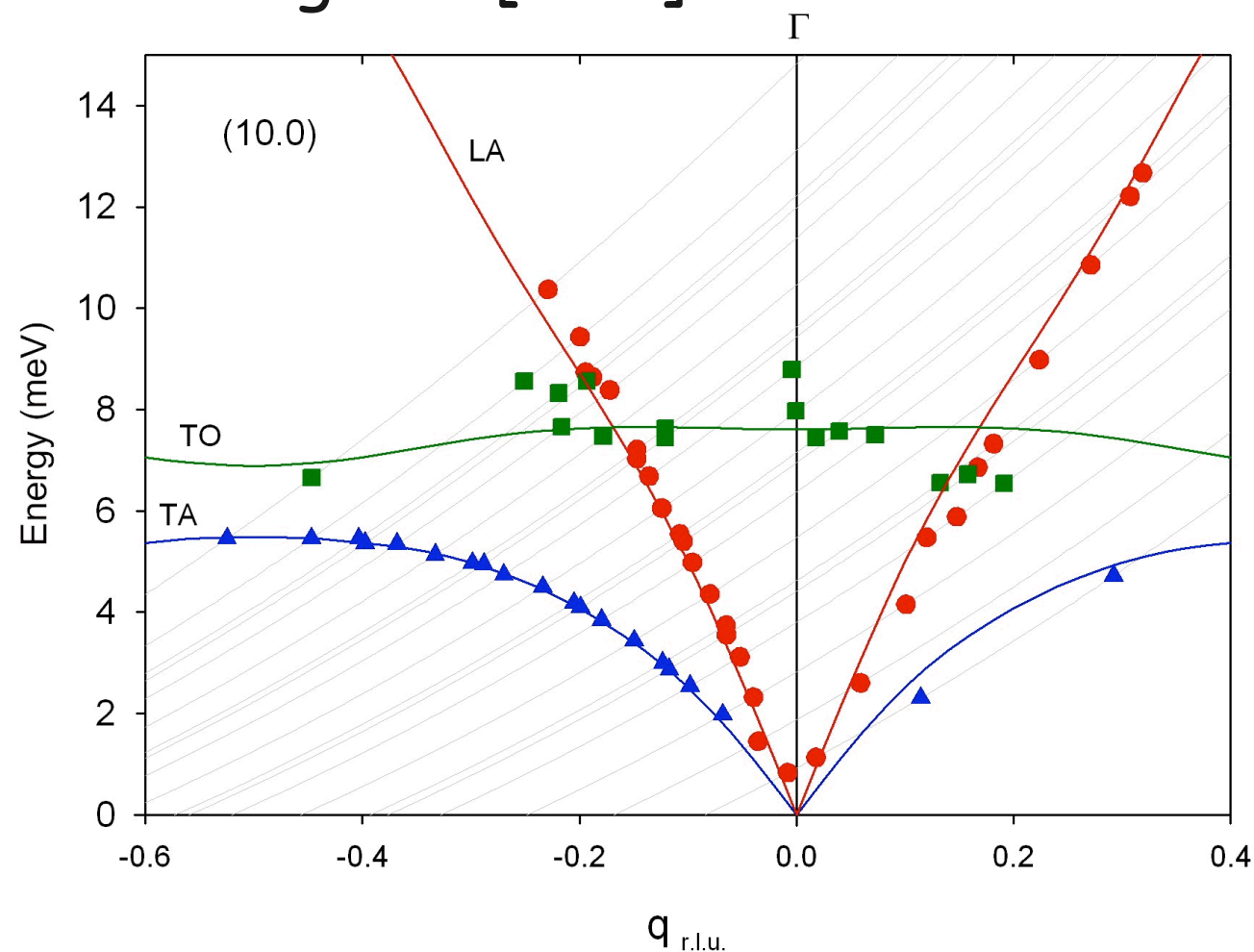




The reciprocal space construction for a single detector is shown above.  $\underline{k}_f$  is fixed by the analyzer d-spacing  $d_A$  and  $2\theta_A$  the scattering angle. Each time bin in the time-of-flight spectrum corresponds to a different  $\underline{k}_i$  and hence a different scattering triangle.

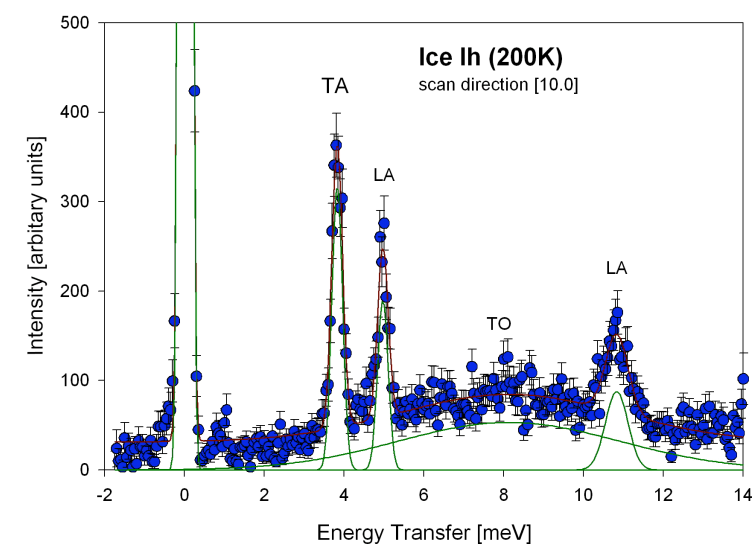
# The Dynamics of Ice Ih

The scan along the [10.0] direction.



- ⊙ The optic modes are very broad. This is probably due to a coupling to the lattice disorder.

- ⊙ The flattening of the TA-mode is similar to that seen in the covalent semiconductors such as Ge or GaAs.



# Magnetic Cross Section

$$\frac{d^2\sigma}{d\Omega dE'} = \frac{(\gamma r_0)^2}{2\pi\hbar} \frac{k'}{k} \sum_{\alpha,\beta} (\delta_{\alpha\beta} - \hat{Q}_\alpha \hat{Q}_\beta) \sum_{ld'l'd'} F_{d'}^*(\vec{Q}) F_d(\vec{Q})$$

$$\times \int_{-\infty}^{\infty} dt \langle \exp\{-i\vec{Q} \cdot \vec{R}_{l'd'}(0)\} \exp\{i\vec{Q} \cdot \vec{R}_{ld}(t)\} \rangle \langle S_{l'd'}^\alpha(0) S_{ld}^\beta(t) \rangle e^{i\omega t}$$

- If we assume that the motion of an ion is independent of its spin orientation:

$$\frac{d^2\sigma}{d\Omega dE'} = \frac{(\gamma r_0)^2}{2\pi\hbar} \frac{k'}{k} \left\{ \frac{1}{2} g F(\vec{Q}) \right\}^2 \exp\{-2W(\vec{Q})\} \sum_{\alpha,\beta} (\delta_{\alpha\beta} - \hat{Q}_\alpha \hat{Q}_\beta)$$

$$\times \sum_{ld'l'd'} \exp\{i\vec{Q} \cdot (\vec{R}_{ld} - \vec{R}_{l'd'})\} \int_{-\infty}^{\infty} dt \langle S_{l'd'}^\alpha(0) S_{ld}^\beta(t) \rangle e^{i\omega t}$$

- i.e. the inelastic cross section is just the Fourier transform in time and space of the spin-spin correlation function.

# Fluctuation-Dissipation Theorem

- We have written the cross section as proportional to a correlation function, i.e.  $\langle S_{i'd'}^\alpha(0)S_{id}^\beta(t) \rangle$
- In fact, what the neutron is doing is applying a very small perturbation to the spin system.
- If the perturbation is small, then the response of the system is proportional to the spectrum of spontaneous fluctuations.  
(Fluctuation-Dissipation Theorem).

$$\frac{d^2\sigma}{d\Omega dE'} \propto (\gamma r_0)^2 \frac{k'}{k} \left\{ \frac{1}{2} g F(\vec{Q}) \right\}^2 \exp\{-2W(\vec{Q})\} \{n(\omega) + 1\} \\ \times \frac{1}{\pi (g\mu_B)^2} \sum_{\alpha,\beta} (\delta_{\alpha\beta} - \hat{Q}_\alpha \hat{Q}_\beta) \text{Im}\{\chi^{\alpha\beta}(\vec{Q}, \omega)\}$$

where  $S^\alpha(\vec{Q}, \omega) = \chi^{\alpha\beta}(\vec{Q}, \omega) H^\beta(\vec{Q}, \omega)$

- i.e., the inelastic cross section is just the dissipative part of the  $(\vec{Q}, \omega)$ -dependent magnetic susceptibility.

# Kramers-Kronig Relations

- This dynamic susceptibility is related to the static susceptibility measured in a conventional susceptometer by the Kramers-Kronig relations:

$$\chi'(\vec{Q},0) = \frac{1}{\pi} \int_{-\infty}^{\infty} d\omega \frac{\chi''(\vec{Q},\omega)}{\omega}$$

- So the cross section can be rewritten:

$$\frac{d^2\sigma}{d\Omega dE'} \propto \frac{k'}{k} S(Q,\omega) \propto \frac{k'}{k} \{n(\omega) + 1\} \chi'(\vec{Q},0) \omega P(\vec{Q},\omega)$$

- $P(Q,\omega)$  is just a normalized spectral or "shape" function
  - e.g. a delta function or a Lorentzian
- $\chi'(Q \rightarrow 0,0)$  is the bulk static susceptibility

N.B.  $S(Q,\omega)$  is the neutron scattering law here, not the F.T. of the spin.

# Simple Examples

- I will discuss three simple model systems before showing examples of inelastic neutron scattering experiments.
- The first two are single-ion models, i.e. there is no interaction between spins on neighboring sites. Therefore:
  - The excitation energies are  $Q$ -independent
  - The cross sections follow a single-ion form factor
- The models are:
  1. Simple Curie paramagnet
  2. Van Vleck paramagnet
  3. Spin waves in an ordered system (ferromagnet or antiferromagnet)

# Curie Paramagnet

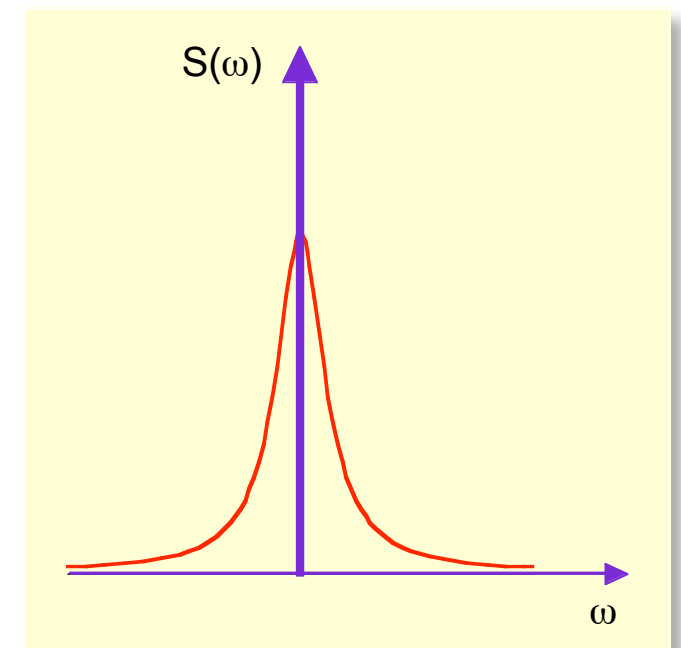
$$S(Q, \omega) = \{n(\omega) + 1\} \chi'(\vec{Q}, 0) \omega P(\vec{Q}, \omega)$$

- The bulk susceptibility for a simple paramagnet, with non-interacting spins is simply:

$$\chi'(0, 0) \propto \frac{S(S + 1)}{3k_B T}$$

- Since the spins are non-interacting, we can assume that it costs no energy for them to flip, i.e.  $P(\omega) = \delta(\omega)$
- In the limit of  $\omega \rightarrow 0$ ,  $\{n(\omega) + 1\} \rightarrow k_B T / \omega$

$$S(\omega) \propto \frac{2}{3} S(S + 1) \delta(\omega)$$



- If the spins are fluctuating, the peak is broadened (quasi-elastic).

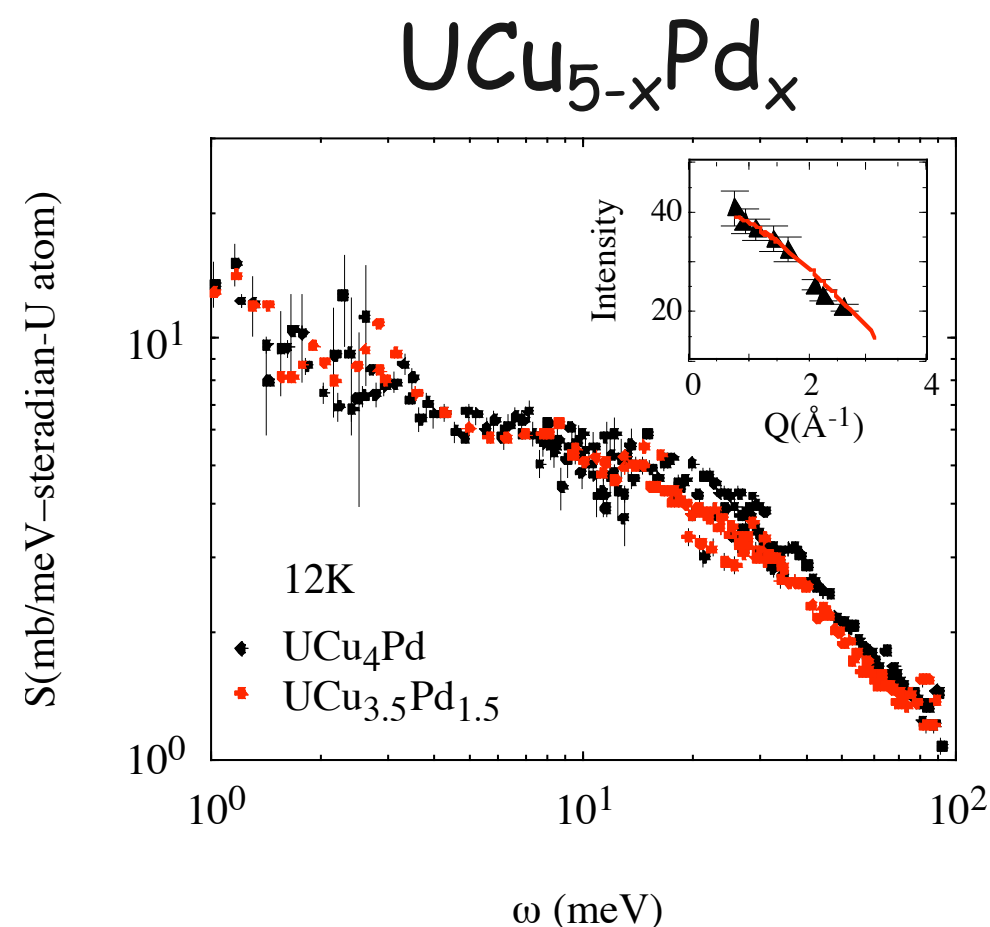
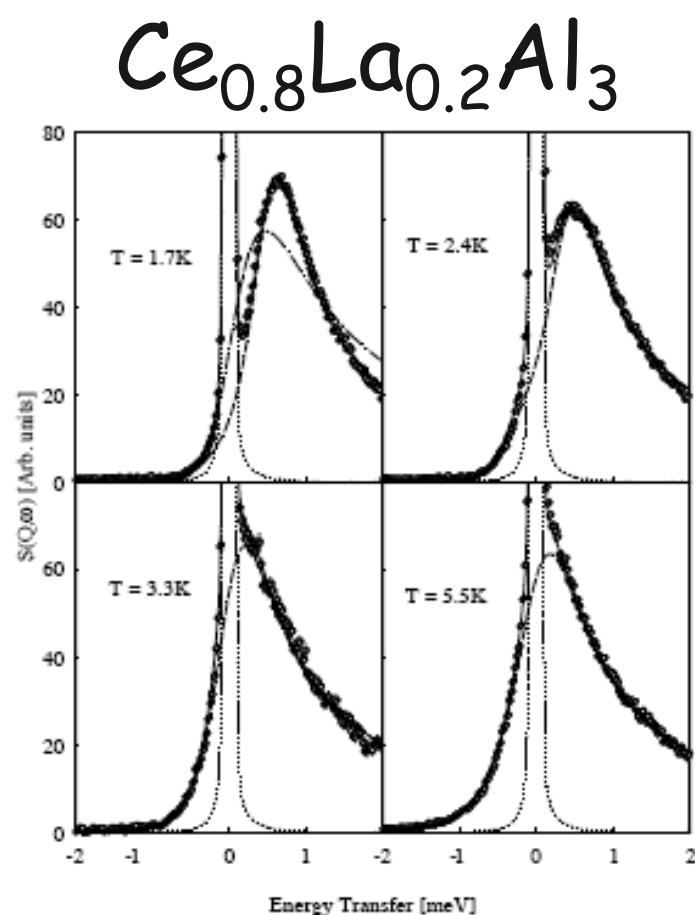
$$\langle S^z(t) S^z(0) \rangle \propto \exp(-t/\tau) \Rightarrow S(\omega) \propto \{n(\omega) + 1\} \omega \Gamma / \{\omega^2 + \Gamma^2\}$$

# Fluctuating Moment Systems

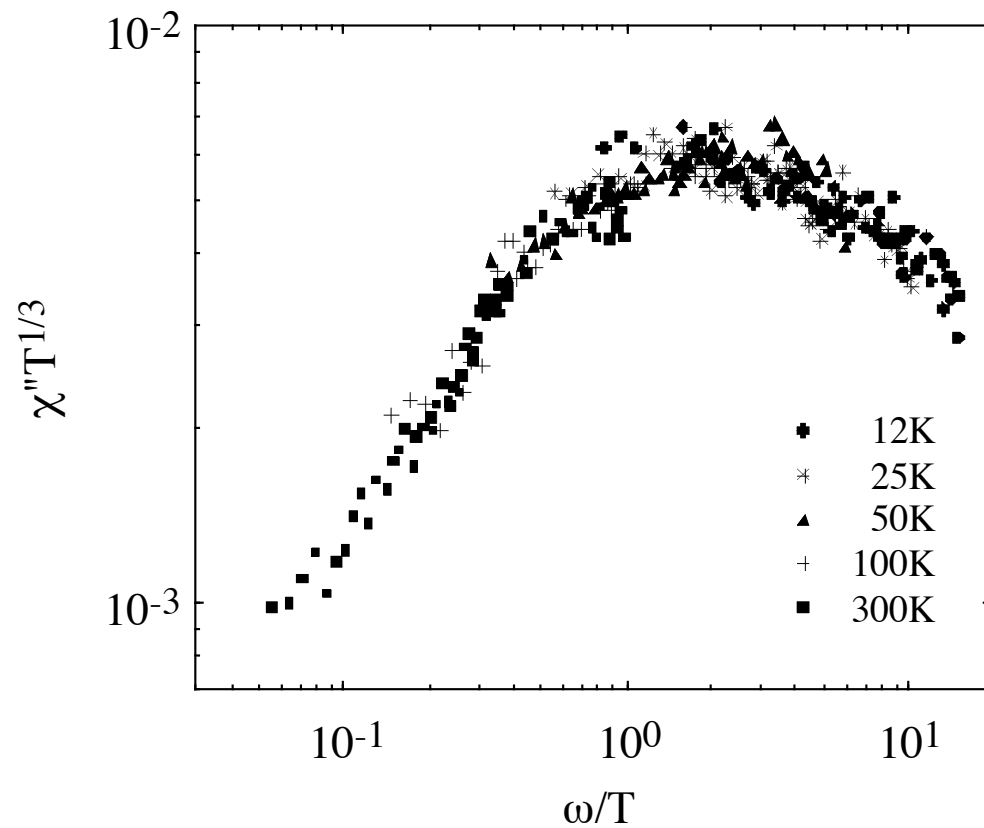
Neutron measurements of spin dynamics have been important for measuring relaxation rates of local moments coupled to conduction electrons .

The temperature dependence  $\Gamma(T)$  has distinctive behaviour in heavy fermions, Kondo lattice and intermediate valence materials.

In particular  $\Gamma(T \rightarrow 0)$  gives a measure of the "Kondo temperature", a key parameter in strongly correlated electron systems.



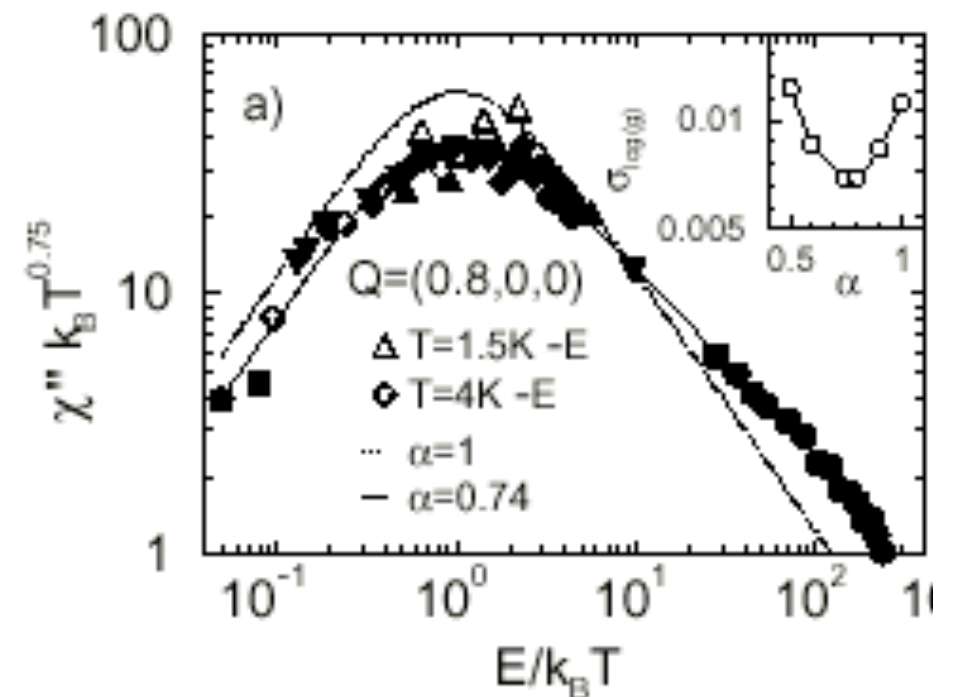
# Quantum Critical Scaling in $UCu_{5-x}Pd_x$



$$\chi''(\omega, T) T^{\frac{1}{3}} = \left(\frac{T}{\omega}\right)^{\frac{1}{3}} Z\left(\frac{\omega}{T}\right)$$

M.C.Aronson *et al*, Phys. Rev. Lett. **75**, 725 (1995)

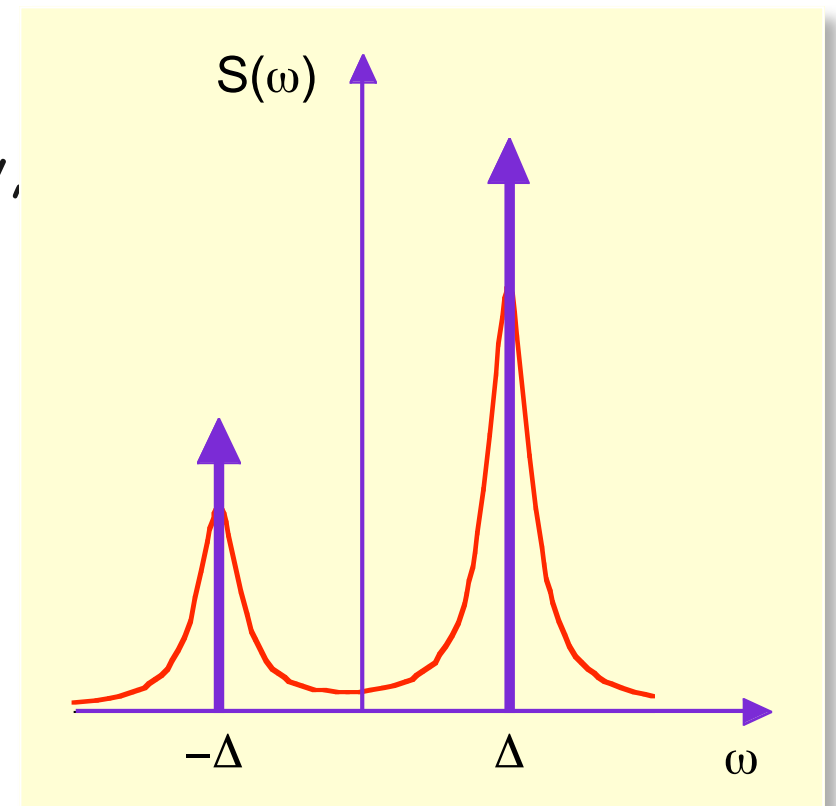
*cf*  $CeCu_{5.9}Au_{0.1}$



A. Schroder *et al*, Nature **407**, 351 (2000)

# Van Vleck Paramagnet

- In a Van Vleck paramagnet, the ground state is non-magnetic, but there is a magnetic state at finite energy, e.g. at  $\omega = \Delta$ , with transitions from the ground state induced by a dipole matrix element.
- To calculate the neutron cross section, let's start with the spin-spin correlation function, which is really a sum of dipole matrix elements:



$$\int_{-\infty}^{\infty} dt \langle S_{l'd'}^{\alpha}(0) S_{ld}^{\beta}(t) \rangle e^{i\omega t} = \sum_{i,j} p_i \langle i | S_{l'd'}^{\alpha} | j \rangle \langle j | S_{ld}^{\beta} | i \rangle \delta(\omega + E_i - E_j)$$

$$\langle S^{\alpha}(0) S^{\beta}(t) \rangle = \frac{|M_{\alpha\beta}|^2}{1 + \exp(-\Delta/k_B T)} \{ \delta(\omega - \Delta) + \exp(-\Delta/k_B T) \delta(\omega + \Delta) \}$$

if we assume:

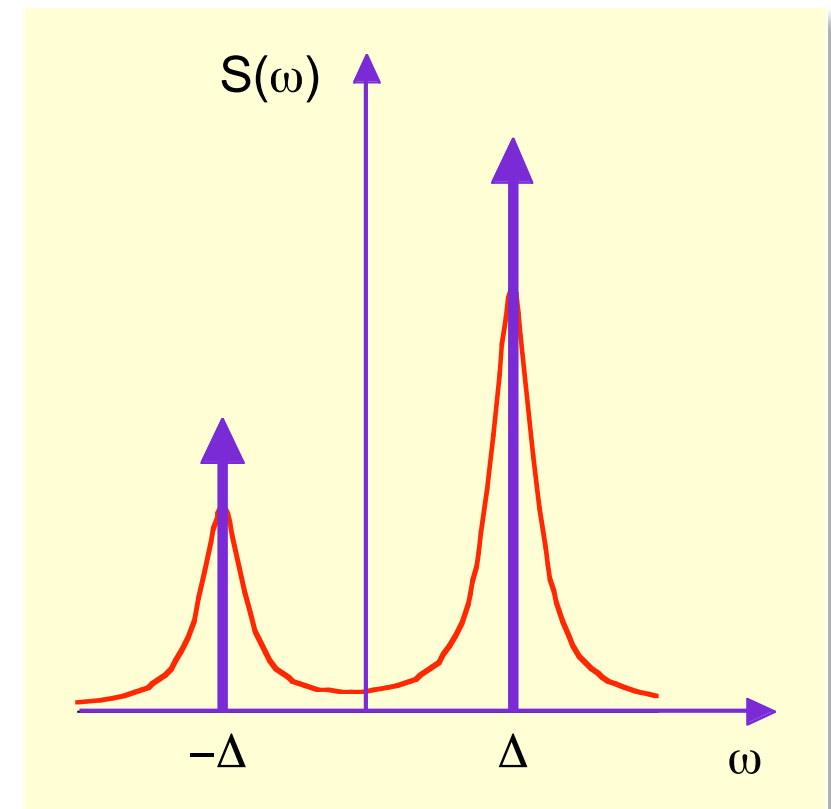
- that both levels are singlets
- spins on different sites do not interact ( $M_{\alpha\beta}$  is the dipole matrix element)

# Van Vleck Paramagnet (contd)

- We can show that both forms of the cross section are equivalent if we set:

$$P(\omega) = \frac{1}{2} \{ \delta(\omega - \Delta) + \delta(\omega + \Delta) \}$$

and use  $\{n(\omega)+1\} = 1/\{1-\exp(-\omega/k_B T)\} = -n(-\omega)$



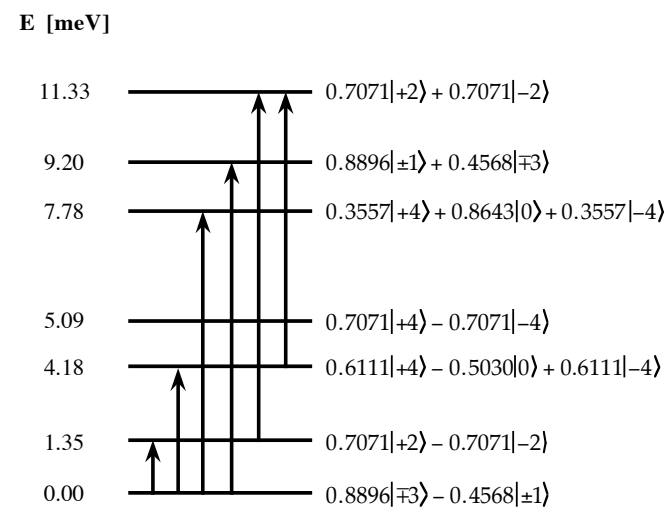
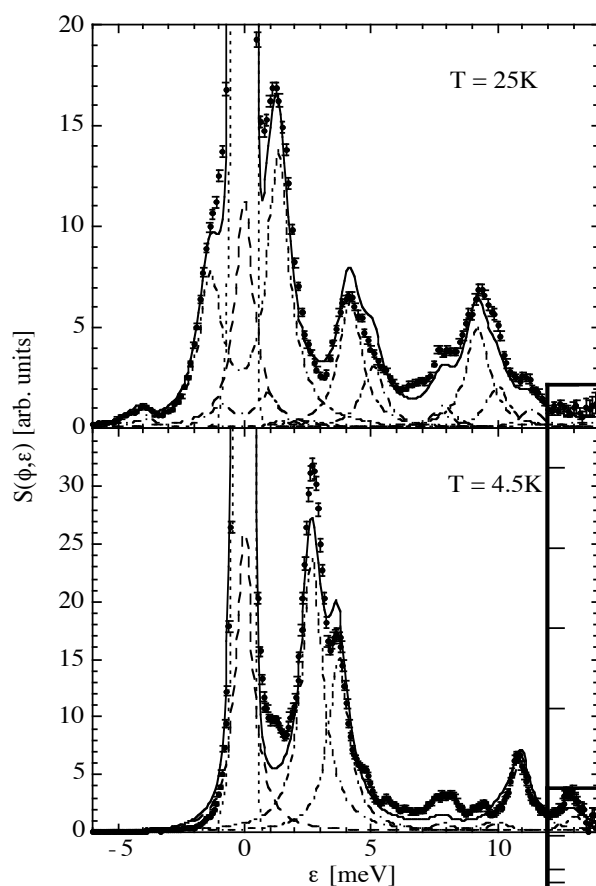
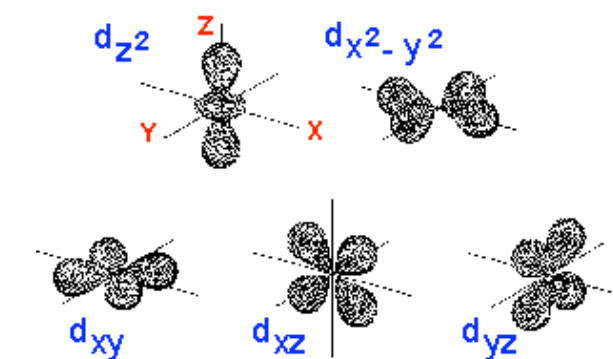
$$\{n(\omega) + 1\} \chi'(0) \omega P(\omega) = \frac{|M_{\alpha\beta}|^2}{1 + \exp(-\Delta / k_B T)} \{ \delta(\omega - \Delta) + \exp(-\Delta / k_B T) \delta(\omega + \Delta) \}$$

$$\chi'(0) = \frac{|M_{\alpha\beta}|^2}{\Delta} \tanh\left(\frac{\Delta}{2k_B T}\right)$$

- This is the standard expression for a Van Vleck paramagnet.

# Crystal Field Spectroscopy

- Localized electronic  $4f^n$  wavefunctions may be split by Coulomb repulsion from neighboring anions
- Neutrons can induce transitions between the energy levels if there is a dipole matrix element



- The crystal field wavefunctions can be determined from the inelastic peak energies and intensities.

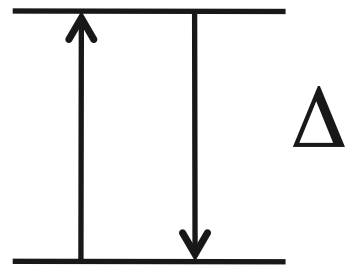
$$S(Q, \omega) \propto f^2(Q) p_i |M_{ij}|^2 \delta(\omega - \Delta_i)$$

$$\text{where } p_i = \exp(-\Delta_i/k_B T) / Z$$

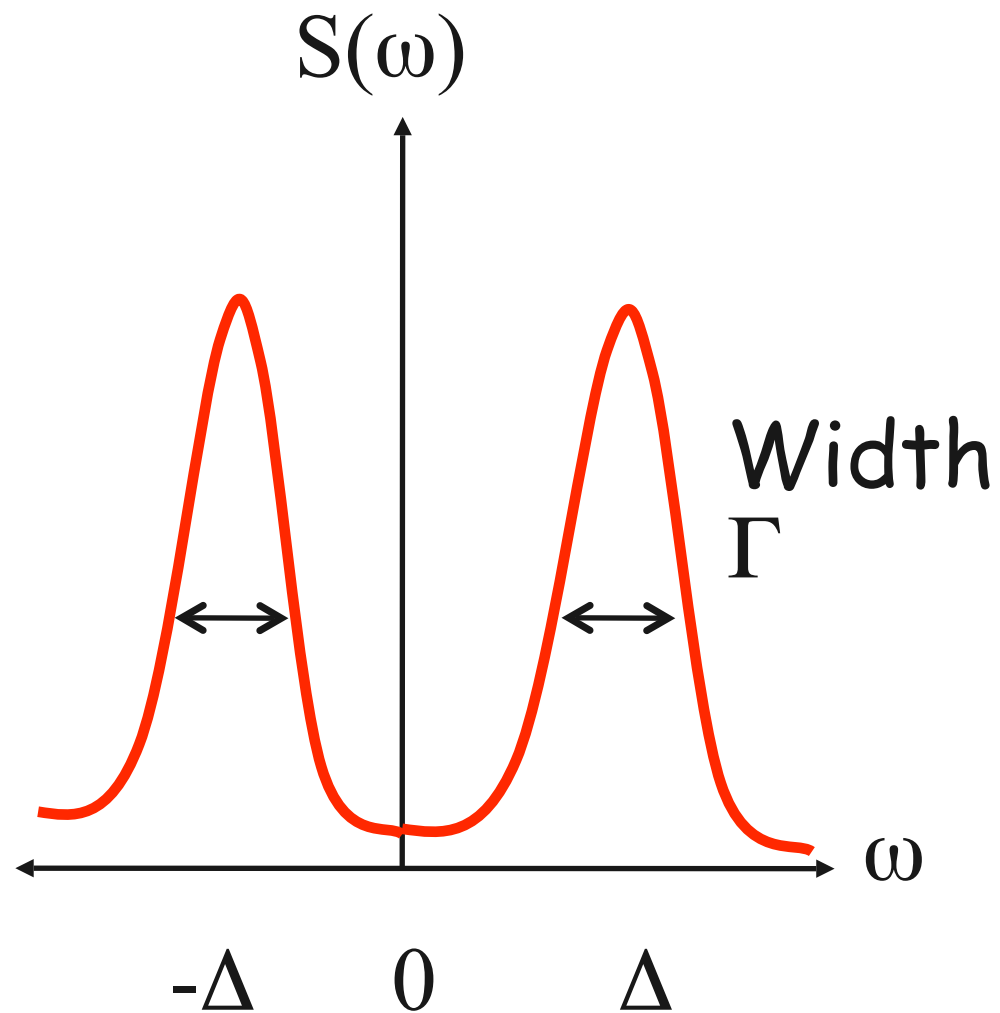
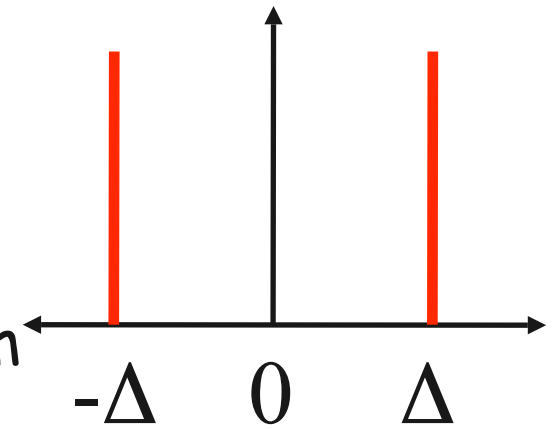
$$\text{and } Z = \sum_i n_i \exp(-\Delta_i/k_B T)$$

# Spin Lattice Relaxation

Simple example of excitations between two CF states.



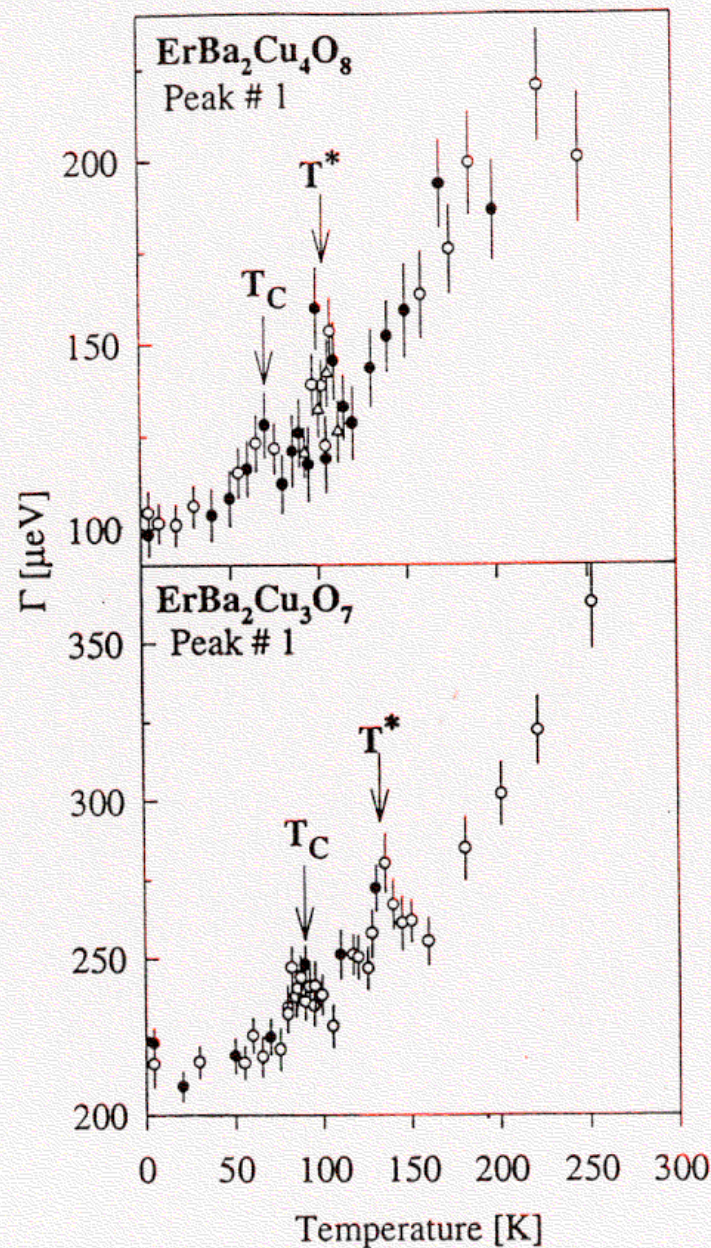
In the absence of interactions the spectrum consists of two delta functions at  $\pm\Delta$



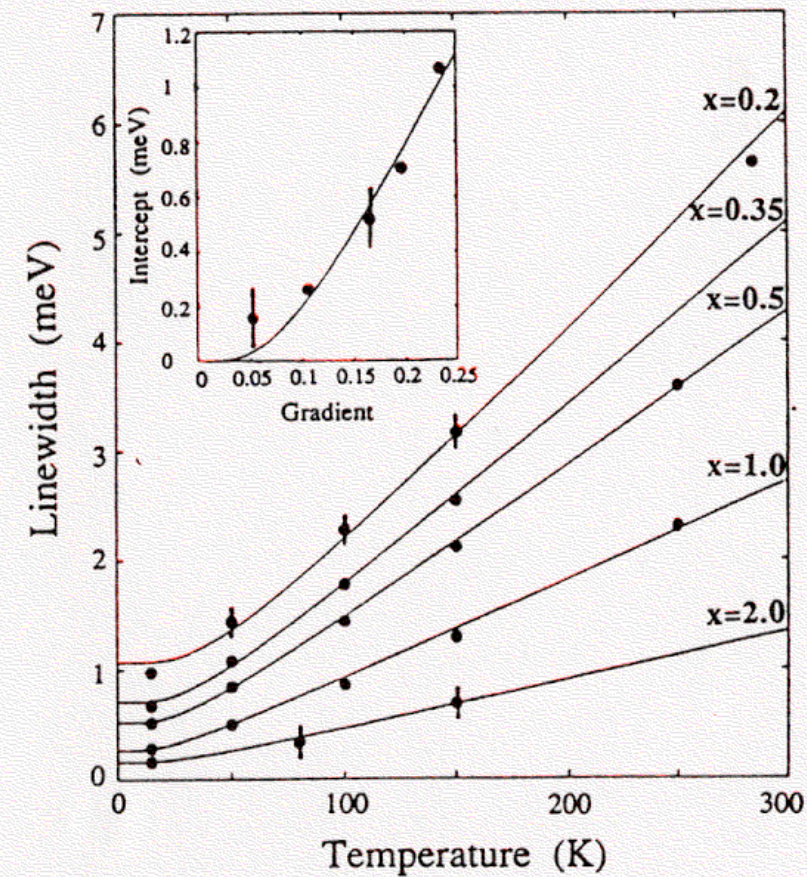
Spin-lattice relaxation, due to spins interacting with phonons or conduction electrons results in the excitations having a linewidth  $\Gamma$  equal to the reciprocal of the relaxation time,  
 $\Gamma = 1/\tau$

# Examples of Spin Lattice Relaxation

Example 1 : Linewidths of CF excitations of  $\text{Er}^{3+}$  in  $\text{ErBa}_2\text{Cu}_4\text{O}_8$  (Goremychkin et al.)



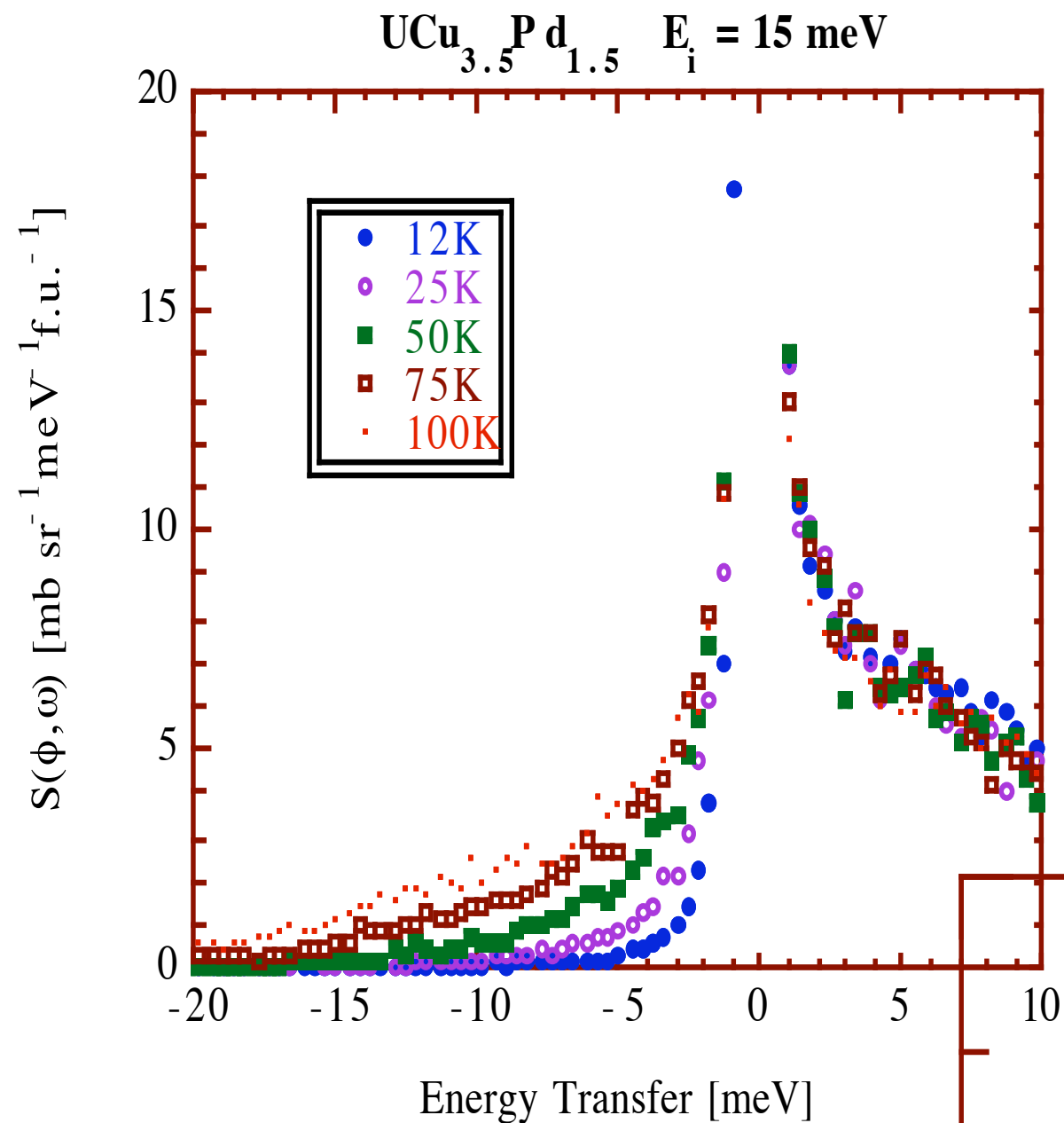
Example 2 : Single ion component of linewidth in Kondo alloys  $\text{CeRu}_2\text{Si}_{2-x}\text{Ge}_x$  (Rainford and Dakin).



$$\text{Intercept} \approx k_B T_K = D(J\rho)^{-1/2} \exp(-1/J\rho)$$

$$\text{Gradient} \approx (J\rho)^2$$

# Principle of Detailed Balance



- In the Van Vleck example, the energy gain peak was smaller than the energy loss peak.
- The ratio between the two is given by the principle of

## Detailed Balance

$$S(-\omega) = \exp(-\omega/k_B T) S(\omega)$$

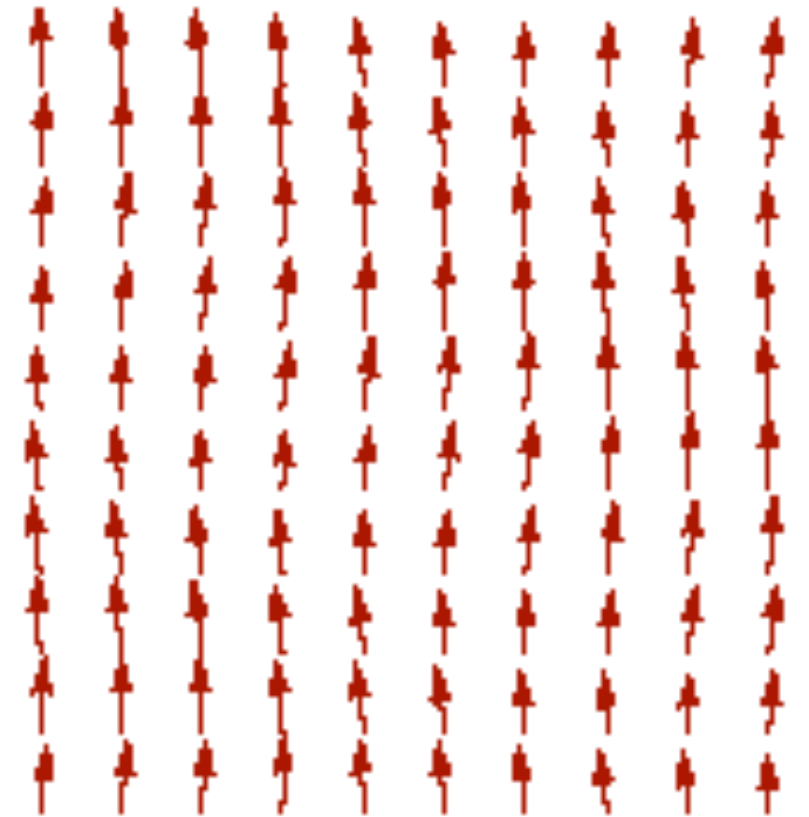
- All systems in thermal equilibrium obey this principle.
- This can be a useful sanity check:
  - self-consistency of data analysis
  - the cryostat is working

# Spin Waves

- In most magnetic systems, there is a coupling between neighboring spins
  - e.g, Heisenberg exchange

$$H_{ex} = - \sum_{i,j} J_{ij} \vec{S}_i \cdot \vec{S}_j$$

- When one spin changes direction, it induces a wave-like disturbance of all the neighboring spins.



# Spin Waves (contd)

- The elementary excitations of an ordered magnet are propagating spin deviations, i.e., spin waves.
- Because neighboring spins are coupled, their excitation energies are  $q$ -dependent, with dispersion relations, e.g.,

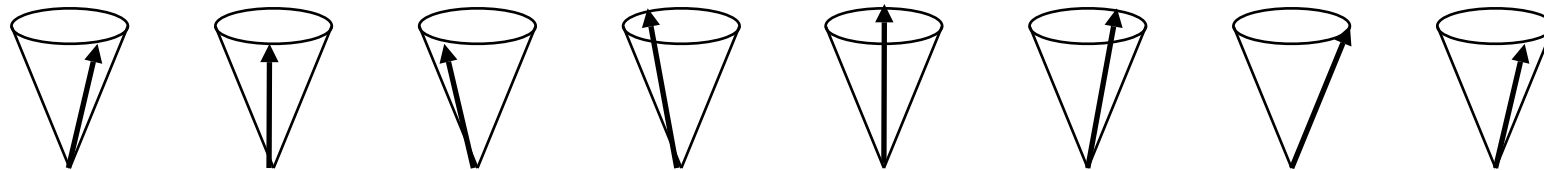
Where 
$$\hbar\omega_q^{ferro} = S [ J(0) - J(q) ] \approx Dq^2$$

$$\hbar\omega_q^{antiferro} = S \sqrt{J(0)^2 - J(q)^2}$$

- A quantized spin wave excitation is known as a magnon.

In cubic symmetry

$$D = 2JSa^2$$



# Spin Waves Correlation Functions (formal)

- The spin wave cross section can be derived from the earlier formulae by defining "creation" and "annihilation" operators

$$S_i^+(t) = \sqrt{\frac{2S}{N}} \sum_q \exp\{i[\vec{q} \cdot \vec{R}_i - \omega_q t]\} \hat{a}_q \quad S_i^-(t) = \sqrt{\frac{2S}{N}} \sum_q \exp\{i[\vec{q} \cdot \vec{R}_i - \omega_q t]\} \hat{a}_q^+$$

where  $\hat{a}_q |n_q\rangle = \sqrt{n_q} |n_q - 1\rangle$  and  $\hat{a}_q^+ |n_q\rangle = \sqrt{n_q + 1} |n_q + 1\rangle$

- Using  $\langle \hat{a}_q^+ \hat{a}_q \rangle = \langle n_q \rangle$  and  $\langle \hat{a}_q \hat{a}_q^+ \rangle = \langle n_q + 1 \rangle$  and  $S^x = \frac{1}{2}(S^+ + S^-)$   $S^y = \frac{1}{2i}(S^+ - S^-)$

$$\langle S_i^x(0) S_j^x(t) \rangle = \frac{S}{2N} \sum_q \exp\{-i\vec{q} \cdot (\vec{R}_i - \vec{R}_j) - \omega_q t\} \langle n_q + 1 \rangle + \exp\{i\vec{q} \cdot (\vec{R}_i - \vec{R}_j) - \omega_q t\} \langle n_q \rangle$$

$$\langle S_i^y(0) S_j^y(t) \rangle = \langle S_i^x(0) S_j^x(t) \rangle$$

$$\langle S_i^z(0) S_j^z(t) \rangle = S^2 - \frac{2S}{N} \sum_q \langle n_q \rangle$$

$$\langle n_q \rangle = \left\{ \exp\left(\frac{\omega_q}{k_B T}\right) - 1 \right\}^{-1}$$

# Spin Wave Cross Section (Heisenberg Ferromagnet)

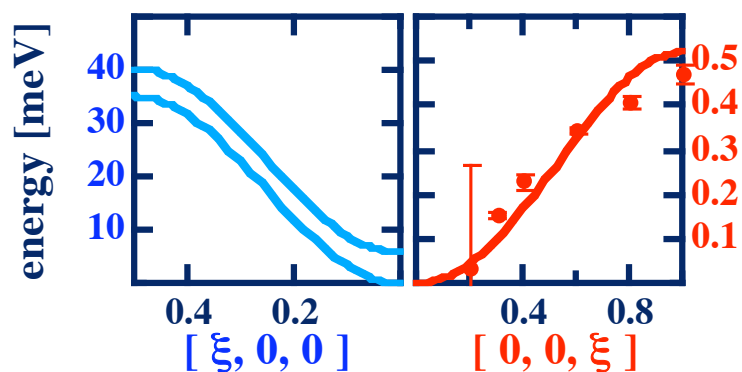
■ Using 
$$\sum_{i,j} \exp\{i\vec{Q}\cdot(\vec{R}_i - \vec{R}_j)\} = \frac{(2\pi)^3}{V} \sum_{\vec{\tau}} \delta(\vec{Q} - \vec{\tau})$$

$$\frac{d^2\sigma}{d\Omega d\omega} = (\gamma r_0)^2 \frac{(2\pi)^3}{V} \frac{k'}{k} \left\{ \frac{1}{2} g F(\vec{Q}) \right\}^2 \exp\{-2W(\vec{Q})\} (1 + \hat{Q}_z^2) \frac{1}{2} S$$

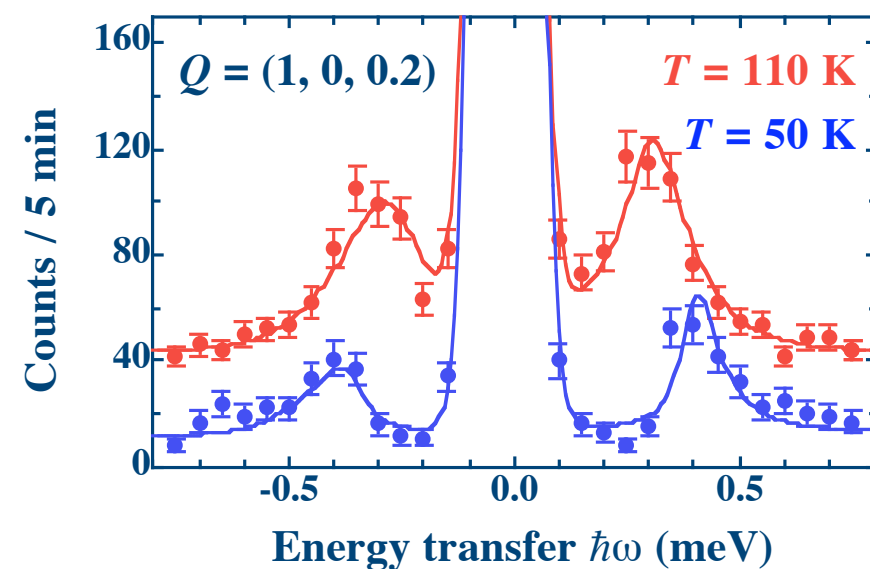
$$\sum_{\tau, q} \langle n_q + 1 \rangle \delta(\vec{Q} - \vec{q} - \vec{\tau}) \delta(\omega - \omega_q) + \langle n_q \rangle \delta(\vec{Q} + \vec{q} - \vec{\tau}) \delta(\omega + \omega_q)$$

## Spin Wave Creation

- e.g. spin waves in  $\text{La}_{1.2}\text{Sr}_{1.8}\text{Mn}_2\text{O}_7$ 
  - cf Van Vleck Paramagnet



## Spin Wave Annihilation



# Kinematics Again (in a single crystal)

Can also be expressed in terms of the components of  $Q$  parallel and perpendicular to the incident wavevector  $k_i$ :

$$Q_{\perp} = k_f \sin(\psi) \quad Q_{\parallel} = k_i - k_f$$

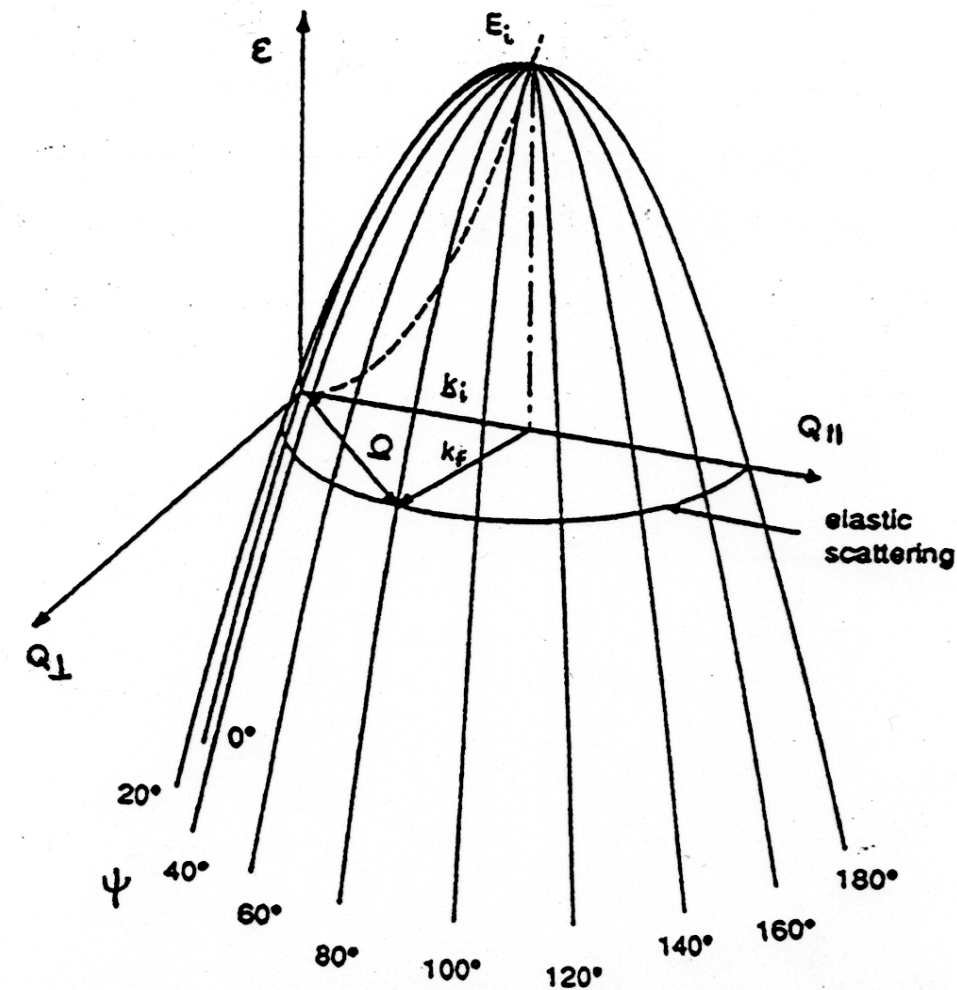
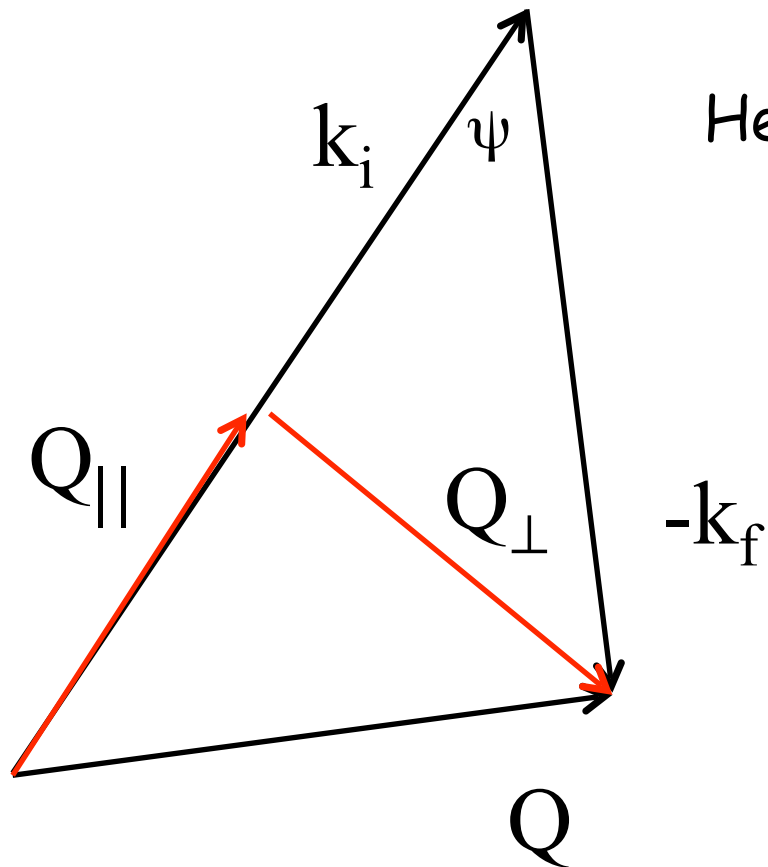
Hence it follows that

$$Q_{\perp} = \sqrt{\frac{2m(E_i - \varepsilon)}{\hbar^2}} \sin(\psi)$$

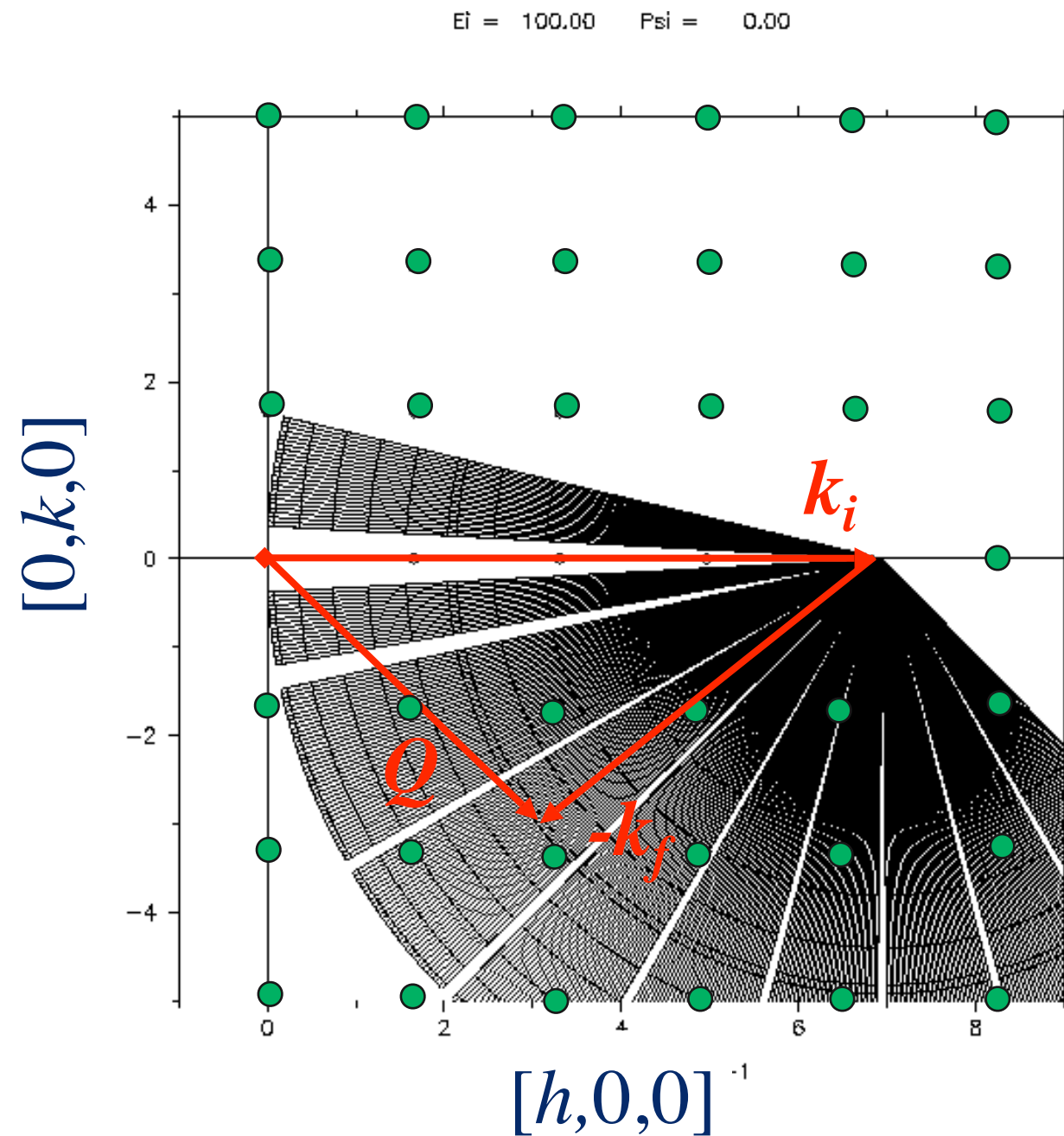
and

$$Q_{\parallel} = \sqrt{\frac{2m}{\hbar^2}} [\sqrt{E_i} - \sqrt{(E_i - \varepsilon)} \cos(\psi)]$$

This results in the surface of a paraboloid, with the apex in  $(Q_{\parallel}, Q_{\perp}, \varepsilon)$ -space at the point  $(k_i, 0, E_i)$ .



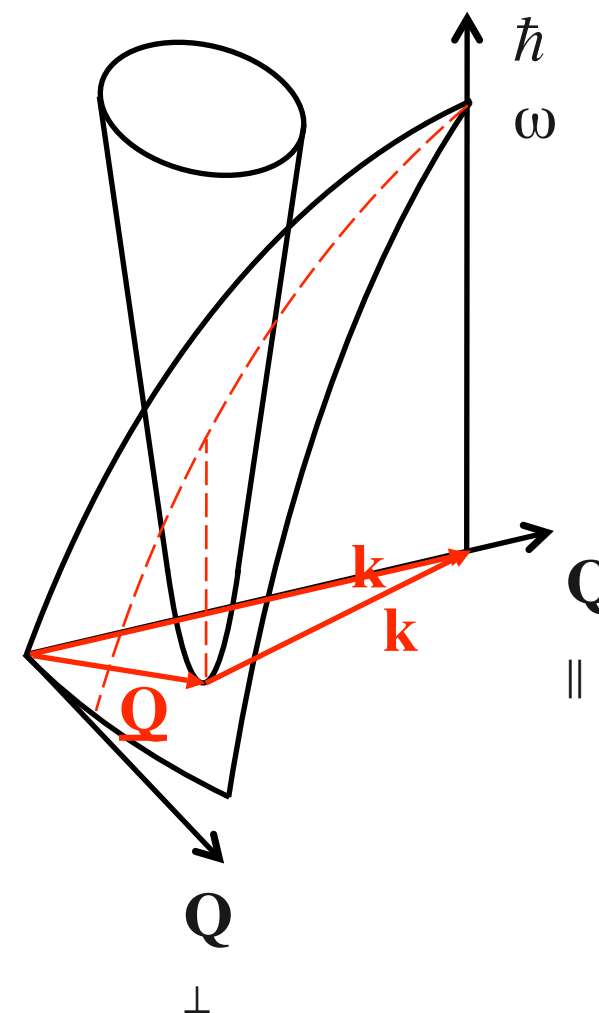
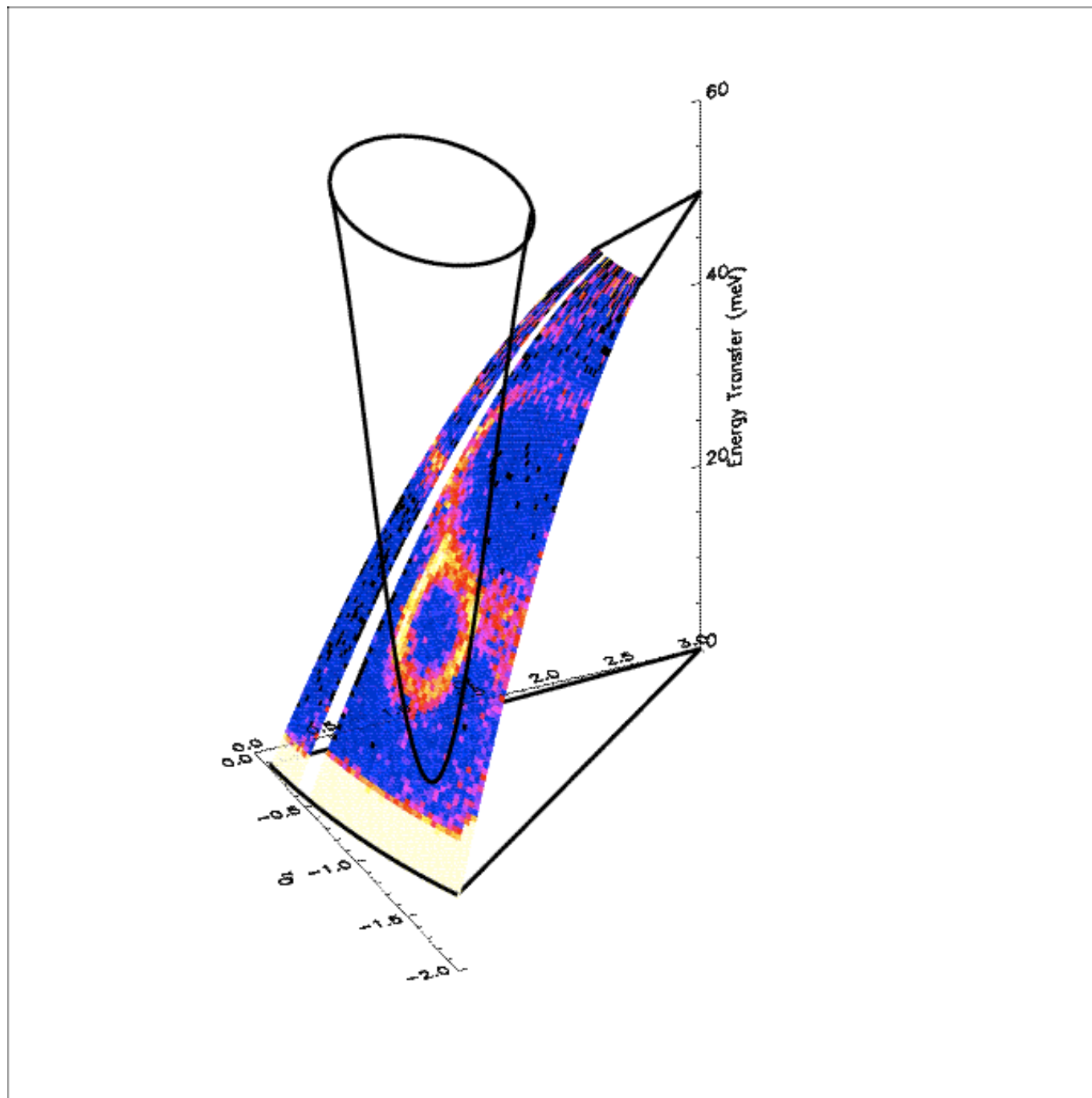
# Kinematics in a Single Crystal (contd)



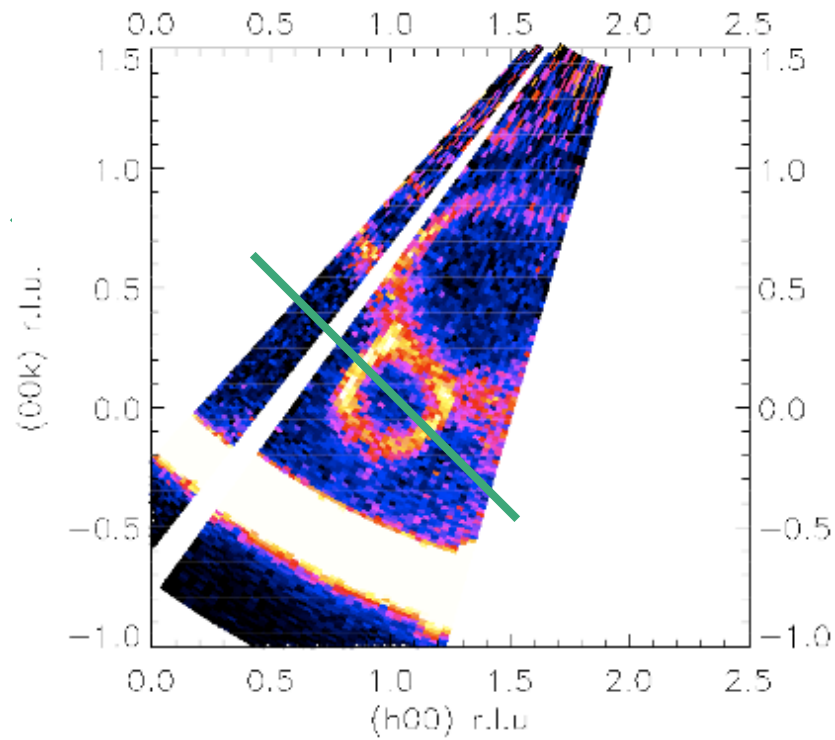
In a single crystal experiment, we need to superimpose the scattering triangle on the reciprocal lattice.

Locus of constant  $w$  is a Q-circle of radius  $k_f$  centered on  $Q = k_i$

# $\text{La}_{0.7}\text{Pb}_{0.3}\text{MnO}_3$ - CMR Ferromagnet



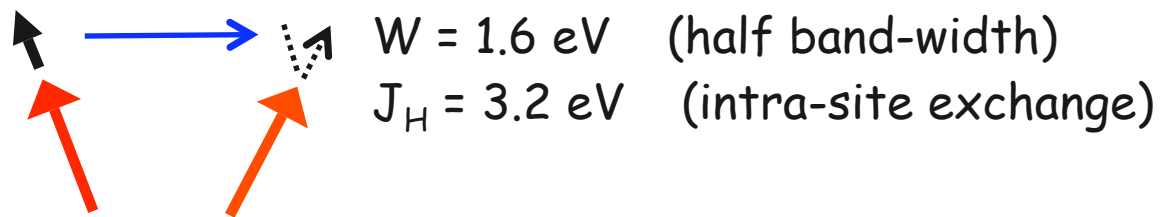
# Spin Waves in a CMR Ferromagnet



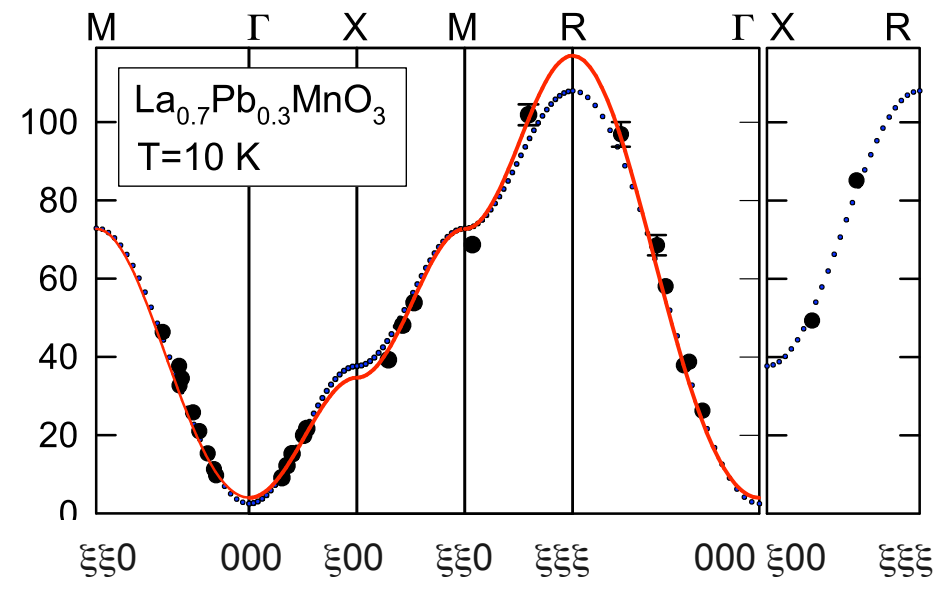
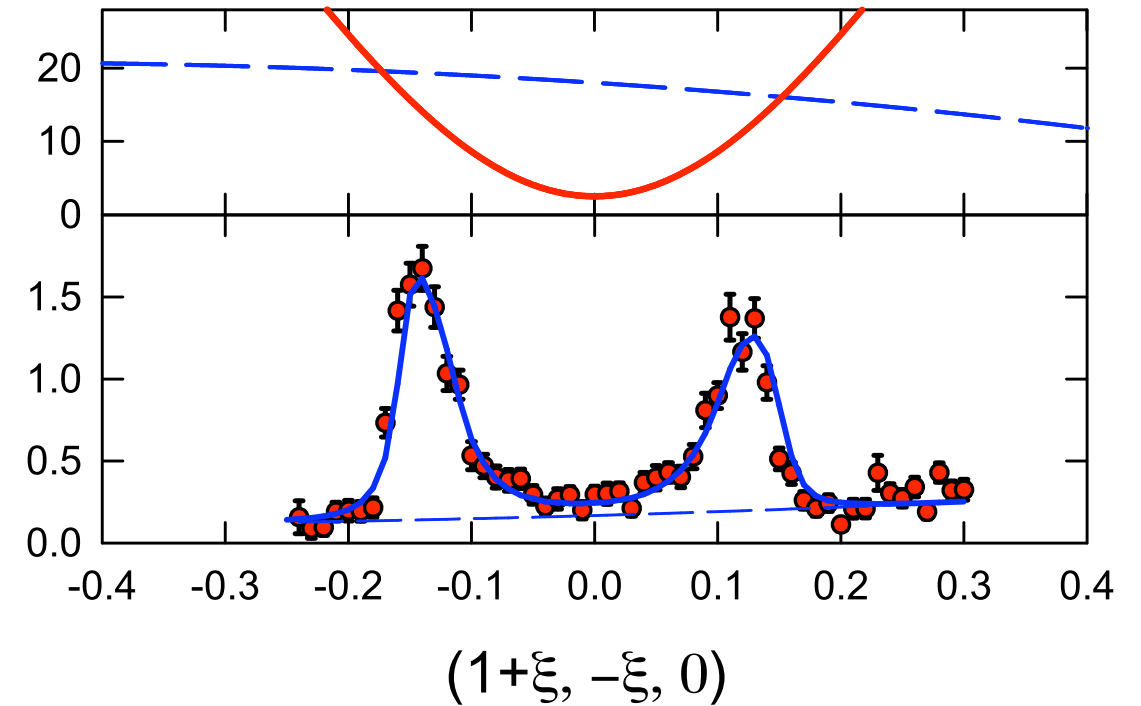
Heisenberg ferromagnet (nearest neighbor)

$$2JS = 8.8 \pm 0.2 \text{ meV}$$

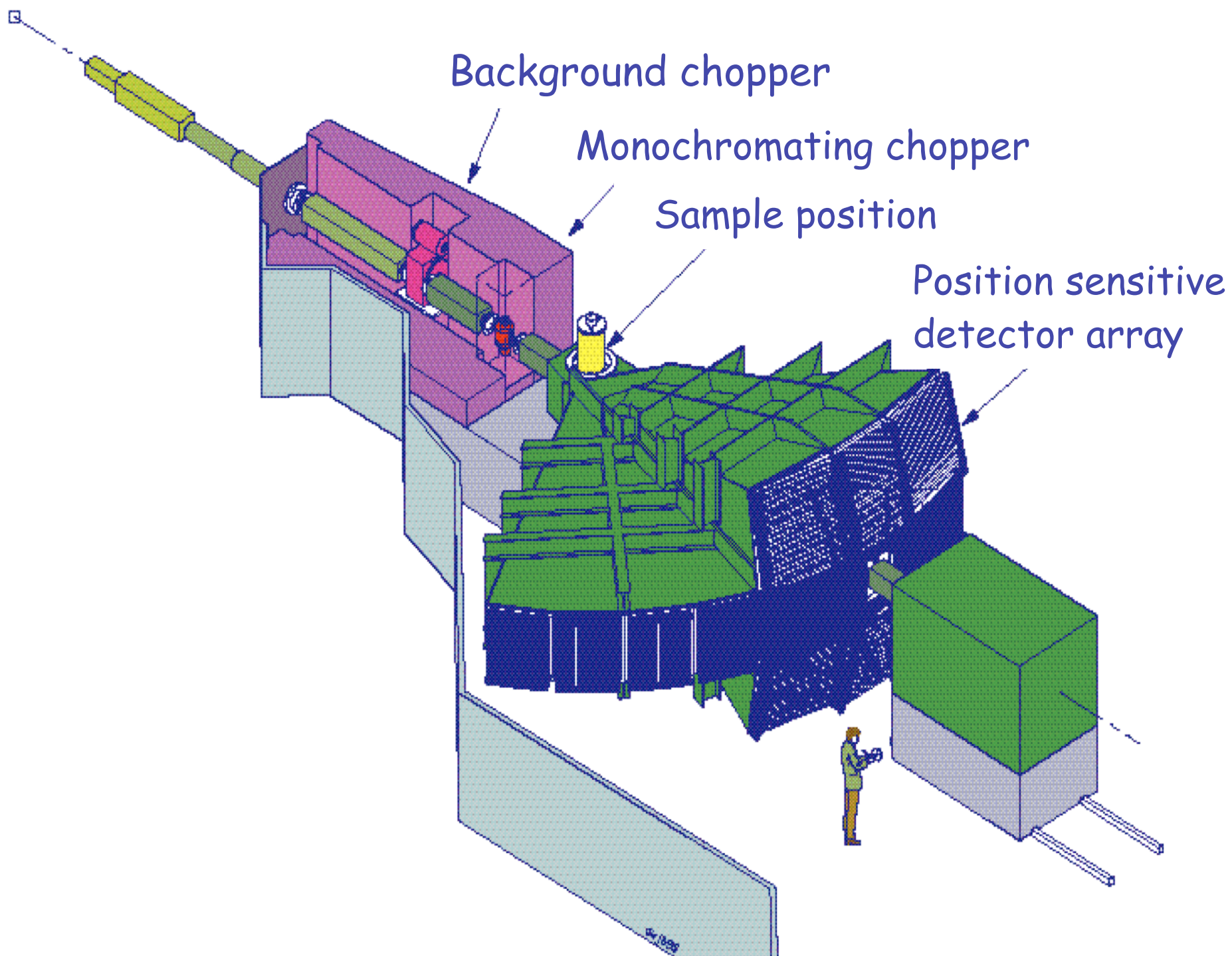
Double exchange model:



Perring et al., Phys Rev. Lett. 77, 711 (1996)



# MAPS spectrometer

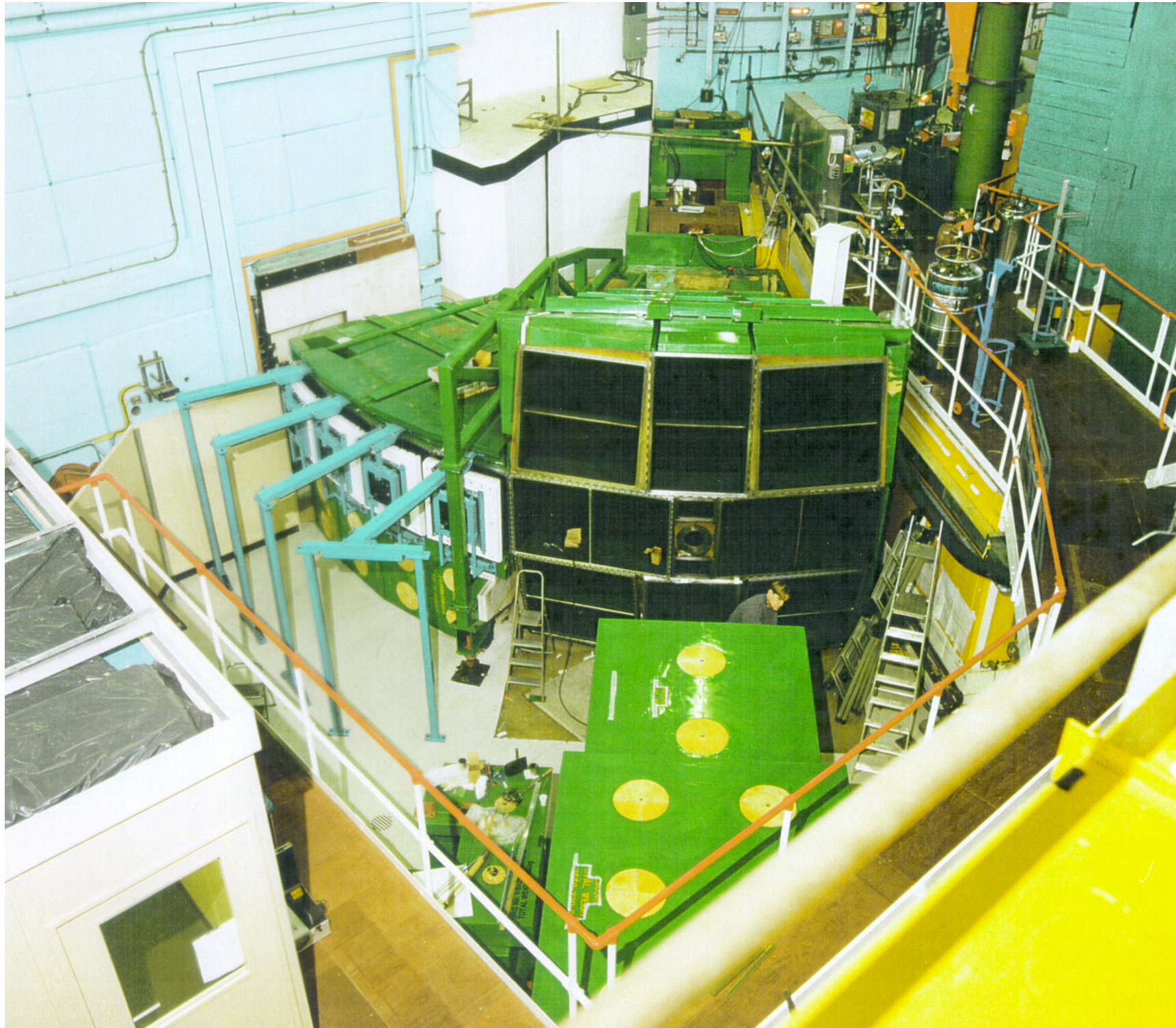


## Specification:

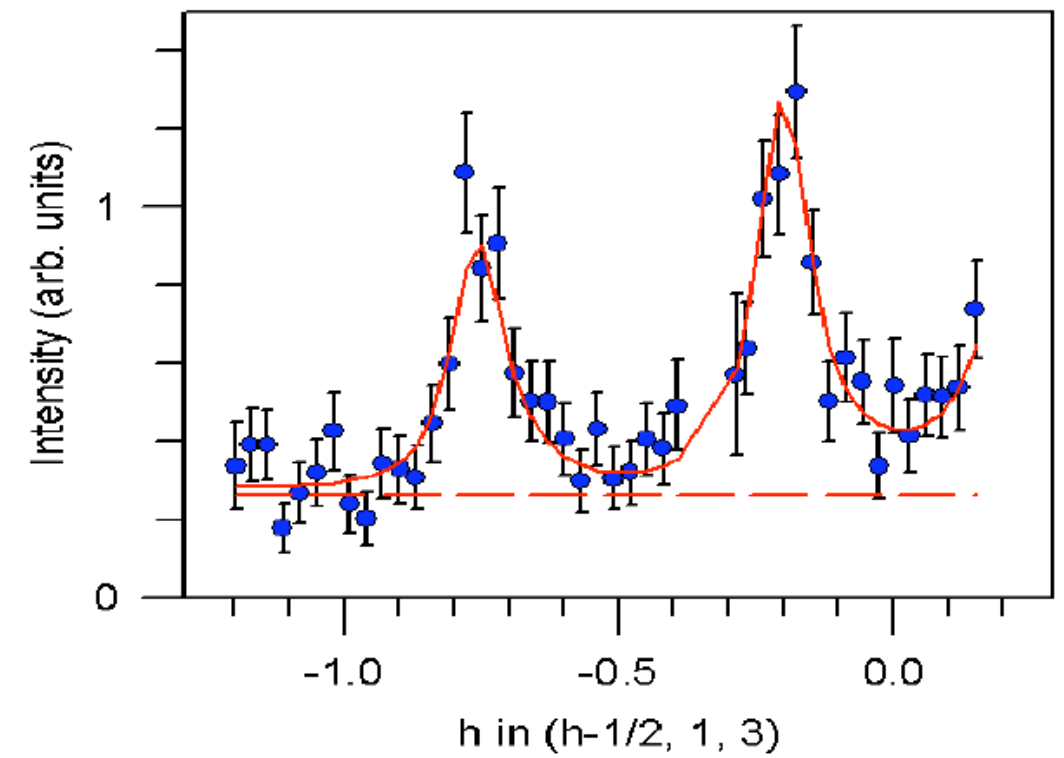
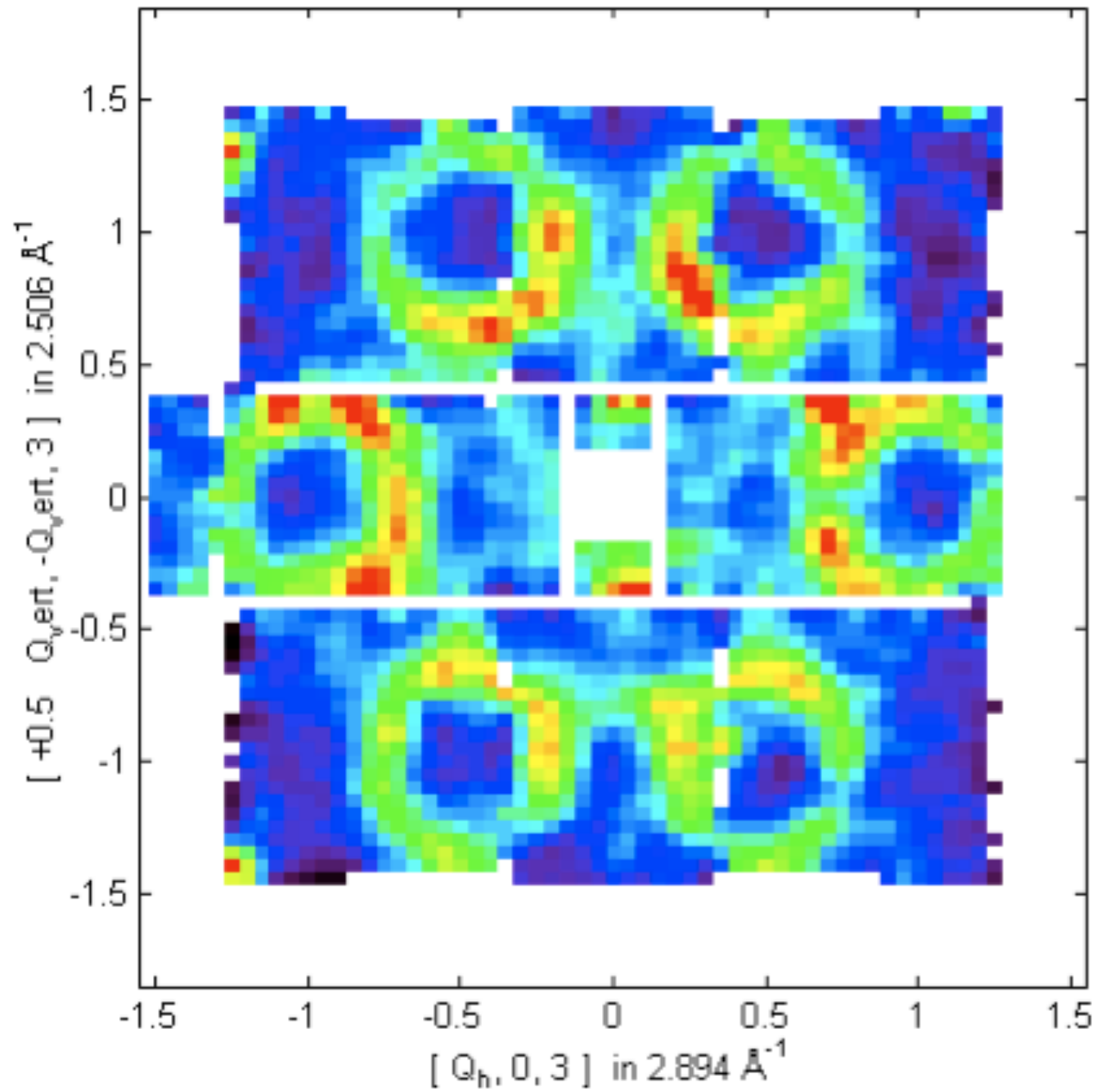
- $20\text{meV} < E_I < 2000\text{meV}$
- $I_{\text{mod-chop}} = 10\text{m}$
- $I_{\text{sam-det}} = 6\text{m}$
- low angle bank:  $3^\circ\text{-}20^\circ$   
high angle bank:  $\rightarrow 60^\circ$
- $\Delta h\nu/E_I = 1\text{-}5\%$  (FWHH)  
~ 50% more flux  
or ~ 25% better resln.
- 40,000 detector elements  
2500 time channels  
 $\rightarrow 10^8$  pixels  $\equiv$  0.4GB datasets

cf SEQUOIA and ARCS at SNS

# MAPS Under Construction



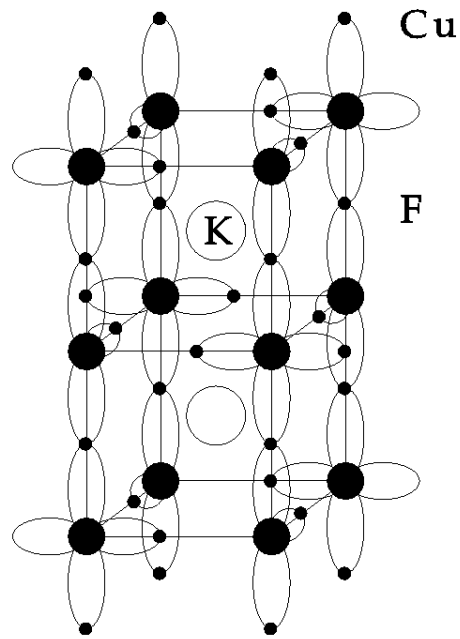
# Spin Waves in Cobalt



$$H = -J \sum \mathbf{S}_i \cdot \mathbf{S}_j$$

$$12SJ = 199 \pm 7 \text{ meV}$$
$$\gamma = 69 \pm 12 \text{ meV}$$

# KCuF<sub>3</sub> - 1D Spin-1/2 Antiferromagnet



Faddeev and Takhtajan

(Phys. Lett 85A 375 1981)

suggested excitation spectrum:

not spin waves :  $S=1$

but pairs of "spinons" :  $S=1/2$

$$\omega = \omega_1(q_1) + \omega_2(q_2)$$

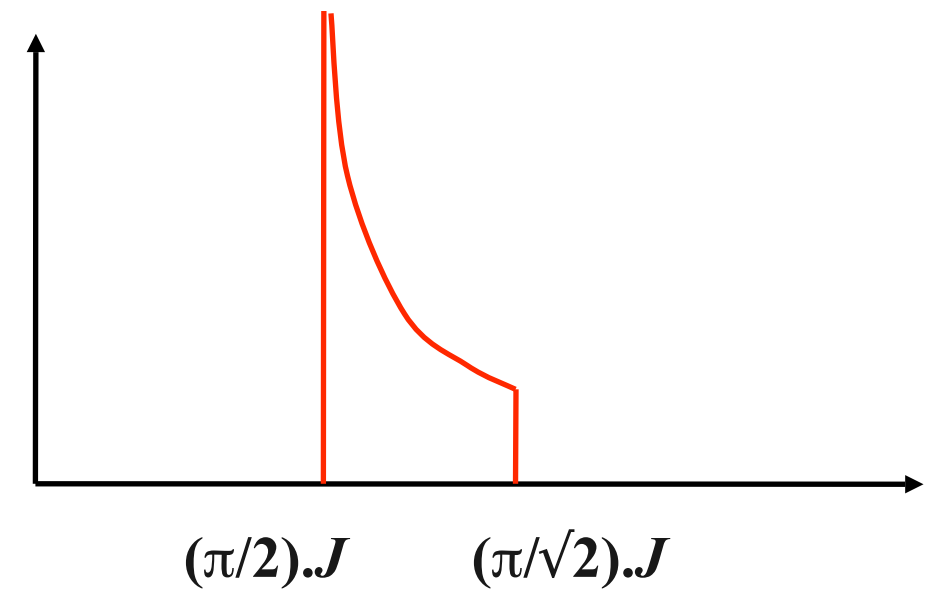
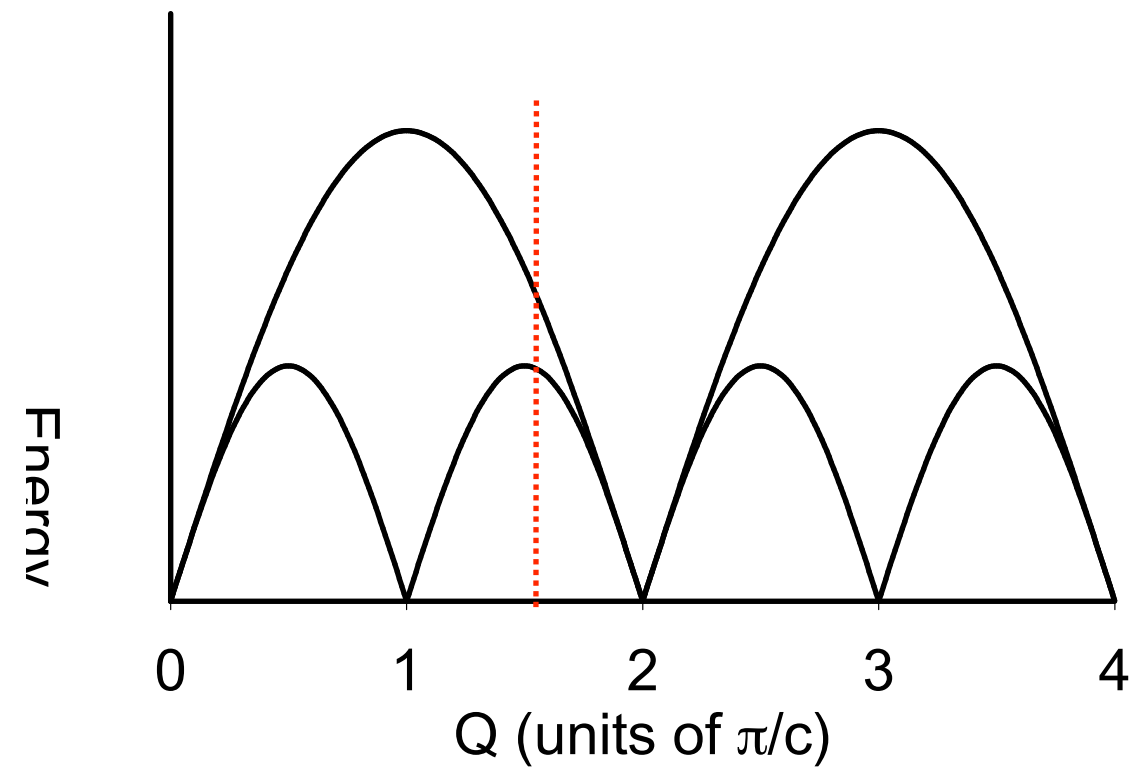
$$q = q_1 + q_2$$

→ continuum of excitations

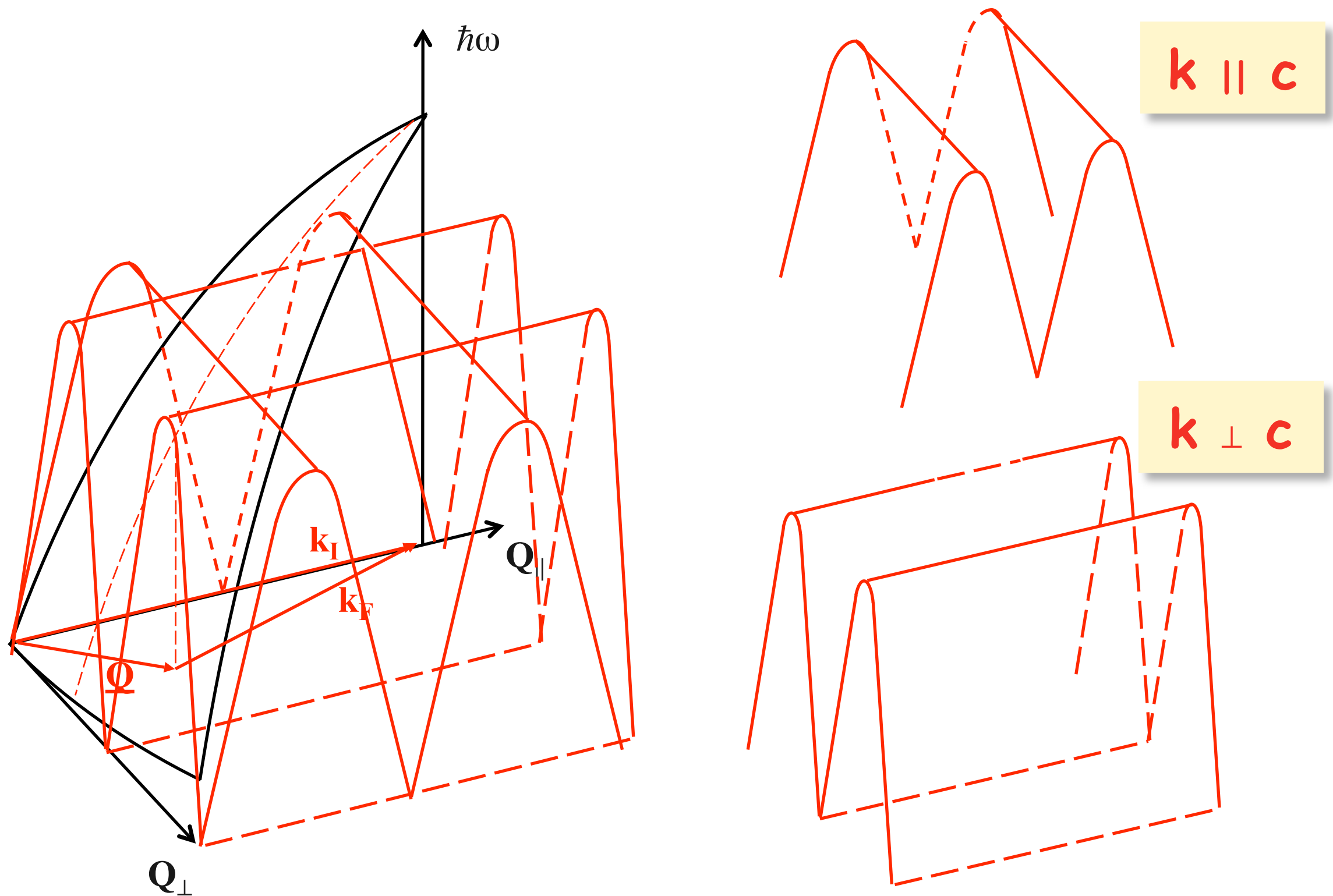
$$\omega_L = (\pi/2) J | \sin(\pi q) |$$

$$\omega_U = \pi J | \sin(\pi q/2) |$$

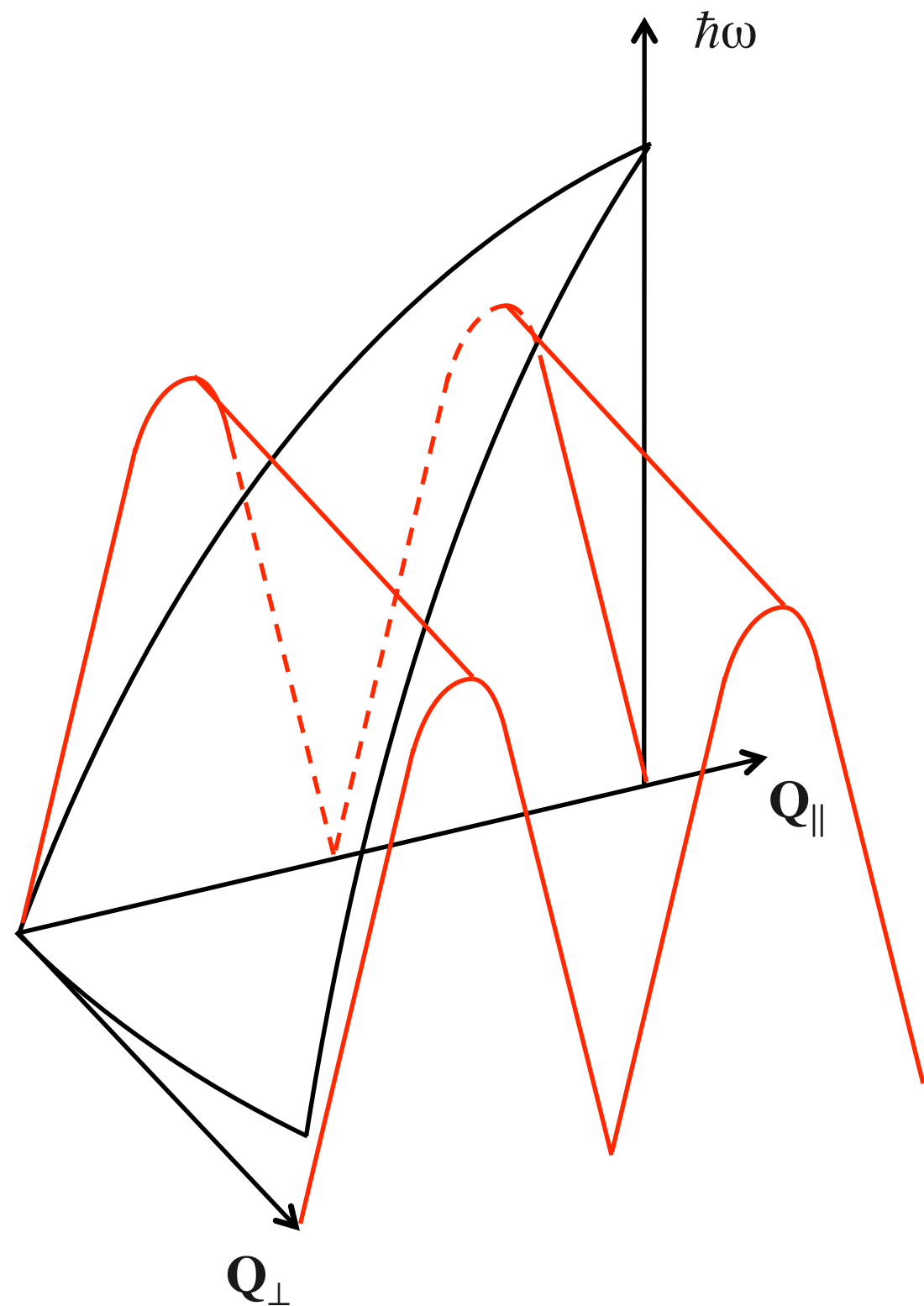
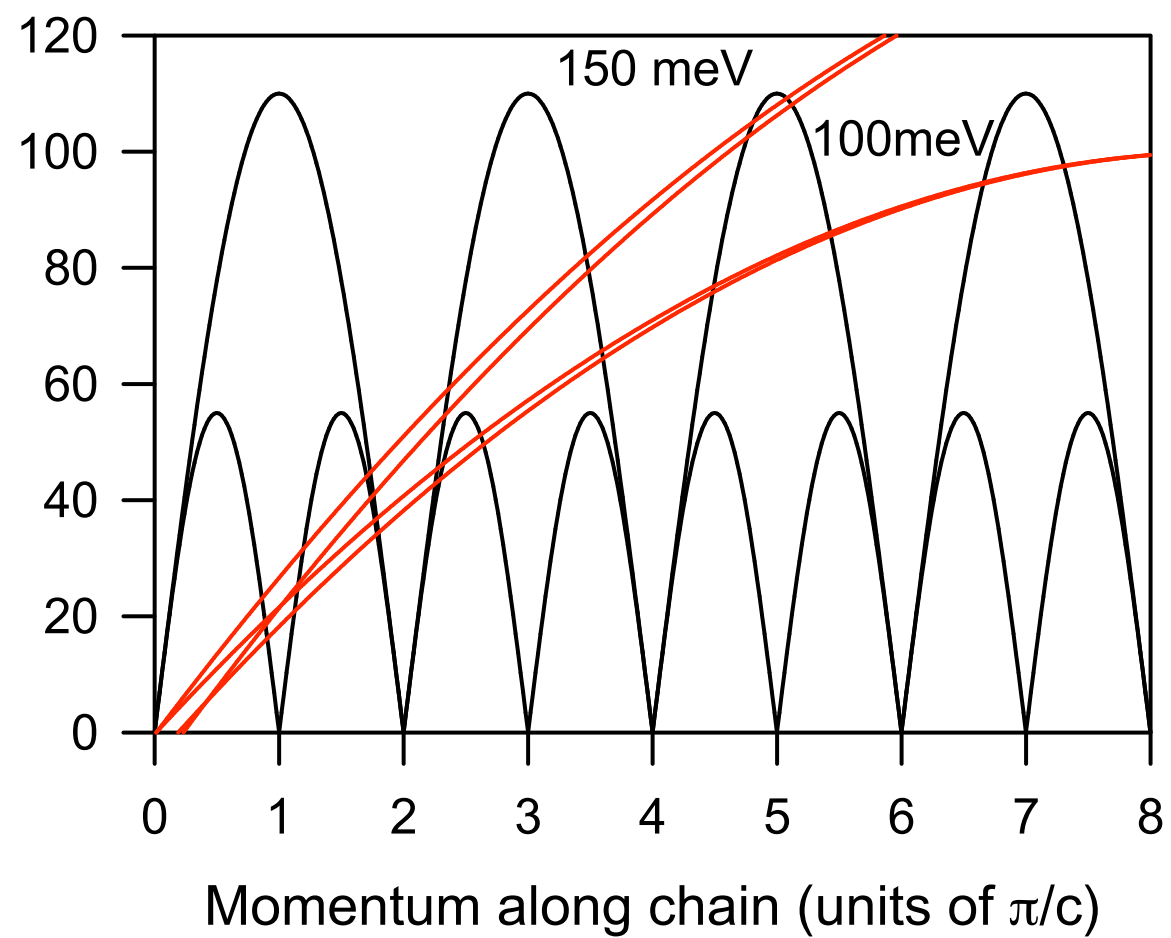
Numerical and analytic work:



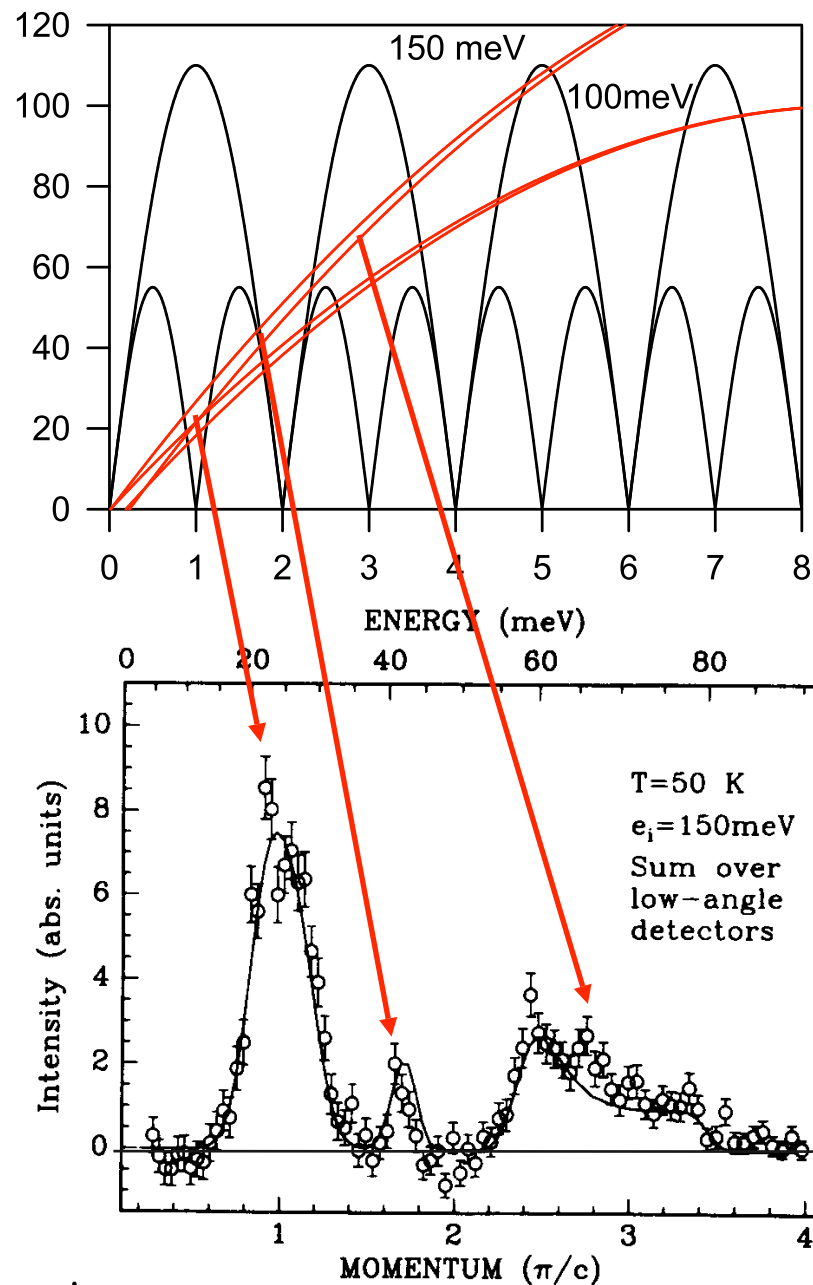
# Low-Dimensional Excitations



# $k$ II $c$



# KCuF<sub>3</sub> Excitations



- Broad peak can only be explained by continuum

First clear evidence of continuum scattering in  $S=1/2$  chain

- Intensity scale:

$$A = 1.78 \pm 0.01 \pm 0.5$$

c.f. numerical work:

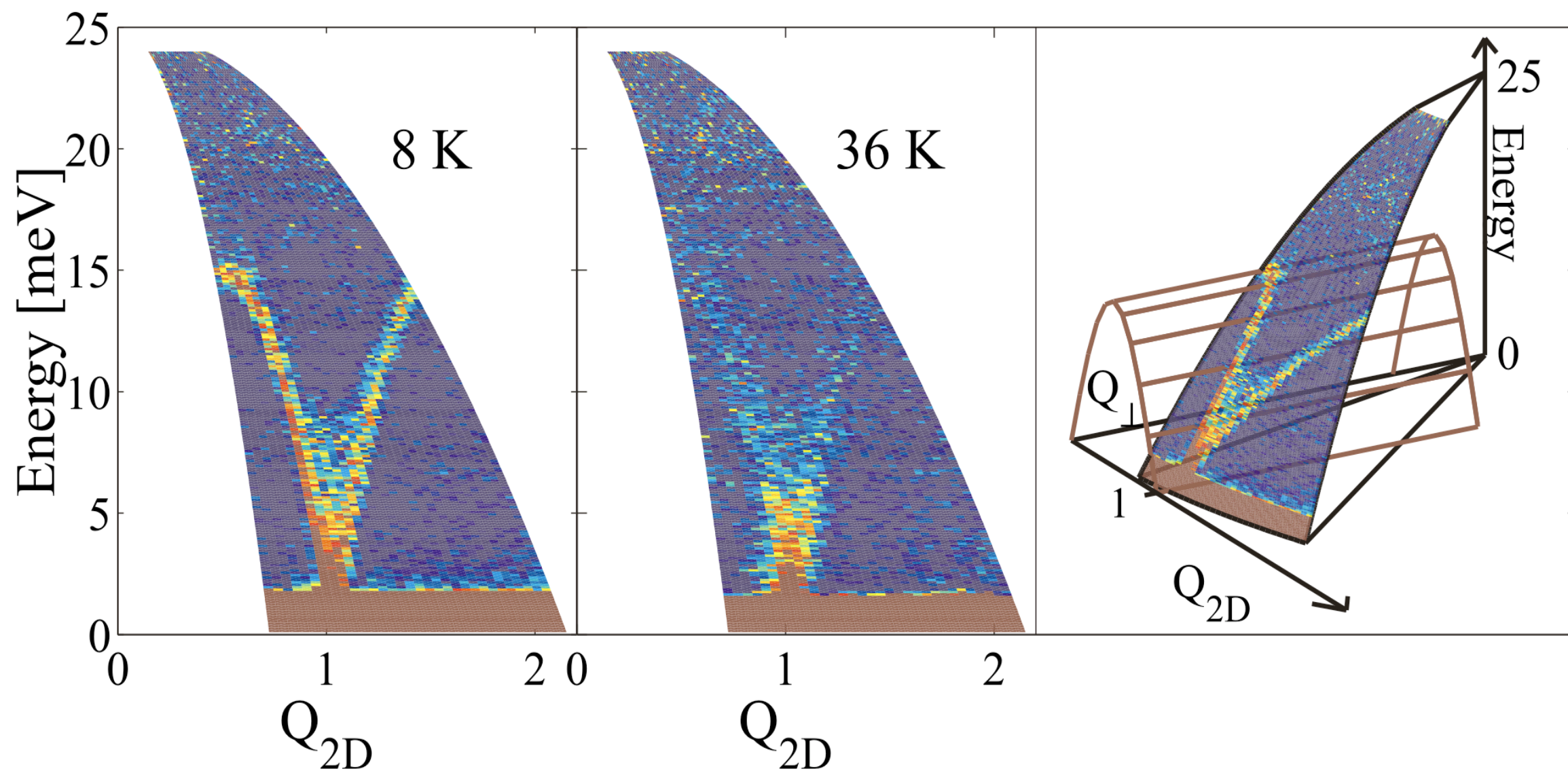
$$A = 1.43$$

- Coupling constant:

$$J = 34.1 \pm 0.6 \text{ meV}$$

D.A. Tennant et al, Phys. Rev. Lett. 70 4003 (1993)

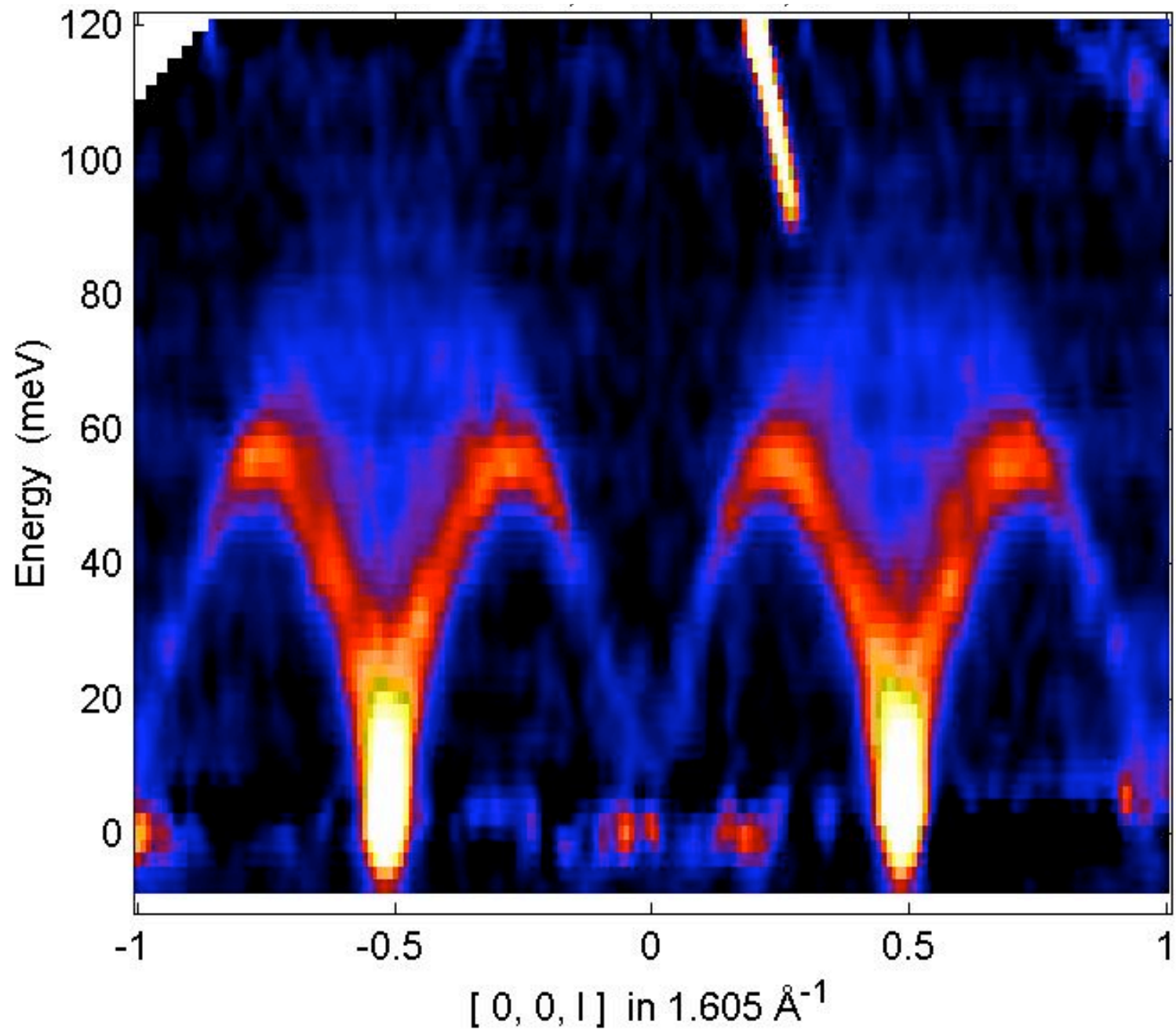
$k \perp c$



# KCuF<sub>3</sub> Excitations (again)

Direct observation  
of the continuum

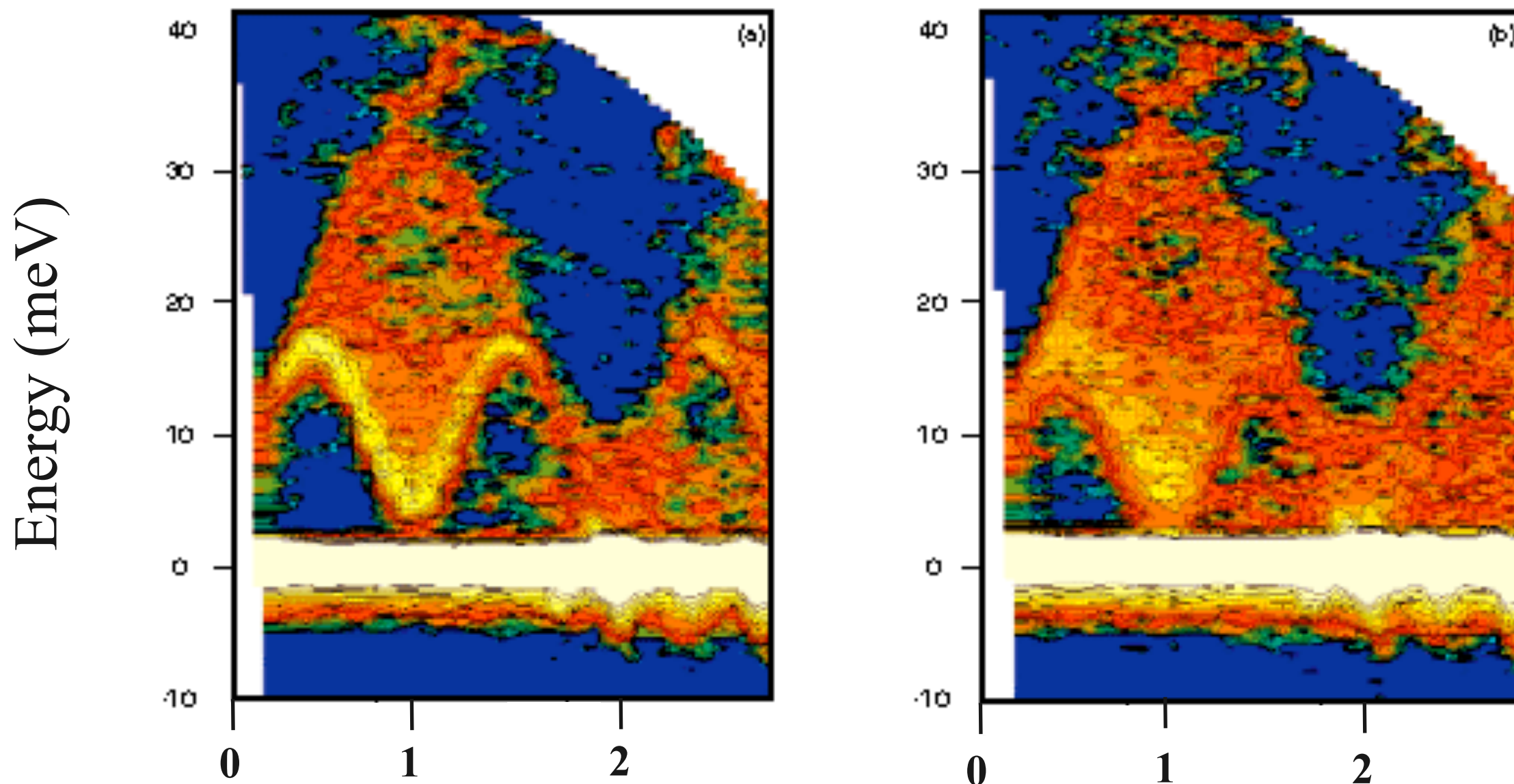
Stephen Nagler (ORNL)  
Bella Lake(Oxford)  
Alan Tennant (St. Andrews)  
Radu Coldea(ISIS/ORNL)



# $\text{CuGeO}_3$ 1D Spin-Peierls Compound

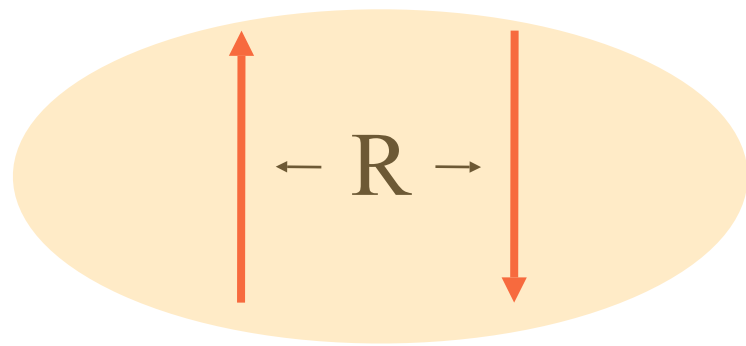
10K

50K

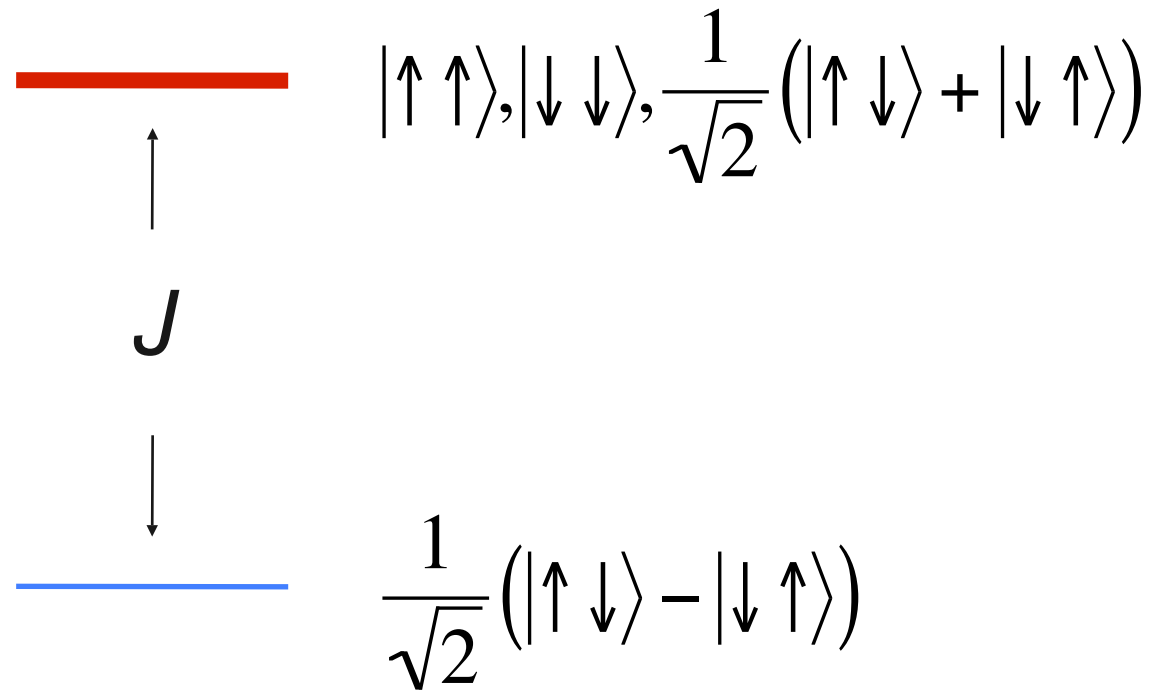


M.Arai et al., Phys. Rev. Lett **77** 3649 (1996)

# Antiferromagnetic Dimers

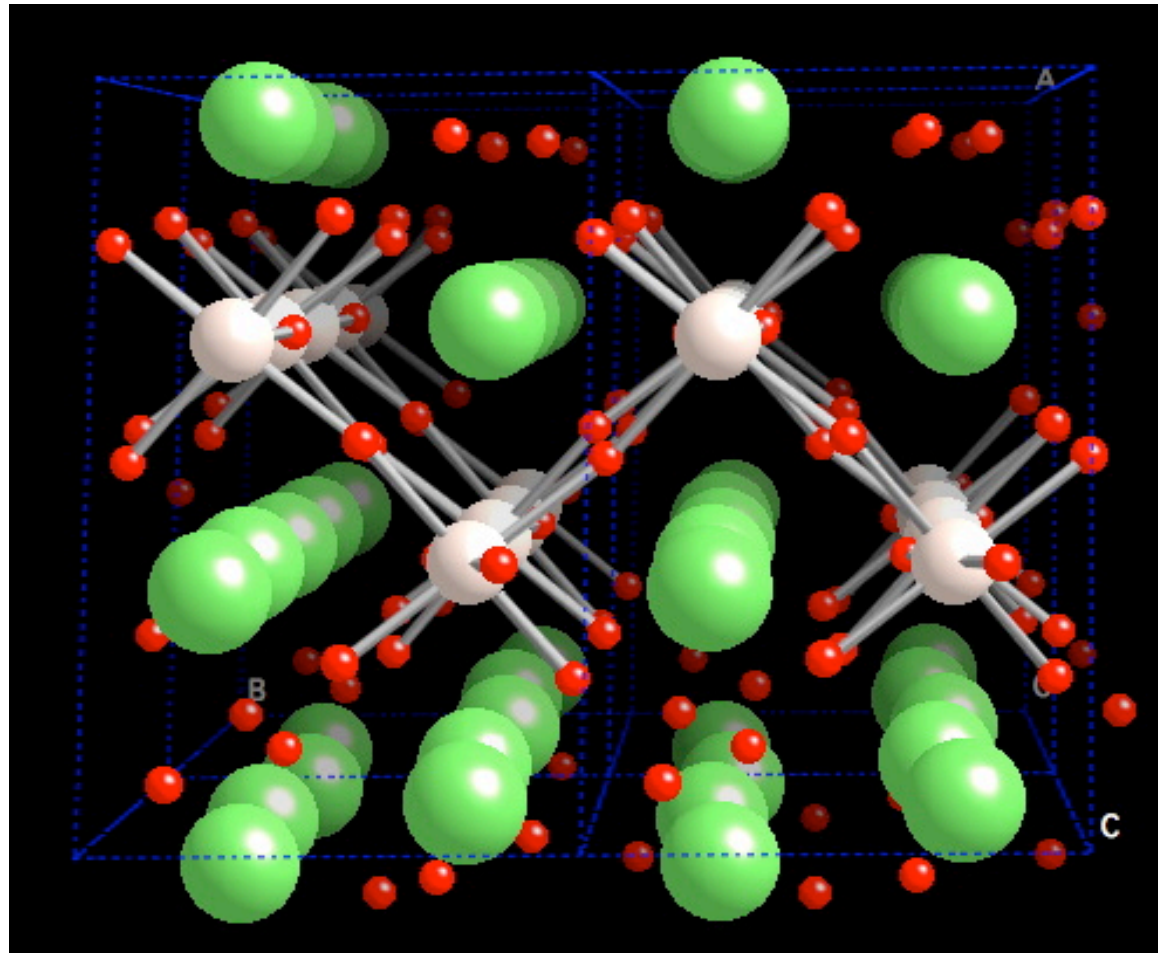


Hamiltonian:  $J\mathbf{S}_1 \cdot \mathbf{S}_2$



$$S^{\alpha\alpha}(\vec{Q}, \omega) = \sin^2\left(\frac{\vec{Q} \cdot \vec{R}}{2}\right) \delta(\omega - J)$$

# Orbitally-Driven Dimerization in $\text{La}_4\text{Ru}_2\text{O}_{10}$

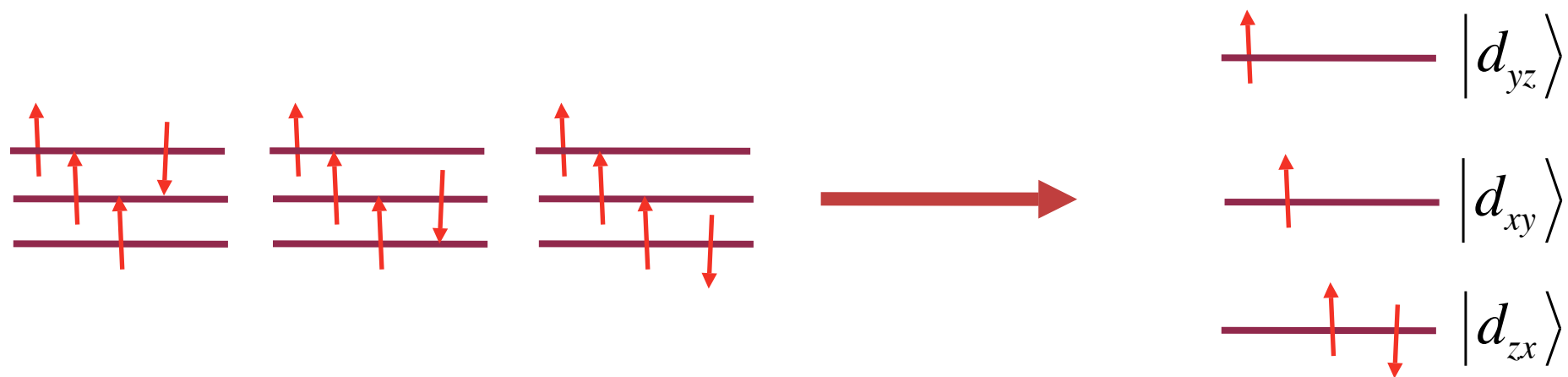


$$J_y = 2J_0(1 + \delta)$$

$$J_x = J_0(1 - \delta)$$

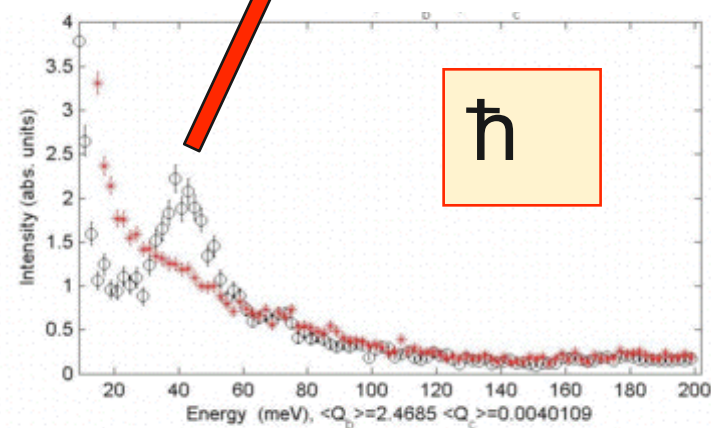
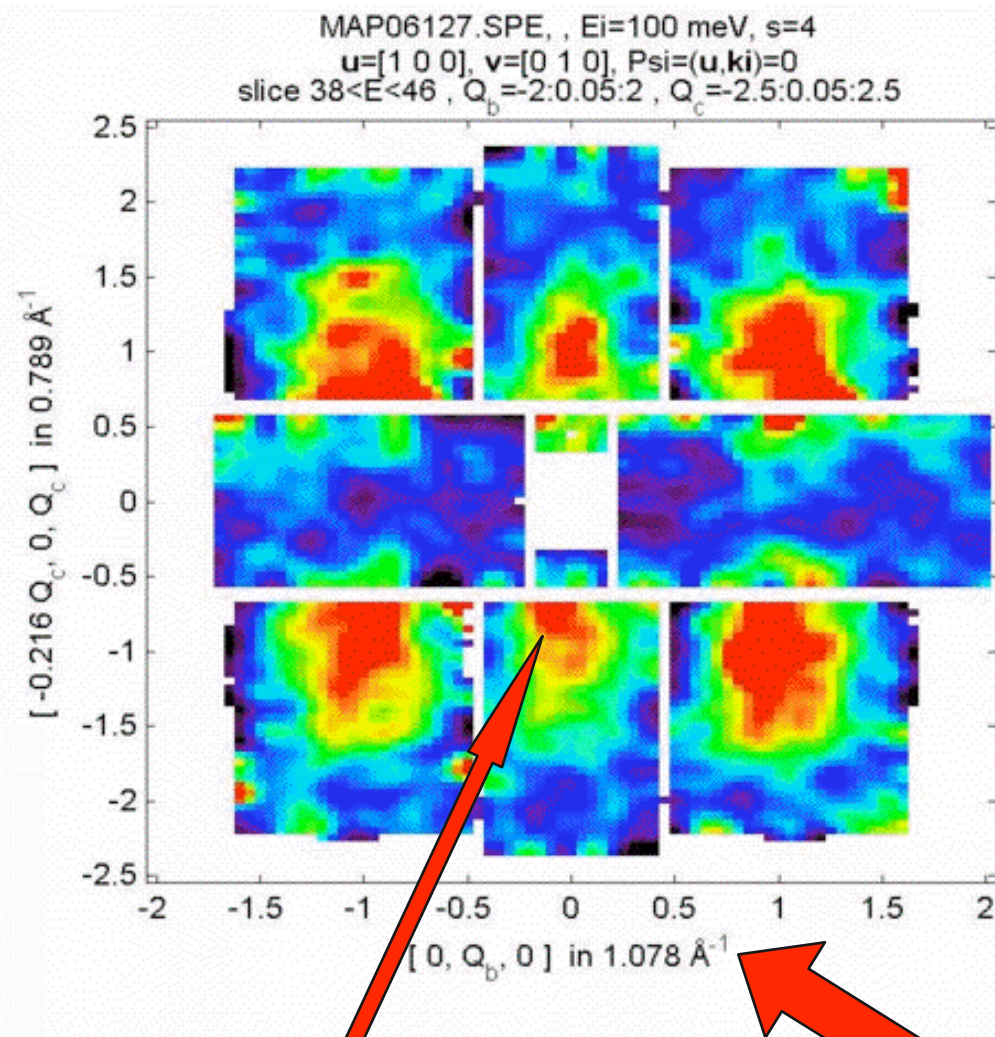
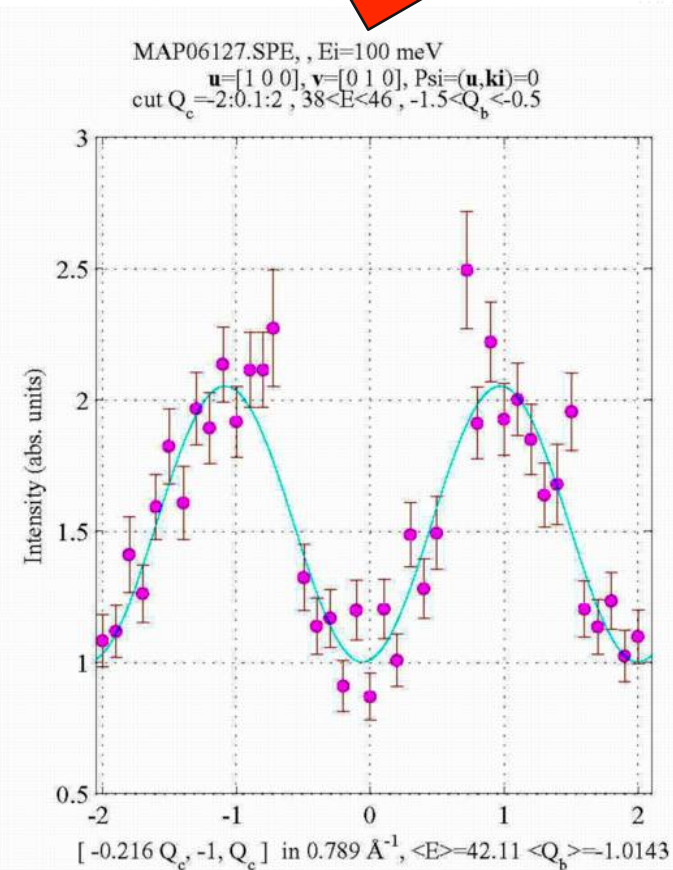
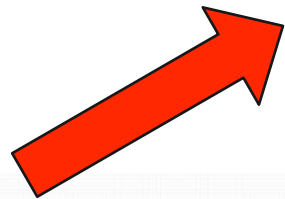
$$J_z = J_0$$

$|d_{yz}\rangle$   
 $|d_{xy}\rangle$   
 $|d_{zx}\rangle$



# Dimerization in $\text{La}_4\text{Ru}_2\text{O}_{10}$

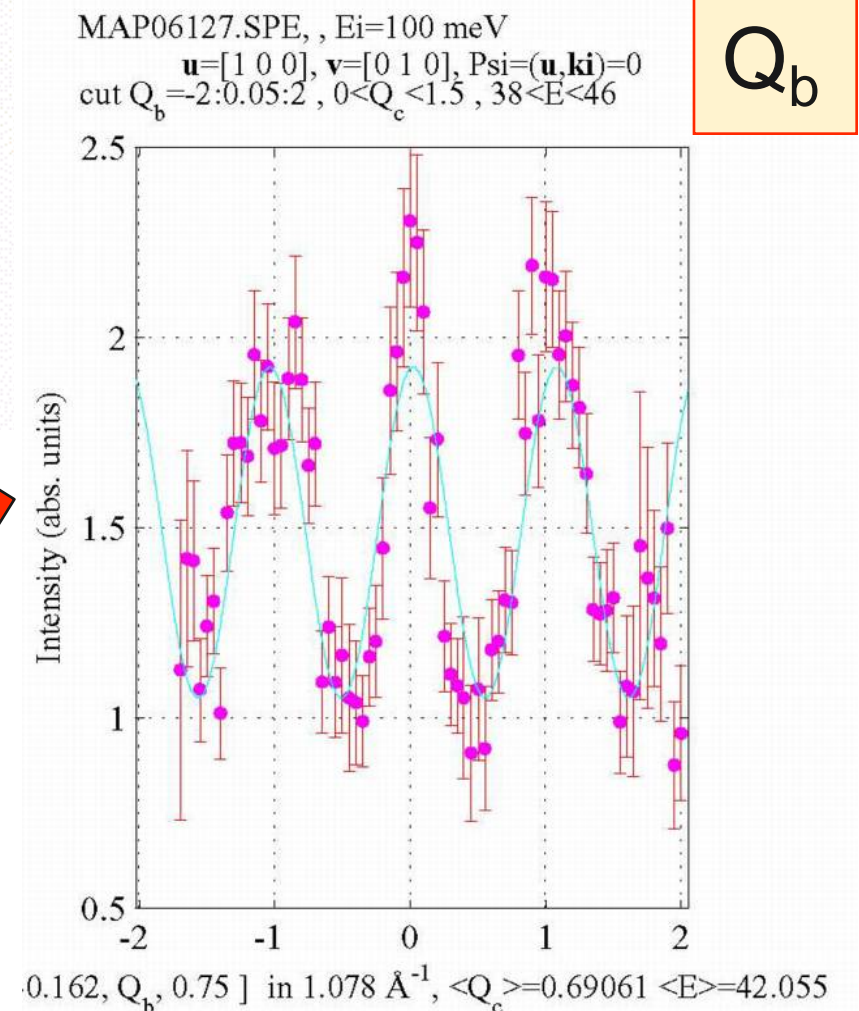
$Q_c$



$\hbar$

The intensity of the inelastic peak at  $\sim 45$  meV shows the strong  $|\sin(q)|^2$  modulation characteristic of dimer interactions with a length scale consistent with neighboring ruthenium ions.

$Q_b$



# Pixel Power\*

- Computing power + good analysis software

visualization + analysis

Integral part of the spectrometer :  
("tertiary spectrometer")

	detector elements	energy bins	pixels
Typical	200-2000	200	$10^5$
MAPS	40000	200	$\sim 10^7$

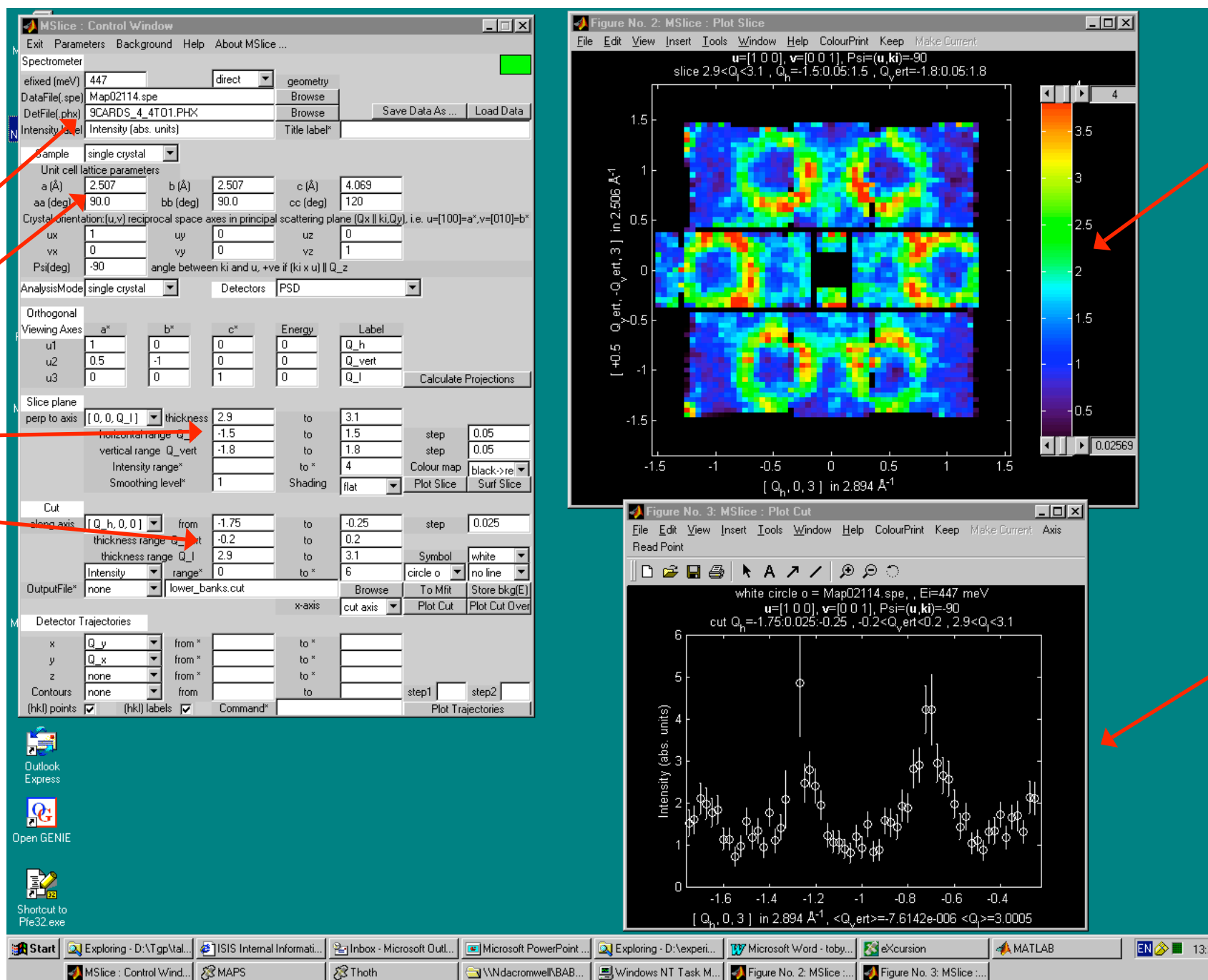
\* © Gabriel Aeppli

# Current Analysis Software

## MSLICE - Radu Coldea (ISIS/ORNL)

GUI interface

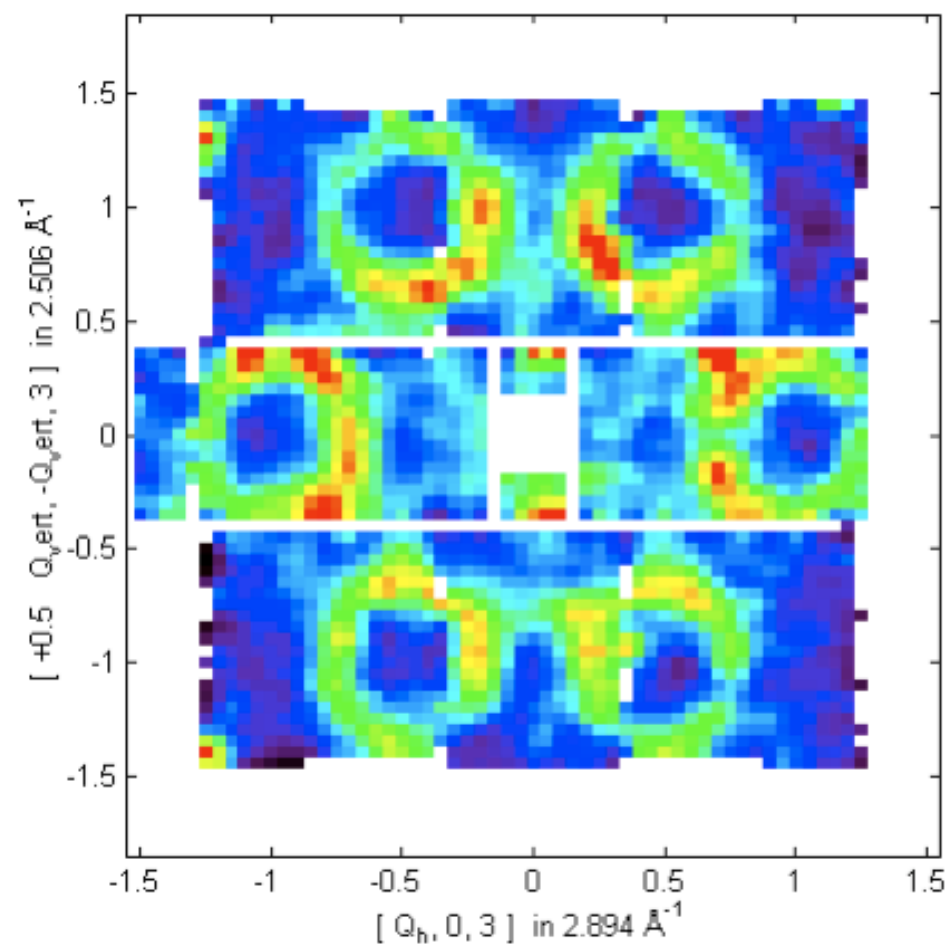
run info.  
sample  
2D &  
1D cuts



2D slices  
in  $(Q, \omega)$

1D cuts  
in  $(Q, \omega)$

# What Now?



- Inelastic neutron scattering has made a vital contribution to our understanding of condensed matter.
- Triple-axis and time-of-flight methods play complementary roles.
- New techniques revitalize the subject and present new challenges.
- The Spallation Neutron Source will continue this process into the future.